Bridging sensory perception to developmental decision-making in Caenorhabditis elegans

Thesis by
Mark Guangde Zhang

In Partial Fulfillment of the Requirements for the
Degree of
Doctor of Philosophy in Biology

CALIFORNIA INSTITUTE OF TECHNOLOGY
Pasadena, California

2024
Defended April 23rd, 2024

Mark Guangde Zhang
ORCID: 0000-0002-0802-300X

Acknowledgements

"Our chief want in life is somebody who will make us do what we can."
- Ralph Waldo Emerson

I must begin by acknowledging my advisor, Paul Sternberg, for being the best advisor I could have asked for during my graduate studies. I knew Paul was the right mentor for me when he asked me at our first lunch together, "what do you need from me as an advisor?" I hope to ask the same question to every future person I mentor.

I did not come to Caltech thinking that I would work in Paul's lab. In fact, Paul's lab was not even on my radar. But after a difficult first rotation, I needed to find a mentor who I knew would support me, grant me independence, and respect the choices I needed to make for myself. Paul has been all of this and more. Even though he boasts immaculate academic credentials and accolades, Paul has been a wonderfully accessible mentor. I will forever miss his roaming the hallways of Kerckhoff and the offices of Chen to learn what his lab members have been up to and how he could best support them.

I need to thank numerous mentors during my undergraduate years at Pomona College, including Professors Sara Olson, Dan O'Leary, Elizabeth Glater for making science worth pursuing. I also owe it to Dr. Fabian Blombach and Finn Werner at University College London, who provided me my first taste of independent research and showed me how rewarding it could be.

I owe so much to my undergraduate thesis advisor Jane Liu, who shepherded my love for research while also teaching me the fundamentals of molecular biology. Throughout my Ph.D., I used methods that I learned in Jane's lab, and I taught many of my students in the Sternberg Lab the same techniques. Thank you, Professor Liu, for making this thesis work possible in ways you may not have ever foreseen.

At Caltech I have met some of the best humans on the planet. I came to Caltech in part because of meeting wonderful friends during recruitment weekend, like Matthew Langley, Mackenzie Strehle, Morgan Schwartz, and Fayth Tan. And once I arrived, I found people I will cherish forever: Katie Page and Reina Buenconsejo (also friends from Pomona), Marta Gonzalvo, Sean Byrne, and Lincoln Ombelets. Thank you to members of the Graduate Christian Fellowship who have helped remind me of my worth beyond the bench: Albert Wandui, VoonHui Lai, Widi Moestopo, Andy Ylitalo, Beckah Silva, Sami Chang, Grigory Heaton, Caroline Paules, Hannah Manetsch, Grace Chen, Nathan Wei, and Maria Camarca.

I would like to thank my committee members, Professors David Prober, Ellen Rothenberg, and Betty Hong, for pushing me to become the best scientist I can. Thank you for your insightful questions and staunch support during our thesis committee meetings.

I am immensely grateful to my mother, Ning Liu, and father, Peng Zhang, for their unwavering support during these past 5.5 years. I thank my brother, Michael Zhang, for always believing in me and encouraging me, even when I found it difficult to do for myself.

And of course, thank you to my partner and soon-to-be wife, Hyeji (Julie) Cho, for being the best human being I have ever met. Thank you for your notes on my desk that remind me that I am capable but also that I am cherished. Thank you for your hugs at night and for listening to me rant about my worms not cooperating. But mostly, thank you for loving me in ways I never knew I needed to be loved. You make all things possible.

Abstract

Amidst uncertain environmental flux, organisms must be able to appropriately adapt their physiology in response to or in preparation for harsh conditions. To accomplish this task, organisms need to accurately perceive current environmental cues, make informed decisions about how the future environmental landscape might unfold, and execute the genetic programs to manifest the proper physiological changes. As a prime example, the roundworm Caenorhabditis elegans makes multiple developmental decisions during its life cycle in response to environmental cues. During larval growth, C. elegans can forego reproductive growth and instead enter diapause (also called dauer), a developmentally arrested state resistant to environmental stress, in response to unfavorable growth conditions. The decisions to enter and exit dauer involve complex neurogenetic computations that integrate environmental cues, yet despite decades of research in the field of C. elegans dauer biology, we still do not fully understand how such sensory integration occurs. Furthermore, how the dauer entry and exit decisions compare and contrast to one another remains unclear.

In this thesis, I comprehensively analyze the C. elegans dauer exit decision using behavioral analyses, neuronal imaging, and gene reporter technologies. In Chapter Two, I I demonstrate how, during dauer exit, the ASJ chemosensory neurons integrate food availability and population density at both the levels of neuronal calcium dynamics and gene expression. I show that expression of the insulin-like peptide encoding gene ins-6 within the ASJ neurons is responsive to dauer-relevant cues, dependent on ASJ neuronal activity, and participates in an autoregulatory feedback mechanism that enforces decision commitment. In Chapter Three, I analyze how steroid hormones are essential for the dauer exit decision, and I illustrate how the spatiotemporal dynamics of steroid hormone regulation during dauer exit compares with that of dauer entry. Taken together, this thesis significantly advances our knowledge of the C. elegans dauer exit decision and helps us better understand how animals coordinate decisions over long timescales in response to changing environments.

Published Content and Contributions

M.G. Zhang, M. Seyedolmohadesin, S. Mercado, H. Park, N. Finnen, F. Schroeder, V. Venkatachalam, P.W. Sternberg, Sensory integration of food availability and population density during the diapause exit decision involves insulin-like signaling in Caenorhabditis elegans. bioRxiv (2024). http://doi.org/10.1101/2024.03.20.586022

M.G.Z. participated in the conception of the study, experimental design, data acquisition, and manuscript writing (original and final drafts).

M.G. Zhang, P.W. Sternberg, Both entry to and exit from diapause arrest in Caenorhabditis elegans are regulated by a steroid hormone pathway. Development 149, dev200173 (2022). https://doi.org/10.1242/dev.200173

M.G.Z. participated in the conception of the study, experimental design, data acquisition, and manuscript writing (original and final drafts).

Table of Contents

List of illustrations and tables

Chapter 1

Introduction

"Uncertainty is the only certainty there is."

– John Allen Paulos, Mathematics Professor

All organisms face uncertain environments. From unicellular bacteria to multicellular animals, all of life must endure sporadic periods of unfavorable stresses and sustainably thrive under seasons of plenty. Doing so requires perceiving environmental changes and executing the appropriate physiological responses. The overarching goal of this thesis was to add to our understanding of how animals use sensory perception to interpret the environment and deploy the necessary genetic programs to appropriately react.

This introduction comprises three sections. First, I discuss the concept of developmental decisions and provide examples across taxa to illustrate how such decisions can help organisms manage environmental uncertainty. I also argue that studying how sensory perception informs developmental decisions has important ramifications for both basic science and human health. Second, I discuss how the nematode Caenorhabditis elegans provides a tractable platform through which we can analyze developmental decisions, and I describe two of the most important developmental decisions that C. elegans makes: the dauer entry and dauer exit developmental decisions. And third, I underscore the various challenges and questions that remain in studying the C. elegans dauer entry and exit decisions, and I preview how this thesis has addressed these important questions.

1.1 Developmental decisions such as diapause are an evolutionary conserved strategy to manage environmental uncertainty

All organisms face the challenge of modulating their behavior, development, and/or morphology to accommodate environmental changes. To overcome this challenge, organisms have evolved the capacity of phenotypic plasticity, wherein organisms of the

same genotype can adopt different phenotypes in response to changing environmental circumstances. These phenotypic changes occur in traits that can be defined along either a continuous axis (e.g., quantifiable traits such as size, shape, and weight) or a discretized axis (i.e., the phenotype is categorized as type A or type B). In the case of discrete phenotypes, such phenotypic plasticity is referred to as polyphenisms (1, 2). In this thesis, one of the key polyphenisms I address is a phenomenon referred to as diapause, a developmentally arrested, stress-resistant state that an organism enters in response to or in preparation of unfavorable environmental conditions (3, 4).

Diapause can be considered a developmental decision, a type of polyphenism in which the phenotype category is one of multiple discrete developmental stages. While there does not exist a unified definition of "developmental decision," I argue that the instances in which the term is invoked (5–9) share a set of common features. Typically, a developmental decision describes a process that:

- results in one of multiple mutually exclusive developmental outcomes
- occurs in response to appropriate environmental stimuli (although some developmental decisions may occur stochastically (10))
- features commitment and irreversibility (i.e., past a certain point, one cannot easily regress to the pre-decision state)

Developmental decisions can occur both at the single-cell level, such as for unicellular organisms or for cell fate decisions in animals including stem cell differentiation and immune cell development (5, 11), or at the multicellular level to affect development of parts (or even the whole) animal.

Below I provide examples of developmental decisions across various taxa, focusing primarily on life cycle decisions whose primary inputs are environmental cues and whose primary purpose is to aid in protecting against environmental stressors.

- Bacteria, fungi, protozoa, and plants boast a strategy called sporulation that involves a developmental decision to form spores. The spore is a stress resistant and dormant state whose primary purpose is to survive amidst harsh conditions while waiting for more favorable growth conditions, after which they germinate and resume growth (8, 9, 12). Many spores deploy dispersal mechanisms that facilitate travel, either actively or passively, to new environments that may be more suitable for germination (9, 13).

- Nematodes, insects, and fish deploy a strategy called diapause, mentioned earlier in this introduction. Similar to the spore state, diapause is a developmentally arrested state characterized by stress resistance and metabolic quiescence (3, 4). Animals enter diapause under unfavorable conditions and exit once environmental conditions sufficiently improve. In many cases, diapause is facultative; animals may decide between two alternative developmental paths, diapause vs. non-diapause, based on environmental factors. Depending on the organism, diapause may occur at different stages during larval development. In nematodes, diapause occurs midway through larval development, whereas different species of insects undergo diapause at different stages from embryonic through adulthood. In fishes such as annual killifishes, which can survive in unstable aquatic environments that include a dry season, diapause occurs at three different stages during embryonic development in response to anaerobic conditions, low temperatures, and the presence of adult fishes (14).

- Social insects including termites and ants use phenotypic plasticity to enforce caste differentiation within their colonies, allowing for a division of labor by morphologically and behaviorally distinct castes produced from the same genotype (15). Environmental cues induce different proportions of ants or termites to grow into a particular caste with specialized roles including defense, brood care, foraging, and sexual reproduction. Researchers argue that the proportion of the different caste members is optimally matched to maximize efficiency of the colony. For instance,

nascent colonies may prioritize workers that gather food to grow the colony, while populated colonies may invest more in soldiers to defend the larger colony, which has now become a lush food source for predators (16, 17). In another example, a colony that experiences a depletion of food in the surrounding area would want to relocate, therefore triggering induction of winged adults, termed alates, which can disperse to distant areas with the goal of starting a new brood in a more replete environment (18).

The variety of these developmental decisions and their existence across multiple domains of life highlight how they are an effective and evolutionarily conserved biological strategy to combat environmental uncertainty. While developmental decisions may appear different from one species to the next, they share a basic flow of information: organisms perceive and interpret environmental conditions and relay that information through various signal transduction cascades to culminate in a physiological response (i.e., the genetic programs that instruct the developmental decision). Studying this flow of information is helpful for at least two reasons, including enhancing our understanding of biological systems as well as helping us address human health and disease.

Enhancing our understanding of biological systems: Developmental decisions such as diapause involve a complicated dance of sensory inputs leading to an all-or-nothing decision that must be adequately reinforced and, in some instances, maintained (2, 19). Consequently, many important questions arise that, when answered, would contribute to our understanding of how biological systems interpret a complex set of inputs to orchestrate a coordinated response. For instance, studying developmental decisions would contribute to our understanding of how organisms process multiple sensory cues, coordinate various signal transduction pathways, manage timescale discrepancies between input detection (which occur quickly) and gene expression programs (which occur more slowly), and incorporate feedback loops to reinforce proper discretized outcomes. I will further discuss each of these points in detail throughout this thesis.

Helping us understand the link between stress and development in mammals: At the organismal level, humans are generally not considered to engage in developmental decisions such as diapause (20–22). However, studying sensory processing of developmental decisions may aid us in understanding human health and disease by providing insights into how stress affects development in mammals.

Because diapause is inextricably linked to stress, we have much to learn from diapause that may reflect patterns used in the mammalian stress responses, particularly as these stresses impact future developmental outcomes. For instance, studying how organisms detect stress in the context of diapause may help us better understand how processing of stress-related inputs in humans over long periods of time regulates the onset of puberty (23) or diseases including anxiety, depression, and PTSD (24). As another example in mammals, rats that experience attentive maternal care demonstrate lower stress responses compared to those reared under lower levels of maternal care, indicating that stress-related experiences during a critical period in early growth greatly impact adult physiology (25). These findings display strong parallels with diapause in that stressors during early critical periods of growth dictate future developmental trajectories. Thus, studying stress processing during growth in the case of developmental decisions such as diapause may help us better understand the impact of stress of mammalian development.

In order to study information flow between sensory perception to execution of developmental decisions such as diapause, it would be ideal to utilize a system wherein the developmental decision occurs in a time frame reasonable for repeated study, and in which the organism's sensory apparatus and gene expression profile can be easily measured and manipulated. In the following section, I describe how the roundworm Caenorhabditis elegans aptly fits those criteria and therefore is well-suited for the study of developmental decisions.

1.2 Caenorhabditis elegans as a model system to study sensory perception during developmental decision-making

First proposed in the 1970s a model biological system by the late Sydney Brenner, the roundworm (nematode) Caenorhabditis elegans has become a staple of biological research spanning multiple subdisciplines including developmental biology, genetics, neuroscience, and more (26, 27). Below I list key reasons that makes C. elegans such a powerful system, particularly for analyzing the intersection between genes, neurons, development, and behavior.

- Fast generation time that is easily cultivated in the laboratory on petri dishes
- Transparent body that can be observed under Nomarski DIC optics and is accessible using fluorescence microscopy
- Amenable to genomic manipulations through mutagenesis, microinjection, transgenic integration, and precise genome-level edits through CRISPR and MosSCI (28–31)
- Amenable to numerous neurobiological measurement and perturbation tools, including electrophysiology, calcium imaging via genetically encoded calcium indicators, optogenetics, chemogenetics, and more (32–34).
- A fully sequenced genome, with thousands of conserved genes that play similar roles between nematodes and mammals (including humans) (27)
- A fully mapped wiring diagram, or "connectome," describing the physical connections between the 302 neurons in the adult hermaphrodite (35)

Although compact, the C. elegans hermaphroditic nervous system comprises merely 302 neurons and yet is capable of complex behaviors such as chemosensation, nociception, thermosensation, short- and long-term memory, and adaptive learning (36). While C. elegans was the first to have its connectome (or "wiring diagram") fully mapped via

electron microscopy (35), it has become clear that knowing the synaptic connections alone cannot fully account for the various neuronal circuits that govern the distinct behaviors One important reason is because of neuropeptides and neuromodulators, which further sculpt the nematode's nervous system by allowing wireless signaling between physically disconnected neurons as well as by limiting or permitting specific circuits (37).

C. elegans dauer entry and exit are two closely related developmental decisions: The nervous system of C. elegans orchestrates the decision to enter and exit diapause, mentioned earlier in this introduction as a developmental decision designed to protect the nematode against harsh environmental conditions. When C. elegans grow in favorable conditions (characterized by abundant food, low crowdedness, and cool temperatures), they develop through 4 larval stages into reproductive adults. However, if conditions prove less favorable, animals may choose the alternative developmental route to enter dauer. German for "enduring," the word "dauer" refers to a stress resistant state of diapause characterized by resistance to environmental insults, feeding cessation, slowed metabolism, a thinner radial width, and immobility (although dauers can readily move when prompted) (38, 39).

The dauer developmental decisions consist of the dauer entry decision and the dauer exit decision (also commonly referred to as dauer recovery decision). The dauer entry decision itself comprises two subdecisions. The first subdecision is made during early larval growth at the L1 stage in which larvae will choose between entering L2 (the reproductive route) versus L2d (a pre-dauer state). L2d larvae will then calculate a second subdecision and choose between returning to reproductive development as L3 larvae or commit to become dauer larvae (40). Finally, the dauer exit decision takes place as dauers assess their environment to determine the appropriate time to exiting the dauer state and return to reproductive development by becoming an L4 animal. Strikingly, L4s that originated from standard reproductive growth are nearly identical to L4s that originated from dauers, although some nuanced differences exist (41, 42).

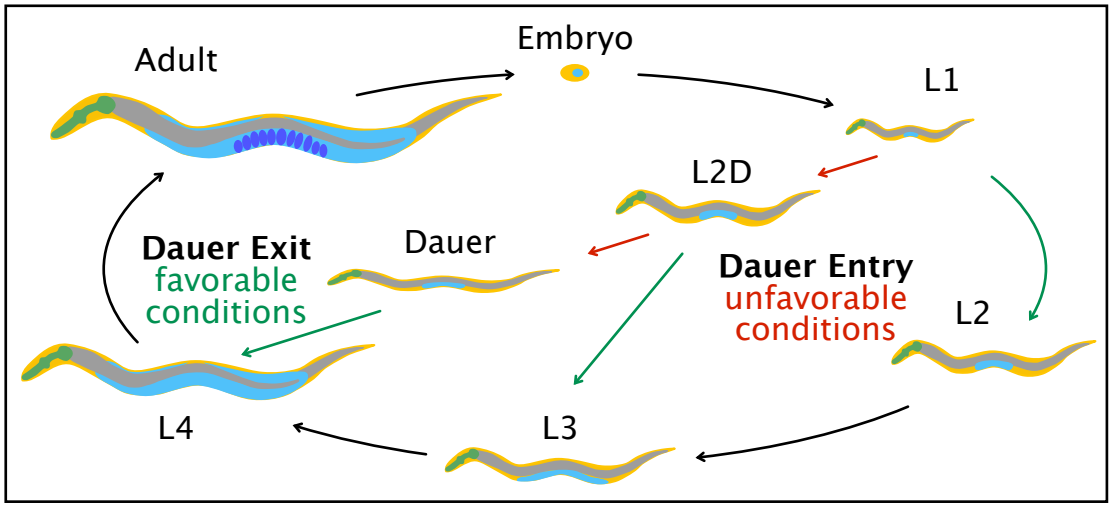

Figure 1.1: The C. elegans life cycle includes developmental decisions to enter and exit the dauer state depending on environmental conditions

The dauer entry decision comprises two subdecisions. The first decision is made during the L1 stage to enter a pre-dauer L2d state or undergo reproductive growth as an L2 larvae. A second decision is made during the L2d state to enter dauer or undergo reproductive growth as an L3 larvae. Dauers make the dauer exit decision to return to reproductive growth as L4 larvae. Colored arrows indicate decisions made under unfavorable (red) or favorable (green) conditions.

The dauer developmental process has been one of the most well-studied topics in the C. elegans community. A search of "C. elegans dauer" on Google Scholar yields over 24,000 search results, attesting to its history of extensive scientific scrutiny. These studies have unearthed key insights into the genetic pathways, neuroendocrine mechanisms, neuronal circuits, and more governing the dauer decisions. Here, I briefly describe the key principles underlying how C. elegans makes the dauer entry and exit decisions.

Environmental inputs into the dauer entry and exit decisions: Since the C. elegans dauer state specializes in protecting against environmental stress, the inputs to the dauer decisions convey future environmental status. The three critical environmental inputs to both the

dauer entry and dauer exit decisions are food supply, population density, and temperature. While there likely exist additional inputs, such as touch (Lee et al., unpublished), these three inputs have been the most well characterized:

1. Food supply: The most direct predictor of future availability is current food availability. C. elegans' primary food source is bacteria, abundantly present in the rotting vegetable matter where C. elegans can commonly be found (43, 44). Early reports described the food signal to be "heat-stable, dialyzable, neutral, and hydrophilic" and was mimicked via a purified component of yeast extract (45). While the precise chemical composition of what the food signals are remain elusive, some studies suggest it may be a combination of bacterial metabolites (including fatty acids) (46, 47). Although unlikely to be the same food signal used by Golden and Riddle, volatile odors emitted by appetitive bacteria such as isoamyl alcohol might also serve as a food signal (48, 49). Food availability is also the predominant environmental input for another developmental decision: L1 arrest, which occurs immediately following egg hatching (50).

2. Population density: C. elegans sense population density by detecting the concentrations of secreted pheromones from other nearby C. elegans worms. The general term "pheromone" collectively describes a mixture of glycosides of the dideoxysugar ascarylose, which are individually referred to as "ascarosides." Each ascaroside possesses a unique aliphatic side chain which dictates its functional activity, often by acting as a secreted molecular signal that regulates a number of biological processes including mating, developmental timing, and developmental decision-making (i.e., the dauer decisions) (51). Different ascarosides are also produced in different concentrations during different developmental stages, providing chemical snapshots of population composition at a given point in time (52). Notable ascarosides that regulate the dauer decisions include ascr #1, #2, #3, #5, #8, and icas#9 by promoting dauer entry at nanomolar concentrations (51). By

reflecting population density, ascaroside concentrations could serve as a food derivative calculator by indicating how quickly food will be depleted.

3. Temperature: Arguably one of the least understood inputs into the dauer decisions, temperature regulates the dauer decisions in that high ambient temperature promotes dauer entry and inhibits dauer exit (40). The role of temperature is poorly understood because the exact molecular nature of how temperature influences the dauer process remains unclear. Neither impairing the C. elegans singular thermosensory neuron AFD nor mutating thermotaxis pathways abolishes the temperature-dependent regulation of dauer entry, suggesting that the typical neuronal pathways associated with temperature sensation in C. elegans do not fully account for the temperature sensitivity of the dauer decisions (53, 54). Many Daf-C mutants are temperature sensitive despite not encoding temperature-sensitive gene products, indicating that the dauer process itself has some type of temperature dependence (54). One possibility is that temperature affects the biochemical rates at which dauer-relevant gene products or signaling molecules are produced, and that these altered rates bias the worms to enter dauer at specific temperatures.

The signal transduction pathways underlying dauer entry and exit: Genetic studies have highlighted multiple genetic pathways that control the dauer entry and exit decisions, including a guanylyl cyclase pathway, a TGF-β-like pathway, an insulin-like pathway, and a steroid hormone signaling pathway (Fig. 1.2). Below, I briefly describe each pathway as it relates to the dauer entry and exit decisions.

1. Guanylyl cyclase pathway: Genetic analysis places the guanylyl cyclase pathway relatively upstream in the dauer signal transduction process. Consistent with this notion, the guanylyl cyclase pathway contains genes encoding for receptors expressed in many of the chemosensory neurons known to regulate dauer entry. A major gene of this pathway is daf-11, which encodes a subunit of a receptor-like guanylyl cyclase that converts GTP to cyclic GMP (cGMP) (55). Loss-of-function mutants for daf-11 form dauers even under favorable conditions and are therefore

considered dauer formation abnormal – constitutive (Daf-C). As a secondary messenger, cGMP activates downstream proteins including the cGMP-gated cation channel heterodimer TAX-2/TAX-4 (56, 57) as well as cGMP-dependent kinases such as EGL-4 (58, 59). Cyclic GMP analogs such as 8-bromo-cGMP rescues the Daf-C phenotype of daf-11 but does not rescue the Daf-C phenotype of mutants defective for genes in other pathways, suggesting that cGMP acts earlier in the dauer process (55). Current models propose that chemosensory neurons such as ASI express GPCRs that detect food and/or pheromone, which upon ligand binding trigger a G-protein signaling pathway that eventually activates DAF-11 (39, 60).

2. TGF-β-like pathway: Conserved throughout animal development, the TGF-β pathway involves TGF-β ligands that bind cell surface transmembrane receptors that leads to the phosphorylation and subsequent nuclear translocation of SMAD transcription factors that regulate transcription (61). Mutants defective for a gene encoding the homolog of a TGF-β ligand, daf-7, are Daf-C, indicating the TGF β signaling normally acts to promote reproductive development and inhibit dauer formation (62). Homologs for TGF-β receptors (including DAF-1 and DAF-4) and SMAD transcription factors (including DAF-8, DAF-14, and DAF-3) have been identified (63). daf-7 expresses in the chemosensory neurons ASI during favorable, reproductive growth conditions, while daf-7 expression is downregulated by unfavorable, dauer-inducing growth conditions (62). Conversely, expression of TGF-β receptors and SMAD transcription factors occurs broadly throughout the animal (63). Binding of DAF-7/TGF-β causes the SMAD transcription factor DAF-3 (and its co-SMAD DAF-5) to translocate to the nucleus and promote reproductive, non-dauer growth (64).

3. Insulin-like pathway: Like in mammals, the C. elegans insulin/insulin-like growth-factor 1 (IGF-1) signaling (IIS) pathway bridges nutritional state to development, metabolism, and longevity (i.e., aging) (65). Although the C. elegans genome encodes only one ortholog of the insulin/IGF receptor (IGFR), DAF-2, (66), the

same genome contains at least 40 genes predicted through genetic and bioinformatics to encode insulin-like peptides (ILPs). While many of these ILPs diverge biochemically from human insulin (67), the ILP INS-6 has been demonstrated to bind the human insulin receptor at high affinity despite lacking a C peptide that is highly conserved in vertebrate insulin (68). Activation of DAF-2/IGFR triggers a signal transduction cascade involving numerous kinases and phosphoinositide signaling that ultimately control the subcellular localization of the DAF-16/FoxO transcription factor (65). daf-2 loss-of-function mutants are Daf-C (66), while daf-16 loss-of-function mutants do not enter dauer even under unfavorable conditions and are therefore termed dauer-formation abnormal – defective (Daf-D). Genetic analyses indicate DAF-16 to be the culminating transcription factor in the insulin-like pathway when it comes to dauer formation (39, 65), resulting in a model whereby in the absence of insulin-like pathway activity, DAF-16/FoxO translocates to the nucleus (69) where it promotes reproductive development and/or inhibits dauer development.

4. Steroid hormone pathway: A steroid hormone pathway centered on the nuclear hormone receptor DAF-12/NHR has been shown to be genetically downstream of most elements of the cGMP, TGF-β-like, and insulin-like signaling pathways described above (39). As neuroendocrine signals, steroid hormones facilitate organism-wide developmental decisions by relaying information from sensory processing centers to the rest of the organism. Indeed, steroid hormones regulate virtually all of the polyphenisms described earlier in section 1.1 (3, 4, 70). DAF-12 shows homology to vertebrate vitamin D receptors and thyroid hormone receptors (71). Hormonal regulation of DAF-12 occurs via binding of bile acid-like steroids called Δ4- and Δ7-dafachronic acid (DA), whose syntheses requires the cytochrome P450 DAF-9/CYP450 (72). DAF-12 assembles with different coregulators in a ligand-dependent manner to regulate genes related to development, gonadal maturation, longevity, and fat metabolism (73). daf-9 loss-of-function mutants are Daf-C, but they arrest as “partial dauers” under favorable growth conditions in that

they exhibit some non-dauer morphological and behavioral properties (74). Loss-of-function mutants for daf-12 are Daf-D, indicating that steroid hormones, whose production is catalyzed by DAF-9, antagonize DAF-12 function (74). Absence of ligand binding causes DAF-12 to associate with DIN-1/CoR, a homolog of mammalian SHARP corepressor, and promote dauer development (75). On the other hand, the ligand binding of Dafachronic Acids causes DAF-12 to disassociate DIN-1/CoR, resulting in reproductive growth.

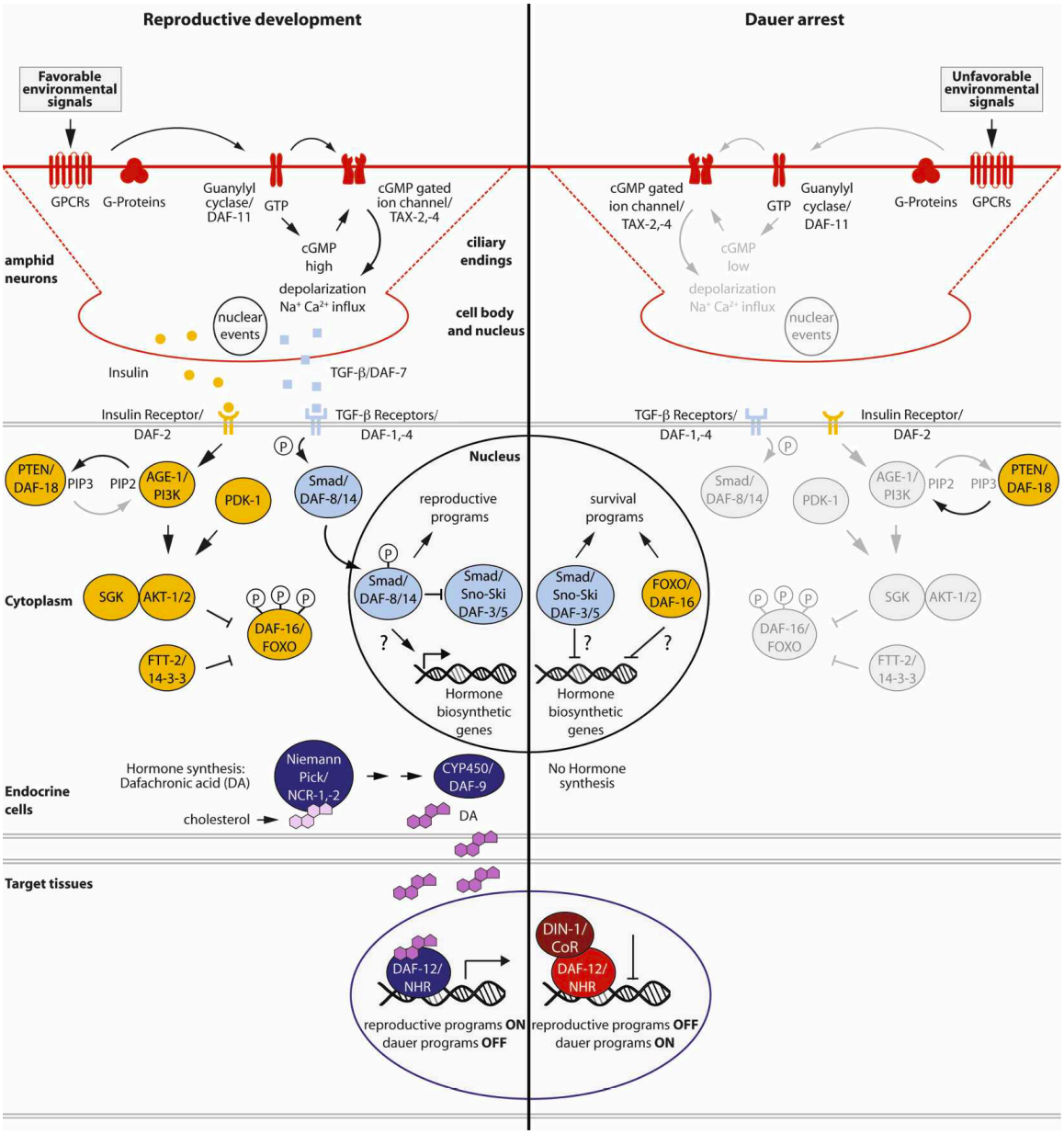

Figure 1.2. Genetic pathways controlling the dauer entry decision

Unmodified figure taken from Fielenbach and Antebi, 2008. Shown are the active (opaque) and inactive (greyed out) signal transduction components during the dauer entry decision (and by extension, likely applies to dauer exit decision as well) to enter reproductive growth (left half) or dauer development (right half). See main text for descriptions of individual genetic pathways. Pathways are color-coded red for the cGMP pathway, light blue for the TGF-beta-like pathway, yellow for the insulin-like pathway, and dark blue and dark red for the steroid hormone pathway.

The C. elegans dauer decision-making process has been studied for over 50 years, making it one of the most well-characterized phenomena in nematodes and perhaps even in animal biology. And yet, despite our wealth of knowledge concerning the genetic components and signaling mechanisms that underlie the dauer entry and exit decisions, many fundamental questions remain unanswered. In the next section, I highlight important outstanding questions that pertain to the dauer entry and exit decisions and then provide an overview of how this thesis addresses those questions.

1.3 How this thesis addresses longstanding questions pertaining to the dauer entry and exit developmental decisions

There exist thousands of papers pertaining to the C. elegans dauer entry and exit decisions, and yet there are numerous outstanding questions, many of which are foundational to understanding how C. elegans calculate the dauer entry and exit decisions. The bulk of previous studies also tend to skew towards genetic analyses (i.e., identifying individual genetic components and analyzing genetic pathways) and focus more on dauer entry than dauer exit, resulting in numerous gaps in our knowledge. Herein, I discuss a number of important questions in the dauer field that, despite over half a century of study, remain to be adequately addressed.

How do neurons perceive sensory signals and convey that information to downstream tissues? In 1991, Cori Bargmann and Bob Horvitz demonstrated the crucial role that C. elegans chemosensory neurons play in mediating the dauer entry and exit decisions (76). Laser ablation of specific neurons in isolation and/or in combination resulted in abnormal rates of dauer entry and exit compared to wild type. And while studies since then have offered clues as to how these chemosensory neurons partake in the dauer decision-making process (62, 77–81), we still lack a clear understanding of how these neurons perceive environmental cues, communicate with each other, and propagate that information into the various signaling pathways mentioned in Section 1.2. In particular, studies have often treated C. elegans neurons as traditional cell types, neglecting to consider how their neuron-specific properties (such as specialized morphologies, ion channels, and signal transduction mechanisms) are involved in computation of the dauer entry and exit decisions.

In Chapter Two of this thesis, I describe how the chemosensory neuron ASJ mediates the sensory integration process during the dauer exit decision at both the levels of intracellular calcium dynamics as well as gene expression. I demonstrate how the insulin-like peptide INS-6, a signaling molecule associated with the insulin-like pathway, contributes to the dauer exit decision-making process. I analyze the relationships among neuronal activity, ins-6 expression, and signal transduction pathways including cGMP signaling to elucidate a model of how dauers upregulate ins-6 expression after being moved to favorable conditions to promote exit from the dauer state.

What are the key similarities and differences between dauer entry and dauer exit? The vast majority of studies concerning dauer in C. elegans pertains to the dauer entry decision, while only a handful of studies specifically examine dauer exit. While early genetic evidence suggested that the genetic pathways underlying both are similar, recent studies have highlighted key differences. For example, ablation studies using a laser microbeam showed that the chemosensory neurons ASI, ASG, and ADF promote reproductive growth during the dauer entry decision specifically, while the chemosensory neuron ASJ promotes reproductive growth during the dauer exit decision specifically (76). In another example,

studies have shown that even though both the insulin-like peptides DAF-28 and INS-6 promote reproductive growth over dauer in both the entry and exit decisions, DAF-28 plays a more critical during dauer entry, while INS-6 plays a more critical role during dauer exit (82, 83). As a final example, mutants defective for the genes daf-6 or daf-10, which bear structural abnormalities in sensory neurons that impair their ability to sense external stimuli, are defective for their ability to enter dauer and exit dauer (84). In other words, these mutants possess an asymmetrical dauer phenotype: they have a Daf-C phenotype in the dauer entry decision and a Daf-D phenotype in the dauer exit decision. Such asymmetry indicates that the daf-6- and daf-10-dependent sensory processing mechanisms affect the dauer entry and exit decisions in different ways.

Therefore, while the same genetic pathways (e.g., cGMP, TGF-β-like, and insulin-like signaling pathways) may control both the dauer entry and exit decisions, the precise manner through which these genetic pathways function might differ between the two decisions. Such differences might include disparate sensory neurons providing input to those pathways, differential importance of signaling molecules, and differential timing and kinetics of pathway dynamics. In Chapter Three of this thesis, I examine how the DAF-12-dependent steroid hormone pathway (the fourth pathway described in Section 1.2) regulates the dauer exit decision while emphasizing how such regulation differs between the dauer entry and exit decisions. I describe how the steroid hormone pathway promotes reproductive growth during the dauer exit decision and that the spatiotemporal dynamics of steroid hormone production resembles the L2d to L3 subdecision made during dauer entry.

What is the nature of the partial dauer? When grown under favorable, non-dauer-inducing conditions, both daf-9 loss-of-function mutants and specific daf-12 mutants that bear mutations in the DAF-12 ligand binding domain form “partial dauers”. Compared to classical dauers or “full dauers,” partial dauers are radially thicker, have a paler body, and pump their pharynxes occasionally (85). It remains a puzzle as to what these partial dauers are and whether they can provide any meaningful insight into the dauer entry and/or exit

decisions. In Chapter Three of this thesis, I present data to suggest that these daf-9 loss-of-function partial dauers are actually dauers that have partially begun dauer exit. In other words, I argue that these partial dauers are partially exited dauers. These findings collectively suggest that dauer exit can be broken up into at least two phases: an initial phase that is independent of daf-9 dependent steroid hormones and results in distinct morphological and behavioral characteristics such as a wider, paler body and increased motility and pumping frequency, followed by a second phase that is daf-9 dependent and results in the completion of dauer exit including further somatic and gonadal development that results in formation of post-dauer L4 larvae.

Concluding remarks: Despite decades of research on the dauer entry and exit decisions, the field of dauer biology still boasts myriad questions whose answers are instrumental in fully elucidating these complex developmental decisions. The findings I present in the next two chapters enrich our understanding of dauer biology, particularly the dauer exit decision, and bring us closer to deciphering the intricate computations performed by C. elegans while making critical life cycle decisions.

1.4 References

1. T. Flatt, G. V. Amdam, T. B. L. Kirkwood, S. W. Omholt, Life-history evolution and the polyphenic regulation of somatic maintenance and survival. Q. Rev. Biol. 88, 185–218 (2013).

2. C.-H. Yang, J. A. Pospisilik, Polyphenism – A window into gene-environment interactions and phenotypic plasticity. Front. Genet. 10, 132 (2019).

3. D. L. Denlinger, G. D. Yocum, J. P. Rinehart, "Hormonal control of diapause" in Insect Endocrinology, (Elsevier, 2012), pp. 430–463.

4. X. Karp, Hormonal Regulation of Diapause and Development in Nematodes, Insects, and Fishes. Front. Ecol. Evol. 9 (2021).

5. J. A. Bluestone, J. A. Bluestone, Cell fate in the immune system; decisions, decisions, decisions. Immunol. Rev. 165, 5–12 (1998).

6. D. Hochbaum et al., DAF-12 Regulates a Connected Network of Genes to Ensure Robust Developmental Decisions. PLOS Genet. 7, e1002179 (2011).

7. W. L. Hung, Y. Wang, J. Chitturi, M. Zhen, A Caenorhabditis elegans developmental decision requires insulin signaling-mediated neuron-intestine communication. Development 141, 1767–1779 (2014).

8. T. Som, V. S. R. Kolaparthi, Developmental decisions in Aspergillus nidulans Are Modulated by Ras Activity. Mol. Cell. Biol. 14, 5333–5348 (1994).

9. L. Strmecki, D. M. Greene, C. J. Pears, Developmental decisions in Dictyostelium discoideum. Dev. Biol. 284, 25–36 (2005).

10. R. Shinya et al., Possible stochastic sex determination in Bursaphelenchus nematodes. Nat. Commun. 13, 2574 (2022).

11. A. Cumano et al., New molecular insights into immune cell development. Annu. Rev. Immunol. 37, 497–519 (2019).

12. M. Huang, C. M. Hull, Sporulation: How to survive on planet Earth (and beyond). Curr. Genet. 63, 831–838 (2017).

13. T. T. Wyatt, H. A. B. Wösten, J. Dijksterhuis, "Chapter Two - Fungal spores for dispersion in space and time" in Advances in Applied Microbiology, S. Sariaslani, G. M. Gadd, Eds. (Academic Press, 2013), pp. 43–91.

14. J. P. Wourms, The developmental biology of annual fishes. III. Pre-embryonic and embryonic diapause of variable duration in the eggs of annual fishes. J. Exp. Zool. 182, 389–414 (1972).

15. T. Miura, Developmental regulation of caste-specific characters in social-insect polyphenism. Evol. Dev. 7, 122–129 (2005).

16. E. Hasegawa, The optimal caste ratio in polymorphic ants: Estimation and Empirical Evidence. Am. Nat. 149, 706–722 (1997).

17. H. Shibao, M. Kutsukake, S. Matsuyama, T. Fukatsu, M. Shimada, Mechanisms regulating caste differentiation in an aphid social system. Commun. Integr. Biol. 3, 1–5 (2010).

18. J. Korb, S. Katrantzis, Influence of environmental conditions on the expression of the sexual dispersal phenotype in a lower termite: implications for the evolution of workers in termites. Evol. Dev. 6, 342–352 (2004).

19. L. Schiesari, M. B. O'Connor, "Chapter Eight - Diapause: delaying the developmental clock in response to a changing environment" in Current Topics in Developmental Biology, Developmental Timing., A. E. Rougvie, M. B. O'Connor, Eds. (Academic Press, 2013), pp. 213–246.

20. J. Grinsted, B. Avery, A sporadic case of delayed implantation after in-vitro fertilization in the human? Hum. Reprod. 11, 651–654 (1996).

21. G. E. Ptak, J. A. Modlinski, P. Loi, Embryonic diapause in humans: time to consider? Reprod. Biol. Endocrinol. RBE 11, 92 (2013).

22. J. J. Tarín, A. Cano, Do human concepti have the potential to enter into diapause? Hum. Reprod. 14, 2434–2436 (1999).

23. E. C. Walvoord, The timing of puberty: is it changing? Does it matter? J. Adolesc. Health 47, 433–439 (2010).

24. A. Agorastos, G. P. Chrousos, The neuroendocrinology of stress: the stress-related continuum of chronic disease development. Mol. Psychiatry 27, 502–513 (2022).

25. T.-Y. Zhang, C. Parent, I. Weaver, M. J. Meaney, Maternal Programming of individual differences in defensive responses in the rat. Ann. N. Y. Acad. Sci. 1032, 85–103 (2004).

26. S. Brenner, The genetics of Caenorhabditis elegans. Genetics 77, 71–94 (1974).

27. A. K. Corsi, B. Wightman, M. Chalfie, "A Transparent window into biology: A primer on Caenorhabditis elegans" in WormBook: The Online Review of C. Elegans Biology [Internet], (WormBook, 2018).

28. T. Evans, Transformation and microinjection. WormBook (2006). https://doi.org/10.1895/wormbook.1.108.1.

29. C. Frøkjær-Jensen, M. W. Davis, M. Ailion, E. M. Jorgensen, Improved Mos1 -mediated transgenesis in C. elegans. Nat. Methods 9, 117–118 (2012).

30. L. M. Kutscher, S. Shaham, Forward and reverse mutagenesis in C. elegans. WormBook Online Rev. C Elegans Biol. 1–26 (2014). https://doi.org/10.1895/wormbook.1.167.1.

31. J. D. Ward, Rapid and precise engineering of the Caenorhabditis elegans genome with lethal mutation co-conversion and inactivation of NHEJ Repair. Genetics 199, 363–377 (2015).

32. N. Pokala, Q. Liu, A. Gordus, C. I. Bargmann, Inducible and titratable silencing of Caenorhabditis elegans neurons in vivo with histamine-gated chloride channels. Proc. Natl. Acad. Sci. 111, 2770–2775 (2014).

33. C. Schmitt, C. Schultheis, S. J. Husson, J. F. Liewald, A. Gottschalk, Specific expression of channelrhodopsin-2 in single neurons of Caenorhabditis elegans. PLOS ONE 7, e43164 (2012).

34. C. Schultheis, J. F. Liewald, E. Bamberg, G. Nagel, A. Gottschalk, Optogenetic long-term manipulation of behavior and animal development. PLOS ONE 6, e18766 (2011).

35. J. G. White, E. Southgate, J. N. Thomson, S. Brenner, The structure of the nervous system of the nematode Caenorhabditis elegans. Philos. Trans. R. Soc. Lond. B. Biol. Sci. 314, 1–340 (1986).

36. A. C. Hart, “Behavior” in WormBook: The Online Review of C. Elegans Biology [Internet], (WormBook, 2006).

37. C. I. Bargmann, Beyond the connectome: How neuromodulators shape neural circuits. BioEssays 34, 458–465 (2012).

38. R. C. Cassada, R. L. Russell, The dauerlarva, a post-embryonic developmental variant of the nematode Caenorhabditis elegans. Dev. Biol. 46, 326–342 (1975).

39. P. J. Hu, Dauer. WormBook (2007). https://doi.org/10.1895/wormbook.1.144.1.

40. J. W. Golden, D. L. Riddle, The Caenorhabditis elegans dauer larva: Developmental effects of pheromone, food, and temperature. Dev. Biol. 102, 368–378 (1984).

41. S. E. Hall, M. Beverly, C. Russ, C. Nusbaum, P. Sengupta, A cellular memory of developmental history generates phenotypic diversity in C. elegans. Curr. Biol. 20, 149–155 (2010).

42. P.-Y. Shih, J. S. Lee, P. W. Sternberg, Genetic markers enable the verification and manipulation of the dauer entry decision. Dev. Biol. (2019). https://doi.org/10.1016/j.ydbio.2019.06.009.

43. A. Barrière, M.-A. Félix, Isolation of C. elegans and related nematodes. WormBook Online Rev. C Elegans Biol. 1–19 (2014). https://doi.org/10.1895/wormbook.1.115.2.

44. H. Schulenburg, M.-A. Félix, The Natural biotic environment of Caenorhabditis elegans. Genetics 206, 55–86 (2017).

45. J. W. Golden, D. L. Riddle, A pheromone influences larval development in the nematode Caenorhabditis elegans. Science 218, 578–580 (1982).

46. Y.-C. Chen, M. R. Seyedsayamdost, N. Ringstad, A microbial metabolite synergizes with endogenous serotonin to trigger C. elegans reproductive behavior. Proc. Natl. Acad. Sci. 117, 30589–30598 (2020).

47. T. K. Kaul, P. R. Rodrigues, I. V. Ogungbe, P. Kapahi, M. S. Gill, Bacterial fatty acids enhance recovery from the dauer larva in Caenorhabditis elegans. PLOS ONE 9, e86979 (2014).

48. S. H. Chalasani et al., Dissecting a circuit for olfactory behaviour in Caenorhabditis elegans. Nature 450, 63–70 (2007).

49. S. E. Worthy et al., Identification of attractive odorants released by preferred bacterial food found in the natural habitats of C. elegans. PLOS ONE 13, e0201158 (2018).

50. L. R. Baugh, To grow or not to grow: Nutritional control of development during Caenorhabditis elegans L1 arrest. Genetics 194, 539–555 (2013).

51. A. H. Ludewig, F. C. Schroeder, “Ascaroside signaling in C. elegans” in WormBook: The Online Review of C. Elegans Biology [Internet], (WormBook, 2018).

52. F. Kaplan et al., Ascaroside expression in Caenorhabditis elegans is strongly dependent on diet and developmental stage. PLoS ONE 6, e17804 (2011).

53. M. Ailion, J. H. Thomas, Dauer formation induced by high temperatures in Caenorhabditis elegans. Genetics 156, 1047–1067 (2000).

54. J. W. Golden, D. L. Riddle, A pheromone-induced developmental switch in Caenorhabditis elegans: Temperature-sensitive mutants reveal a wild-type temperature-dependent process. Proc. Natl. Acad. Sci. 81, 819–823 (1984).

55. D. A. Birnby et al., A transmembrane guanylyl cyclase (DAF-11) and Hsp90 (DAF-21) regulate a common set of chemosensory behaviors in Caenorhabditis elegans. Genetics 155, 85–104 (2000).

56. C. M. Coburn, I. Mori, Y. Ohshima, C. I. Bargmann, A cyclic nucleotide-gated channel inhibits sensory axon outgrowth in larval and adult Caenorhabditis elegans: a distinct pathway for maintenance of sensory axon structure. Development 125, 249–258 (1998).

57. C. M. Coburn, C. I. Bargmann, A Putative cyclic nucleotide–gated channel Is required for sensory development and function in C. elegans. Neuron 17, 695–706 (1996).

58. T. Hirose et al., Cyclic GMP-dependent protein kinase EGL-4 controls body size and lifespan in C. elegans. Development 130, 1089–1099 (2003).

59. N. D. L'Etoile et al., The cyclic GMP-dependent protein kinase EGL-4 regulates olfactory adaptation in C. elegans. Neuron 36, 1079–1089 (2002).

60. C. I. Bargmann, "Chemosensation in C. elegans" in WormBook: The Online Review of C. Elegans Biology [Internet], (WormBook, 2006).

61. Y. Shi, J. Massagué, Mechanisms of TGF-β signaling from cell Membrane to the nucleus. Cell 113, 685–700 (2003).

62. P. Ren et al., Control of C. elegans larval development by neuronal expression of a TGF-β homolog. Science (1996). https://doi.org/10.1126/science.274.5291.1389.

63. T. L. Gumienny, C. Savage-Dunn, "TGF-β signaling in C. elegans" in WormBook: The Online Review of C. Elegans Biology [Internet], (WormBook, 2018).

64. L. S. da Graca et al., DAF-5 is a Ski oncoprotein homolog that functions in a neuronal TGFβpathway to regulate C. elegans dauer development. Development 131, 435–446 (2004).

65. C. T. Murphy, P. J. Hu, "Insulin/insulin-like growth factor signaling in C. elegans" in WormBook: The Online Review of C. Elegans Biology [Internet], (WormBook, 2018).

66. K. D. Kimura, H. A. Tissenbaum, Y. Liu, G. Ruvkun, daf-2, an insulin receptor-like gene that regulates longevity and diapause in Caenorhabditis elegans. Science 277, 942–946 (1997).

67. S. B. Pierce et al., Regulation of DAF-2 receptor signaling by human insulin and ins-1, a member of the unusually large and diverse C. elegans insulin gene family. Genes Dev. 15, 672–686 (2001).

68. Q. Hua et al., A divergent INS protein in Caenorhabditis elegans structurally resembles human insulin and activates the human insulin receptor. Genes Dev. 17, 826–831 (2003).

69. K. Lin, H. Hsin, N. Libina, C. Kenyon, Regulation of the Caenorhabditis elegans longevity protein DAF-16 by insulin/IGF-1 and germline signaling. Nat. Genet. 28, 139–145 (2001).

70. S. C. Hand, D. L. Denlinger, J. E. Podrabsky, R. Roy, Mechanisms of animal diapause: recent developments from nematodes, crustaceans, insects, and fish. Am. J. Physiol.-Regul. Integr. Comp. Physiol. 310, R1193–R1211 (2016).

71. A. Antebi, W.-H. Yeh, D. Tait, E. M. Hedgecock, D. L. Riddle, daf-12 encodes a nuclear receptor that regulates the dauer diapause and developmental age in C. elegans. Genes Dev. 14, 1512–1527 (2000).

72. D. L. Motola et al., Identification of ligands for DAF-12 that govern dauer formation and reproduction in C. elegans. Cell 124, 1209–1223 (2006).

73. N. Fielenbach, A. Antebi, C. elegans dauer formation and the molecular basis of plasticity. Genes Dev. 22, 2149–2165 (2008).

74. B. Gerisch, C. Weitzel, C. Kober-Eisermann, V. Rottiers, A. Antebi, A hormonal signaling pathway influencing C. elegans metabolism, reproductive development, and life span. Dev. Cell 1, 841–851 (2001).

75. A. H. Ludewig, A novel nuclear receptor/coregulator complex controls C. elegans lipid metabolism, larval development, and aging. Genes Dev. 18, 2120–2133 (2004).

76. C. I. Bargmann, H. R. Horvitz, Control of larval development by chemosensory neurons in Caenorhabditis elegans. Science 251, 1243–1246 (1991).

77. C. M. Chai et al., Interneuron control of C. elegans developmental decision-making. Curr. Biol. 32, 2316-2324.e4 (2022).

78. S. H. Chung, A. Schmalz, R. C. H. Ruiz, C. V. Gabel, E. Mazur, Femtosecond laser ablation reveals antagonistic sensory and neuroendocrine signaling that underlie C. elegans behavior and development. Cell Rep. 4, 316–326 (2013).

79. K. Kim et al., Two chemoreceptors mediate developmental effects of dauer pheromone in C. elegans. Science 326, 994–998 (2009).

80. J. Ouellet, S. Li, R. Roy, Notch signalling is required for both dauer maintenance and recovery in C. elegans. Development 135, 2583–2592 (2008).

81. W. S. Schackwitz, T. Inoue, J. H. Thomas, Chemosensory neurons function in parallel to mediate a pheromone response in C. elegans. Neuron 17, 719–728 (1996).

82. A. Cornils, M. Gloeck, Z. Chen, Y. Zhang, J. Alcedo, Specific insulin-like peptides encode sensory information to regulate distinct developmental processes. Development 138, 1183–1193 (2011).

83. D. A. Fernandes de Abreu, et al., An insulin-to-insulin regulatory network orchestrates phenotypic specificity in development and physiology. PLoS Genet. 10, e1004225 (2014).

84. P. S. Albert, S. J. Brown, D. L. Riddle, Sensory control of dauer larva formation in Caenorhabditis elegans. J. Comp. Neurol. 198, 435–451 (1981).

85. B. Gerisch, A. Antebi, Hormonal signals produced by DAF-9/cytochrome P450 regulate C. elegans dauer diapause in response to environmental cues. Development 131, 1765–1776 (2004).

Chapter 2

Sensory integration of food availability and population density during the diapause exit decision involves insulin-like signaling in C. elegans

M.G. Zhang, M. Seyedolmohadesin, S. Mercado, H. Park, N. Finnen, F. Schroeder, V. Venkatachalam, P.W. Sternberg, Sensory integration of food availability and population density during the diapause exit decision involves insulin-like signaling in Caenorhabditis elegans. bioRxiv (2024). http://doi.org/10.1101/2024.03.20.586022

2.1 Abstract

Decisions made over long time scales, such as life cycle decisions, require coordinated interplay between sensory perception and sustained gene expression. The Caenorhabditis elegans dauer (or diapause) exit developmental decision requires sensory integration of population density and food availability to induce an all-or-nothing organismal-wide response, but the mechanism by which this occurs remains unknown. Here, we demonstrate how the ASJ chemosensory neurons, known to be critical for dauer exit, perform sensory integration at both the levels of gene expression and calcium activity. In response to favorable conditions, dauers rapidly produce and secrete the dauer exit-promoting insulin-like peptide INS-6. Expression of ins-6 in the ASJ neurons integrate population density and food level and can reflect decision commitment since dauers committed to exiting have higher ins-6 expression levels than those of non-committed dauers. Calcium imaging in dauers reveals that the ASJ neurons are activated by food, and this activity is suppressed by pheromone, indicating that sensory integration also occurs at the level of calcium transients. We find that ins-6 expression in the ASJ neurons depends on neuronal activity in the ASJs, cGMP signaling, a CaM-kinase pathway, and the pheromone components ascr#8 and ascr#2. We propose a model in which decision commitment to exit the dauer state involves an autoregulatory feedback loop in the ASJ neurons that promotes high INS-6 production and secretion. These results collectively demonstrate how insulin-like peptide signaling helps animals compute long-term decisions by bridging sensory perception to decision execution.

2.2 Introduction

A fundamental goal of neuroscience is to understand how nervous systems sense, integrate, and interpret diverse stimuli to deliver the appropriate output. The duration over which these processes occur spans from shorter timescales, such as during reflexive responses to harsh stimuli or chemotaxis towards attractive stimuli (1–5), to longer timescales, such as migration or hibernation decisions in response to changing weather patterns, temperature, and food availability (6–9). We lack a clear understanding of how neuronal activity, which occurs over short timescales of milliseconds to seconds, informs downstream processes

that occur over timescales of hours or longer. One such decision that takes place over a longer timescale is the developmental decision to enter (or exit) diapause, a temporarily suspended developmental state that protects against environmental stress and promotes dispersal. Diapause is evolutionarily conserved across metazoans and requires integration of environmental cues to inform a coordinated, organismal-wide decision (10–12)

To better understand how a compact nervous system can interpret sensory signals to coordinate a organismal-wide decision that takes place over multiple hours, we studied the dauer exit decision. During early larval growth, C. elegans choose between two developmental fates depending on environmental conditions (Fig. 2.1A). Under favorable conditions, larvae undergo reproductive growth, whereas under unfavorable conditions, larvae enter the stress-resistant, long-lived developmentally arrested diapause state known as dauer (13–15). While in the dauer state, C. elegans continually assess their surroundings to detect environmental improvement; when conditions sufficiently improve, animals exit the dauer state and return to the reproductive cycle as late-stage larvae. Of the various environmental inputs to the dauer entry and exit decisions, the strongest input is a ratio of food to pheromone (14). Here, “pheromone” refers to a mixture of secreted dauer-regulating signaling molecules, termed ascarosides, that collectively convey population density (16, 17).

The genetic pathways and neuroendocrine signaling mechanisms that govern the dauer entry and exit decisions (18–20) including a cGMP pathway, a TGF-β-like pathway, an insulin/insulin-like growth factor (IGF)-1 signaling (IIS) pathway, and a steroid hormone pathway. While considerably more attention has been paid towards the dauer entry decision, previous studies identified two insulin-like peptides, INS-6 and DAF-28, as regulators of dauer exit that work within the IIS pathway (21, 22).

Despite the wealth of knowledge collected on the C. elegans dauer entry and exit decisions, many fundamental questions remain, including: (1) How does sensory integration of food, pheromone, and temperature (amongst other possible cues) occur? (2) How does short-

term perception of environmental cues translate into the dauer decisions which take place over the course of hours? To address these questions, we studied the dauer exit decision using genetic and molecular neurobiological approaches. Using an ethologically relevant, pheromone-based assay, we demonstrate an essential role for neuropeptide signaling as a whole in dauer exit and validate INS-6 as important for dauer exit.

To understand how INS-6 production relates to sensory perception, we analyzed the spatiotemporal dynamics of ins-6 expression in response to different environmental cues and found that ins-6 expression in a pair of chemosensory neurons, the Amphid Single Cilium J (ASJ) neurons, reflects both food and pheromone levels during dauer exit. We found that high ins-6 expression in the ASJ neurons reflects commitment to exit the dauer state. Through calcium imaging in dauers, we show that sensory integration of food and pheromone can also be seen at the level of sensory neuron activity: ASJ calcium levels increase in response to food, but this response can be suppressed by adding pheromone. We find that ins-6 upregulation during dauer exit depends on ASJ neuronal activity, cGMP signaling, a CaM-kinase pathway, and is inhibited most potently by the pheromone component ascr#8. Altogether, our data show how the ASJ neurons integrate food and pheromone levels both in the short-term through calcium transients and in the longer term through transcription of ins-6, thereby highlighting how neuropeptides can provide the bridge from ephemeral sensory information to sustained physiological changes.

2.3 Results

A screen of ASJ-enriched neuropeptide genes validates ins-6 as critical for dauer exit

Neuronal ablation methods using a laser microbeam or transgenic caspases have shown that the chemosensory ASJ neurons are important for dauer exit (21, 23, 24), but the precise molecular mechanism by which the ASJ neurons promote dauer exit remains unclear. Having previously shown that neuropeptides are collectively required for dauer entry (25), we reasoned that neuropeptides could also be involved in dauer exit. Using a pheromone based dauer exit assay (Fig. 2.1B), we tested five mutants defective in neuropeptide synthesis or secretion and found that four out of the five loss-of-function mutants

(sbt-1/7BT, egl-3/PC2, egl-21/CPE, and unc-31/CAPS) had significantly lower dauer exit rates than that of wild-type (Fig. 2.1C), strongly indicating that neuropeptide signaling is required for exit. By contrast, ric-7 loss-of-function mutants, which are impaired for dense core vesicle secretion (26), exited dauer at rates higher than that of wild-type, suggesting that RIC-7 may impair the secretion of different neuropeptides than those affected by the other four mutants.

We hypothesized that the ASJ neurons may utilize neuropeptides to promote dauer exit and tested this by screening for defects in dauer exit rates in mutants lacking ASJ-enriched neuropeptides. We analyzed loss-of-function mutants for eleven insulin-like peptide genes, two neuropeptide-like peptide genes, and two FMRF-amide-like peptide genes that were predicted to be enriched in ASJ based on single-cell RNA-sequencing data (27) (Fig. 2.1D, Fig. S2.1A). Of the fifteen genes tested, ins-6 mutants showed the most severe dauer exit defect as they exited dauer at the lowest rates compared to wild type. ins-32 mutants showed a modest dauer exit defect, while mutants defective for ins-26, nlp-80, flp-15, or flp-34 showed higher than wild-type dauer exit rates, suggesting that the neuropeptides those genes encode may inhibit dauer exit.

ins-6 transcription and INS-6 secretion increase quickly during dauer exit

We focused on characterizing the expression pattern of ins-6 because it showed the most severe impairment in dauer exit of the neuropeptide genes we tested. To characterize how ins-6 expression responds to environmental improvement during dauer exit, we analyzed ins-6 transcription and INS-6 secretion using genomically integrated fluorescence reporters that were simultaneously integrated into the same strain (Fig. 2.2A; Table S2.1). To measure ins-6 transcription, we constructed ins-6p::destabilized-YFP (dYFP), a transcriptional reporter based off a previous design (21) that fuses both upstream and downstream regulatory regions of ins-6 to dYFP, a modified YFP variant with a shorter half-life which provides higher temporal resolution (28), and measured fluorescence intensity in head neurons. To measure INS-6 secretion, we constructed ins-6::mCherry, a translational reporter that uses the ins-6 promoter to drive expression of a fusion between

the INS-6 propeptide and mCherry, a protein whose secretion can be tracked using a coelomocyte uptake assay (29) in which fluorescence intensity within the coelomocytes reflects the amount of neuropeptide secreted into the body cavity. We built a strain containing simultaneously integrated copies of both these reporters (see Table S2.1) and concurrently measured YFP signal in head neurons and mCherry signal in coelomocytes (Fig. 2.2B).

ins-6 transcriptional reporter activity in the ASJ neurons of dauers increased in just one hour after transfer of dauers to favorable conditions (Fig. 2.2C) and continued to increase for multiple hours thereafter (Fig. 2.2C, F). ins-6 transcriptional reporter activity also increased in the ASI chemosensory neurons albeit at a slower rate and to a lower maximum relative to the ASJ neurons (Fig. 2.2D, G). To validate these results, we performed fluorescence in-situ hybridization (FISH) for ins-6 mRNA (Fig. S2.2I, J). Consistent with our fluorescence reporter results, our FISH data indicate that ins-6 transcripts increased just 1 hour after transfer and continued to increase afterwards. Concordant with results using our ins-6 transcriptional reporter, we observed that ins-6::mCherry translational reporter activity in the coelomocytes increased within the first hour following transfer to favorable conditions and continued to increase for multiple hours thereafter (Fig. 2.2E, H). Under reproductive growth conditions, which result in non-dauer adult development, our ins-6 transcriptional reporter showed no signal in ASJ throughout development (Fig. S2.2A). ins-6 transcriptional reporter activity in ASI (Fig. S2.2B) and translational reporter activity (Fig. S2.2C) in the coelomocytes peaked in L1 larvae and then decreased throughout development. These results suggest that favorable conditions cause increased ins-6 reporter activity specifically in the context of animals in the dauer state. In summary, the transfer of dauers to favorable conditions causes an increase in ins-6 transcription and INS-6 secretion that promotes dauer exit.

The observed increase in INS-6 secretion (as measured by mCherry signal in the coelomocytes) could result from an increase in ins-6 transcription, INS-6 processing, INS-6 packaging, and/or dense core vesicle release. To parse these different factors, we built a

translational reporter driven by a constitutively active ASJ-specific promoter, trx-1p::ins-6::mCherry, and again measured coelomocyte uptake of INS-6::mCherry (Fig. S2.2D). The mCherry signal in coelomocytes increased when dauers were transferred to favorable conditions in a manner similar to animals bearing the ins-6p::ins-6::mCherry reporter transgene (fold-change of 2.14x and 4.8x at "6 h.a.t." versus "Dauer" from two independent lines of the trx-1p::ins-6::mCherry reporter compared to 2.68x using the ins-6p::ins-6::mCherry translational reporter from Fig. 2.2H), suggesting that secretion of INS-6 is also controlled at the level of dense core vesicle release.

daf-28 expression patterns suggest a weaker role in dauer exit versus ins-6

The same studies that identified INS-6 as a major regulator of dauer exit also characterized DAF-28, another insulin-like peptide that promotes the reproductive growth trajectory during the dauer entry decision (30), as a weaker regulator of dauer exit (21, 22). Consistent with those observations, loss of daf-28 gene function did not result in a defect in dauer exit rates in an otherwise wild-type background but did enhance the dauer exit rate defect of ins-6 loss-of-function mutants (Fig. 2.1D, S2.1B). To understand how the spatiotemporal regulation of daf-28 compares with that of ins-6, we performed similar transgenic reporter experiments to study daf-28 (Fig. S2.2E-H).

A daf-28p::dYFP transcriptional reporter showed virtually no activity in the ASJ neurons (Fig. S2.2F) of dauers after being transferred to favorable conditions but did show slight activity increase in the ASI neurons (Fig. S2.2G). daf-28::mCherry translational reporter activity measured in the coelomocytes of dauers did not increase even 6 hours after transfer to favorable conditions (Fig. S2.2H), unlike the ins-6::mCherry translational reporter which increased over two-fold within the first 6 hours (compare with Fig. 2.2H). In contrast, relative to growth under dauer-inducing conditions, growth under non-dauer-inducing conditions resulted in strong daf-28p::dYFP transcriptional reporter activity in the ASI neurons (Fig. S2.2G), weaker activity in the ASJ neurons (Fig. S2.2F), and strong activity in the coelomocytes (Fig. S2.2H), with activity for both reporters peaking after animals reached adulthood. Collectively, our transgenic reporter lines for ins-6 and daf-28 show

inverse expression patterns: ins-6 transcriptional and translational reporter activity increase during dauer exit but less during reproductive growth, and vice versa for the daf-28 reporters. These findings align with both ours' and others' dauer exit assay results in which INS-6 plays a stronger role in regulating dauer exit than does DAF-28 (21, 22).

ins-6 expression reflects commitment in the dauer exit decision

ins-6 expression increases quickly in all dauers when they are transferred to strongly favorable conditions that stimulate 100% of dauers to exit, but what happens when conditions are more ambiguous such that only a fraction of dauers exit? We transferred dauers to a lower pheromone concentration that induces approximately half of dauers to exit (hereby referred to as "intermediate-pheromone conditions") and measured ins-6p::dYFP transcriptional reporter activity (Fig. 2.3A). At three hours after transfer, all worms showed a slight increase in ins-6p::dYFP signal, while at six hours after transfer and beyond, a clear bimodality of the population emerges: the worms that would eventually go on to exit dauer (as evidenced by a wider pharynx (Fig. 2.3B), which is a key morphological characteristic of dauer exit (31)), showed high ins-6 transcriptional dYFP reporter activity, whereas the worms that should remain as dauers showed a return to baseline levels of dYFP signal, resembling the level of signal seen in dauers.

To determine whether ins-6 expression could be used to distinguish dauers that are committed versus non-committed, we compared the time course of ins-6 expression with that of dauer exit commitment (Fig. 2.3C). To examine dauer commitment transferred dauers from high-pheromone, dauer-maintaining conditions to intermediate-pheromone conditions that permitted approximately half the animals to exit dauer, then after different amounts we transferred the animals back onto high pheromone conditions so that animals that had not committed to exiting dauer would be induced to remain as dauers (Fig. 2.3C, top); this protocol was analogous to previous work that established commitment to exiting dauer (13). Within three hours of exposure to intermediate-pheromone conditions, approximately half the animals that might exit dauer under such conditions committed to exiting dauer (18% committed, compared to a baseline of 42%), while roughly the total

pool of dauers that would eventually exit under intermediate-pheromone conditions committed within six hours (43%) (Fig. 2.3C). These observations indicate that while some dauers irreversibly commit in one hour following transfer to intermediate-pheromone conditions, other dauers can take between three to six hours to commit to the exit decision. This six hour mark matches the time point in our imaging experiments in which the clearest bimodality of both ins-6p::dYFP signal as well as pharynx width emerges (Fig. 2.3B), suggesting that such bimodality can reflect decision commitment.

The bimodality of the population in Fig. 2.3A at 6 hours after transfer led us to hypothesize that animals that cross a threshold of ins-6 expression are irreversibly committed to exiting the dauer state, meaning that they will exit even if transferred back onto unfavorable, high pheromone conditions. Conversely, we reasoned that animals that do not cross that threshold are less likely to exit dauer. To test this hypothesis, we performed a longitudinal imaging experiment wherein we measured ins-6 transcriptional reporter activity in the ASJ neurons of the same individual worms over time (Fig. 2.3D). We imaged dauers induced under high pheromone conditions, transferred these dauers to an intermediate pheromone concentration for six hours (to prompt a fraction of them to exit) and imaged them, returned these animals to high pheromone conditions, and imaged them 18 hours later.

The twenty-one dauers followed could be divided into three categories. Category A (n=3) animals showed a distinctly higher ins-6 transcriptional reporter activity (>1000 a.u.) than the rest. All three category A animals exited, and these animals had such high levels of ins-6 expression that even exposure to high pheromone for 18 hours did not noticeably downregulate ins-6 expression. Category B (n=3) animals showed medium levels of transcriptional reporter activity (600-800 a.u.). One out of three category B animals exited, suggesting that ins-6 expression in this range could still lead to either dauer or non-dauer outcomes depending on whether the high pheromone conditions could suppress the modest levels of ins-6 expression. The remaining animals fell into category C (n= 15) and showed low levels of transcriptional reporter activity (<400 a.u.). Only one out of 15 category C animals exited, and many category C animals also showed a slight increase in ins-6

transcriptional reporter activity that then returned to baseline after transfer to high pheromone conditions. These results suggest that dauers must cross a threshold of ins-6 expression to commit to exiting the dauer state, and that if this threshold is not reached, ins-6 expression can be downregulated back to low levels.

ins-6 expression reflects a food:pheromone ratio

Since ins-6 transcriptional reporter activity responded differently when dauers were transferred to no-pheromone versus intermediate-pheromone conditions (compare Fig. 2.2C to Fig. 2.3A), we asked if ins-6 expression responds to a food:pheromone ratio, the principal metric by which dauers decide to exit (14). Dauers bearing the ins-6 transcriptional reporter were transferred onto plates containing differing amounts of pheromone and of a food signal (Fig. 2.4A). We chose crude yeast extract as our food signal because of the following reasons: it promotes dauer exit in our pheromone-based assay (Fig. S2.3A), it is more easily incorporated into agar plates, and because yeast extract is the source material from which a purified food signal was derived in the original dauer exit studies demonstrating the importance of a food:pheromone ratio during dauer exit (14).

We found that ins-6 transcriptional reporter activity correlated positively with food:pheromone ratios (Fig. 2.4A), consistent with ins-6 being upregulated under favorable conditions during dauer exit. Using live OP50 instead of yeast extract was not more effective in increasing transcriptional reporter activity (Fig. S2.3B). To assess whether food or pheromone was the stronger input, we transferred dauers to plates containing either no pheromone or high amounts of pheromone and either no food signal or high amounts of food signal and analyzed ins-6 transcription and INS-6 secretion using our transcriptional and translational reporters, respectively (Fig. 2.4B). At high pheromone levels, both transcriptional and translational reporter activity remained low regardless of whether high yeast extract was present, indicating that pheromone can suppress the ability of food signal to increase INS-6 production and secretion.

Having determined that ins-6 is upregulated under conditions that promote dauer exit, we asked whether this upregulation happens early in the commitment to dauer exit (i.e., happens due to sensory perception of environmental improvement), or whether it might be an effect of the dauer exit process. To explore this possibility, we analyzed our ins-6 transcriptional and translational reporters in a daf-7 mutant background. These animals are defective for daf-7, which encodes a TGF-β-like growth factor and defines a parallel pathway relative to the insulin-like pathway to which ins-6 belongs (20, 32). These mutants constitutively form and remain dauers at 25 °C even under no-pheromone conditions. We repeated the experiment shown in Fig. 2.4B but kept the transferred worms at 25 °C in order to prevent dauer exit. Despite all animals remaining as dauers, these daf-7 mutants exhibited near-identical ins-6 regulation with regards to both transcription and secretion when compared to that in a wild-type background (Fig. 2.4C). INS-6 production and secretion is thus upregulated in response to a high food:pheromone ratio that promotes dauer exit, even in animals incapable of exiting dauer, and such upregulation is not simply a downstream effect of dauer exit.

Calcium imaging in dauers shows integration of food and pheromone in ASJ neurons

To evaluate how the ASJ neurons respond to food and pheromone, we monitored calcium dynamics in dauers expressing the genetically encoded calcium indicator GCaMP6s (33) in the ASJs (34). We exposed dauers to a food signal (the supernatant from an overnight culture of OP50 grown in LB), pheromone, or a combination of both (Fig. 2.5A, S2.5A). We found that the ASJ neurons were activated in response to food signal at both stimulus onset and slightly after stimulus offset. The ASJs did not respond to pheromone, but we observed that when the ASJs were exposed to a mixture of food signal and pheromone, the response looked nearly identical to the response to pheromone alone. This finding suggests that ASJ calcium levels integrate food and pheromone. Although the food signal we used differed between calcium and transcriptional reporter imaging experiments, we found that LB (which contains 0.5% w/v yeast extract) increased calcium levels in the ASJs of L4 larvae (Fig. S2.4C), consistent with yeast extract being an activator of ASJ neuronal activity.

Involvement of other neurons in regulating ins-6 expression within ASJ

We tested if the ins-6 regulation to food and pheromone signals in the ASJ neurons depends on signals received from other neurons by measuring ins-6 transcriptional reporter activity in unc-31/CAPS or unc-13 loss-of-function mutant backgrounds, which are considered defective for neuropeptide secretion and for neurotransmitter release, respectively (29, 35). While loss of unc-31 abrogated ins-6 upregulation (Fig. 2.5C), loss of unc-13 did not produce a noticeable effect (Fig. 2.5D), suggesting that neuropeptide signaling, but not fast-acting synaptic transmission, is essential for ins-6 upregulation. Using an ASJ-specific promoter to express unc-31 cDNA in the unc-31 mutant background partially rescued the low levels of ins-6 transcriptional reporter activity (Fig. 2.5C), implying positive autoregulation: each ASJ neuron might secrete a peptidergic signal to be received by itself or its bilateral partner to increase ins-6 expression. The lack of a full rescue in two of three independent lines suggests additional neurons may contribute to ins-6 upregulation by secreting neuropeptides in an unc-31-dependent manner. In support of an autoregulatory model, we performed calcium imaging in the ASJ neurons of unc-31mutants and found that the responses to food, pheromone, and a mixture of the two remained largely unchanged compared to that of wild type (Fig. 2.5B, S2.5B). Specifically, food signal increased calcium levels in the ASJs while pheromone suppressed the positive response to food signal. Collectively, these results imply that when it comes to calcium response, each ASJ neuron possesses the molecular machinery to process both food and pheromone signals and to integrate the two. In addition, the ASJs communicate within a circuit that feeds back to those same ASJs to increase ins-6 expression in response to food signals.

In accordance with ins-6 partaking in a feedback loop amongst ASJ neurons, we found that in daf-2 loss-of-function mutants, which are defective for the insulin/IGF-1 receptor (IGFR) ortholog DAF-2, ins-6 transcriptional upregulation was impaired (Fig. S2.4D). Transfer of daf-2 mutant dauers to no-pheromone conditions resulted in a small increase in ins-6 transcriptional reporter activity compared to that of wild-type dauers (compare Fig. S2.4D to Fig. 2.2C and 2.4B). This result is consistent with a model in which ins-6 regulation

depends on an autoregulatory mechanism that involves itself and/or other insulin-like peptides that can signal via DAF-2.

Activity dependence of ASJ on ins-6 upregulation

Given the correspondence between ASJ calcium levels and ins-6 expression when exposed to food and pheromone, we evaluated the relationship between neuronal activity and upregulation of ins-6 during dauer exit. To test whether ins-6 upregulation depends on neuronal activity, we chemogenetically silenced the ASJ neurons using cell-specific expression of a histamine-chloride gated channel (36) during dauer exit by transferring dauers to no-pheromone conditions with or without histamine and measuring ins-6 transcriptional reporter activity. We found that inhibiting ASJ activity severely repressed ins-6 upregulation (Fig. 2.5E), and that this effect occurs cell autonomously since, in a mosaic animal in which only one ASJ bears the HisCl transgene, only the non-transgenic ASJ showed an increased ins-6p::dYFP signal (Fig. 2.5F)

We also tested whether chemogenetic or optogenetic activation of ASJ could induce ins-6 expression even under high pheromone conditions (Fig. 2.5G, H). Optogenetic stimulation of ASJ via the red-shifted rhodopsin Chrimson (37) or capsaicin-induced chemogenetic stimulation of ASJ via the TRPV1 channel (38) both slightly increased ins-6 transcriptional reporter activity, but to a much lesser extent when compared to dauers transferred to favorable conditions (compare Fig. 2.5G, H with Fig. 2.2C, 2.4B). These loss- and gain-of-function experiments demonstrate that neuronal activity promotes ins-6 expression during dauer exit.

Molecular regulation of ins-6 in ASJ during dauer exit

We sought to characterize the molecular components responsible for ins-6 upregulation during dauer exit. Since cGMP functions as a messenger in a variety of ASJ-mediated behaviors including dauer development, pathogen avoidance, hydrotaxis, and phototaxis (39–43), we tested mutants defective for genes in the cGMP pathway. Mutations in daf-11 (encoding a transmembrane guanylyl cyclase), tax-2, or tax-4 (which encode subunits of a

cGMP-gated channel) (44, 45) all abrogated ins-6 transcriptional reporter activity in the ASJ neurons of dauers transferred to favorable conditions (Fig. 2.6A). We also tested the cGMP-dependent kinase EGL-4/PKG (46, 47) and found that egl-4(n479) loss-of-function mutants had significantly lower ins-6 transcriptional reporter activity in ASJ (Fig. 2.6A). Addition of the non-hydrolysable cGMP analog, pCPT-cGMP, increased ins-6 transcriptional reporter activity to high levels even in the presence of pheromone (Fig. 2.6B). Collectively, these results demonstrate that cGMP signaling is both necessary and sufficient for ins-6 upregulation during dauer exit.

To test the role of activity-dependent genes, we measured ins-6 transcriptional reporter activity in loss-of-function mutants for cmk-1, encoding the C. elegans homolog of calcium/calmodulin-dependent kinase CaMKI (48), and crh-1, encoding the C. elegans homolog of the CREB transcription factor (49). Both genes have been previously implicated in regulating expression of neuropeptide-encoding genes (43, 50, 51). While cmk-1 mutants displayed a substantial loss in ins-6 transcriptional reporter activity, crh-1 mutants showed only a small decrease in reporter activity (Fig. S2.5A). Thus CMK-1 may help transduce calcium influx into upregulation of ins-6 expression.

Dauer pheromone comprises multiple ascarosides (nematode-specific glycosides of the dideoxy sugar ascarylose) of which ascr#2, ascr#3, ascr#5, and ascr#8 are considered potent inducers of dauer entry (16, 17). To determine which ascaroside components of the dauer pheromone modulate ins-6 expression during dauer exit, we transferred dauers to plates supplemented with individual ascarosides at concentrations previously reported to induce dauer entry (52–54) (Fig. 2.6C). We found that ascr#8 most effectively suppressed ins-6p::dYFP expression, particularly at 1 μM, while ascr#2 mildly suppressed ins-6p::dYFP expression. ascr#3 and ascr#5 did not have a statistically significant effect at either 250 nM or 1 μM. Since ascr#8 most strongly suppressed ins-6 transcriptional reporter activity in dauers, we tested the GPCRs DMSR-12 and SRW-97, previously shown in C. elegans males to be involved in reception of ascr#8 in the context of attraction to hermaphrodites (55), for their roles in regulating ins-6 expression (Fig. 2.6D). A double

mutant defective for both dmsr-12 and srw-97 showed a wild-type ins-6 transcriptional reporter activity response to ascr#8, suggesting additional receptors may be responsible for ascr#8 response in the context of dauer exit.

2.4 Discussion

ins-6 highlighted amongst a screen of ASJ-enriched neuropeptides

Having tested fifteen neuropeptide genes enriched in the ASJ chemosensory neurons, we found that ins-6 loss-of-function mutants had the most severe dauer exit defect in that they exited dauer at the lowest rates compared to wild type (Fig. 2.1D). While ins-6 has previously been implicated in dauer exit (21, 22), this work is the first to test the role of INS-6 function in an otherwise wild-type background for dauer exit. Loss-of-function mutations in ins-32 also resulted in a strong dauer exit defect, indicating that INS-32 may act alongside INS-6 to promote dauer exit. Loss-of-function mutants for neuropeptide genes such as ins-26, nlp-80, flp-15, and flp-34 had higher dauer exit rates than those of wild type, suggesting that those neuropeptide genes may be involved in inhibiting dauer exit. Similar to dauer entry, in which we previously demonstrated that some neuropeptides promote while others inhibit dauer entry (25), the decision to exit dauer may be partially calculated based on a ratio between exit-promoting versus exit-inhibiting neuropeptides and growth factors.

While the C. elegans genome includes over 40 genes encoding insulin-like peptides, ins-6 stands out as being the only gene whose encoded peptide INS-6 has been shown to biochemically bind and activate the human insulin receptor with high affinity despite bearing key structural differences such as the lack of the conserved C peptide compared to human insulin (56, 57). Such biochemical data provides one possible explanation for the potency of INS-6 in regulating dauer exit. While INS-6 plays a major role in regulating dauer exit, the fact that ins-6 loss-of-function mutants can still exit dauer under low-pheromone conditions indicates that INS-6 likely acts alongside other insulin-like peptides (such as DAF-28 and possibly INS-32) to induce dauer exit.

Model for ins-6 upregulation during dauer exit

We analyzed regulation of ins-6 using both fluorescence reporter assays (Fig. 2.2C-H) and mRNA FISH (Fig. S2.2I, J), demonstrating that ins-6 expression and INS-6 secretion increases in just one hour after transfer of dauers onto favorable conditions. In that same time frame, we could not observe any behavioral or morphological changes that would distinguish these dauers as exiting. Our ins-6 transcriptional reporter showed high activity in the ASJ neurons specifically during dauer exit and virtually no activity when animals were raised under reproductive growth conditions leading to non-dauer adults (Fig. S2.2A-C). These data contrast with previous single-cell RNA sequencing data and mRNA FISH data showing that ins-6 transcripts are abundant in the ASJ neurons of L4 larvae raised under reproductive growth conditions (27, 58). This discrepancy suggests that our ins-6 reporters contain regulatory regions responsible for dauer-specific transcriptional activity while lacking additional regulatory regions that promote expression in the ASJ neurons during non-dauer-inducing growth.

Our analysis of ins-6 regulation using fluorescence reporters, gene knockouts, and neuronal perturbations lead us to propose a model of how ins-6 expression facilitates sensory integration and decision commitment during dauer exit (Figure 7). In our model, GPCRs for food signals activate DAF-11 which increases cGMP levels and leads to two parallel outcomes. Firstly, cGMP-gated heterodimeric TAX-2/TAX-4 cation channels open to allow calcium that results in a combination of calcium-dependent transcription mediated through CMK-1/CaMKI as well as exocytosis of neuropeptide-containing dense core vesicles, which has canonically been associated with high calcium levels (29, 59–62). Secondly, cGMP activates transcriptional activity mediated in part through the cGMP-dependent protein kinase EGL-4/PKG to increase ins-6 expression. Since neither cmk-1 nor egl-4 loss-of-function mutants fully prevented ins-6 upregulation (Fig. 2.6A), we suspect that both kinases, each defining a calcium-dependent (via CMK-1/CaMKI) or calcium-independent (via EGL-4/PKG) transcriptional pathway, may be necessary for full ins-6 upregulation during dauer exit. The necessity and sufficiency of cGMP signaling in upregulating ins-6 during dauer exit may help explain why optogenetic or chemogenetic

activation of the ASJ neurons was only sufficient to slightly increase ins-6 expression under high-pheromone conditions (Fig. 2.5G, H), since calcium alone cannot activate cGMP-dependent pathways such as those involving EGL-4.

How does pheromone inhibit ins-6 expression? Since pheromone suppressed calcium transients activated by food signal in both wild-type and unc-31(e169) loss-of-function mutant dauers (Fig. 2.5A, B), the ASJ neurons likely express GPCRs for pheromone which, upon binding to candidate ligands such as ascr#8 or ascr#2, inhibits calcium influx. Pheromone likely acts upstream of cGMP signaling because addition of pCPT-cGMP increases ins-6 expression even under high-pheromone conditions (Fig. 2.6B). Therefore, pheromone could prevent calcium influx by blocking food-based activation of DAF-11.

Our observations suggest that ins-6 expression levels can mark decision commitment. When dauers are transferred to intermediate-pheromone conditions that cause roughly half of dauers to exit within 24 hours, a clear bimodality emerges in ins-6 transcriptional reporter activity around the same time that dauers commit to exiting (Fig. 2.3). The increase in ins-6 transcriptional reporter activity in exit-committed dauers likely results from an autoregulatory positive feedback loop that depends on UNC-31 (to help secrete neuropeptides) and DAF-2/IGFR (as the receptor for insulin-like peptides) (Fig. 2.5D, Fig. S2.4D). We propose that after dauers encounter more favorable conditions, the ASJ neurons produce and secrete small amounts of neuropeptides (which may include INS-6) that bind to receptors (also on the ASJ neurons), thereby triggering an autoregulatory positive feedback loop that promotes further production of INS-6. Our observations that mutating unc-31 nearly abrogated ins-6 expression during dauer exit but spared the ASJ calcium response to food and pheromone (Fig. 2.5B, D) suggests that calcium increases are involved upstream of this putative positive feedback loop. Our observation that chemogenetic silencing of the ASJ neurons (which likely inhibits calcium influx) prevents ins-6 upregulation (Fig. 2.5E, F) further suggests that neuronal calcium may help trigger this positive feedback loop. Such a rampant, irreversible increase in INS-6 production and secretion likely promotes commitment to exit the dauer state by acting on downstream

tissues to induce relevant dauer exit-related genetic programs via insulin-like signaling (57). Our data that ins-6 expression increases even in daf-7 dauers incapable of exiting are consistent with high INS-6 production and secretion as being causes, rather than consequences, of decision commitment.

The nature of this proposed positive feedback loop would explain two features of the dauer exit decision. Firstly, it would explain the all-or-nothing nature of dauer exit in which dauers committed to exiting must proceed fully with decision execution since rampant positive feedback would hinder suppression of that same signaling pathway. Such positive feedback mechanisms have been previously been reported in developmental decisions involving commitment including in yeast, flies, and frogs (63–65). We previously argued that steroid hormone synthesis may similarly utilize positive feedback to force a binary choice between reproductive growth and dauer during the dauer entry decision (66). Secondly, the positive feedback loop would help connect the timescale discrepancy between sensory perception (over seconds) and decision execution (over hours). Dauers must be exposed to favorable food:pheromone ratios for a sufficiently long period of time to trigger the level of positive feedback required for decision commitment.

Ethological significance of ins-6 expression dynamics in ASJ

How does our model relate to what C. elegans may encounter in its natural habitat during dauer exit? In its natural life cycle, C. elegans cycles through periods of favorable conditions and unfavorable conditions (boom and bust), and dauer exit plays a critical role in supporting the transition from bust to boom. Expression levels of ins-6 can convey two important pieces of information: presence of food and absence of pheromone (including ascr#8, which is secreted most by sexually mature hermaphrodites (67)). We envision that, in the wild, C. elegans larvae enter dauer as they grow up in an environment crowded by pheromone-secreting worms and a depleted food source. To exit dauer, C. elegans would need to travel away from its crowded environment and find a new food source. At the chemosensation level, this would equate to perceiving that both food is present and that pheromone levels are low. The presence of food alone is insufficient because high

pheromone levels indicate that, even if food were present, it would be depleted too quickly given the abundance of other worms. Our results are consistent with this scenario in that high pheromone levels suppress food response at both the calcium and ins-6 expression level (Fig. 2.4B, 2.5A).

Our hypothesis for ins-6 upregulation is consistent with a parallel pathway model that includes a calcium (activity dependent) pathway in addition to a calcium-independent pathway (perhaps mediated through the cGMP-dependent kinase EGL-4/PKG). Such a model has previously been reported for the cases of daf-7 upregulation (also in the ASJ neurons) in response to Pseudomonas aeruginosa and in the case of flp-19 regulation in the BAG neurons (43, 51). As postulated previously (43), having a second, activity-independent pathway would prevent ASJ from inappropriately expressing ins-6 during exposure to dauer-irrelevant stimuli that activate ASJ including blue light, electric fields, and sodium chloride (41, 68, 69), thereby conferring specificity with regards to what environmental cues upregulate ins-6 in ASJ.

Sensory integration in a single C. elegans sensory neuron

Our genetic and calcium imaging experiments indicate that ins-6 upregulation during dauer exit occurs cell autonomously within ASJ. unc-13 loss-of-function mutants defective for synaptic transmission had close to wild-type ins-6 upregulation in ASJ (Fig. 2.5D), while unc-31 loss-of-function mutants defective for neuropeptide transmission had low ins-6 expression levels that could be partially rescued by ASJ-specific expression of unc-31 cDNA (Fig. 2.5C) but retained wild-type calcium responses to food and pheromone (Fig. 2.5B). Our data suggest that each ASJ neuron alone can integrate food and pheromone at both the level of neuronal calcium and gene expression, which highlights a stark difference between how C. elegans integrates sensory inputs compared to insects and vertebrates. The compact nervous system of C. elegans requires that it efficiently use its few neurons to discriminate against the vast array of sensory signals. Accordingly, C. elegans employs multiple polymodal sensory neurons that express multiple GPCRs to detect different stimuli (70), such as ASH which can detect a variety of noxious stimuli, AWA which

responds to numerous chemoattractants (71, 72), and AWC which responds to both odors and temperature (73, 74). While vertebrates and insects do utilize polymodal neurons, most notably in nociception (75–77), sensory integration in such organisms is typically performed via a multilayer model in which modality-specific neurons converge onto higher order brain regions (78, 79), a key example being the "one neuron – one receptor" principle observed in mammals and flies wherein each olfactory neuron classes usually only express one olfactory receptor, and signals from each become integrated in further regions of the olfactory bulb (80, 81). Our results help us better understand how a single neuron performs complex computations of multiple sensory inputs and underscores how the computational power of nematode nervous systems (all about 300 neurons) is vastly underestimated by cell number alone.

2.5 Materials and Methods

C. elegans strains and maintenance

C. elegans strains were derived from the wild-type strain N2 (Bristol) and were cultured according to standard laboratory conditions on Nematode Growth Medium (NGM) agar seeded with E. coli OP50 as the food source. A list of strains used in this study, including their genotypes and origins, can be found in Table S1. Curated genetic and genomic information was provided by WormBase (Davis et al., 2022).

Dauer entry induction

To induce for dauer exit and fluorescence imaging assays, 10-20 young adults were placed on 35 mm diameter Petri dishes containing 2 mL of NGM agar (without peptone) supplemented with crude pheromone extract (prepared as previously described; Schroeder and Flatt 2014) at a concentration of 0.5-2.5% w/v, enough to induce >85% animals to enter dauer. Plates were seeded with 10 µL of 8% w/v E. coli OP50, which was prepared by pelleting an overnight culture via centrifugation and resuspending in S-Basal three times (hereby referred to as "S-Basal-washed OP50"). Adults were picked onto the plate and allowed to lay eggs at room temperature (RT; 22-23°C) for 5-9 hours before being removed, during which time they typically laid 300-500 eggs. The plates were then further seeded

with an additional 50 µL of heat-killed 8% w/v E. coli OP50, which was prepared by pelleting an overnight culture via centrifugation, resuspending in S-Basal three times, and placed in a heat block set at 95 °C for 5 minutes (hereby referred to as "heat-killed OP50"). Afterwards, the plates were wrapped with Parafilm (Amcor) and incubated at 25.5-26.1°C for 60-72 hours.

Dauer exit assay

Dauers were formed according to "Dauer entry induction" (above) and then selected for by an SDS wash (2% in M9, 30 minutes, 25°C) to kill non-dauers before being washed 3x in M9 solution (pelleted by centrifuging for 1 minute at RT, 1000 x g). Surviving dauers were then plated onto dauer exit plates seeded with 5 µL 8% w/v heat-killed OP50. Dauer exit plates were prepared similarly to dauer entry plates but contained a lower concentration of crude pheromone extract (typically 0.05% w/v) that had been determined to induce ~40-80% of wild-type dauers to exit within 24 hours. After 24 hours, dauer exit was scored according to morphological and behavioral criteria, including pharyngeal pumping, body thickening, and paler color (31). The few experiments in which the wild-type dauer exit rate was not within the 40-80% range were discarded in order to maintain consistency of dynamic range for scoring.

Molecular cloning and transgenesis

Molecular cloning was performed using NEB HiFi Assembly (New England BioLabs (NEB)) using fragments obtained from PCR with Q5 or Phusion (NEB) or Platinum SuperFi DNA Polymerase (Invitrogen). HiFi Assembly products were transformed into chemically competent DH5α cells via heat shock. Most plasmids used in this study were constructed in a backbone consisting of a derivative of the pSM vector (83), itself a derivative of the Fire vector pPD49.2 (Addgene plasmid # 1686, deposited by Andrew Fire). Plasmids were microinjected into the gonads of young adult animals according to standard protocols (84, 85), with most plasmids first linearized via PCR using oMZ15F and oMZ17R to promote cell-specific expression (86). Contents of injection mixtures can

be found in Table S1. Select transgenes were integrated according to standard X-Ray irradiation protocols and outcrossed at least three times prior to use (87).

To construct the ins-6 transcriptional reporter, we took pQZ10 (which includes mCherry flanked by the 1.7 kb upstream and 2 kb downstream of the ins-6 open reading frame) (21) and replaced the mCherry coding region with that of destabilized YFP, which is a YFP variant that includes a destabilized signal from mouse ornithine decarboxyl at the C terminus that promotes faster degradation (28). To construct the ins-6 translational reporter which includes the INS-6 propeptide fused to mCherry at the C terminus, we took pQZ10 and cloned in the full ins-6 open reading frame (including the sole intron) immediately after the 1.7 kb ins-6 5' upstream fragment. The daf-28 transcriptional and translational reporters were made in an identical manner using the 3 kb upstream and 2.1 kb downstream of the daf-28 open reading frame.

CRISPR Cas9 genome editing

To generate the loss-of-function mutants for ins-24, ins-32, nlp-21, nlp-80, dmsr-12, srg-36, and srx-43, we used the CRISPR STOP-IN method (88). Briefly, C. elegans strain N2 was gene-edited by the insertion of a universal 43-nucleotide-long knock-in cassette (STOP-IN) using CRISPR/Cas9 into an early exon of the target gene to disrupt translation.

Imaging transgenic ins-6 reporter strains throughout development

Transgenic animals bearing an integrated fluorescence reporter were semi-synchronized for growth by allowing young adult hermaphrodites to lay eggs for ~3-5 hours on a 35 mm diameter Petri dish containing 2 mL of NGM agar (without peptone) seeded with 10 µL 8% w/v S-Basal-washed OP50. For experiments involving dauer-inducing conditions, plates contained a high concentration (0.5-2.5% w/v) of crude pheromone and were seeded with 50 µL of 8% w/v heat-killed OP50. For experiments involving non-dauer-inducing conditions, pheromone was omitted, and plates were seeded with 50 µL of 8% w/v S-Basal-washed OP50. Plates were then incubated at 25.5-26.1 °C. For dauer-inducing growth (Fig. 2.2C-H), distinct developmental stages were imaged at the following time points based on

the number of hours spent in the incubator: L2d (40-45 hours), dauer (62-66 hours). For non-dauer-inducing growth (Fig. S2.2A-C, E-F): L1 (22 hours), L2 (32 hours), L4 (46 hours), young adult (56 hours), adult (65 hours). To image dauers during dauer exit, dauers were SDS-selected in a manner identical to that used in the "Dauer exit assay" (above) before being transferred to a new NGM agar (without peptone) plate that lacked crude pheromone and was seeded with 5-10 µL of 8% w/v heat-killed OP50. Dauers were then imaged at the indicated time points based on the number of hours after transfer to the new plate.

Microscopy and image analysis

Animals were immobilized on a pad composed of 4% ultrapure agarose in H2O in 1-2 µL of 5 mM levamisole in H2O or in a suspension of 0.1 µm polystyrene beads (Polysciences) in H2O. Imaging was performed on a Zeiss AxioImager2 equipped with a Colibri 7 for LED fluorescence illumination and an Axiocam 506 Mono camera (Carl Zeiss Inc.). Pharyngeal bulb width measurements were performed using FIJI (ImageJ) software (89) by using the length tool to measure the widest section of the posterior pharyngeal bulb. Images were processed using FIJI. Quantification of YFP in ins-6p::dYFP transgenic animals was performed by drawing an ROI around the neuron of interest (for each animal we measured two ASJ and/or two ASI neurons), measuring the YFP intensity, adjusting for background, and averaging between the two neurons. The ROI was drawn to be approximately the same size and position as that of the neuronal nucleus from the neuron of interest, as estimated by using the DIC channel. Quantification of secreted INS-6::mCherry or DAF-28::mCherry in coelomocytes was performed as described previously (29); in short, the four brightest puncta from a maximum intensity projection of the anterior pair of coelomocytes were measured, adjusted for background, and averaged.

mRNA fluorescence in-situ hybridization (FISH)

FISH was performed similarly to a previously used protocol (58). ins-6 mRNA probes (20 total, see Table S2 for probe sequences) were designed using the Stellaris RNA-FISH Probe Designer 2.0 (LGC Biosearch Technologies) with non-specificity masking level 5

with the target sequence between the entire ins-6 open reading frame along with the 5' and 3' untranslated regions. Probes were labeled with CAL-Fluor 610 at the 3' end. At the appropriate developmental stage, animals were washed 3x with M9 and fixed with 4% paraformaldehyde (PFA) in phosphate-buffered saline (PBS) for 45 minutes. Following three additional washes in PBS containing 0.01% Triton X-100, animals were fixed in 100% methanol overnight at 4 °C. The following day, animals were rehydrated in saline sodium citrate (SSC) buffer at 4x concentration (prepared by diluting 20x SSC buffer 5x in H2O) containing 0.01% Triton X-100 (4x SSCT) and then incubated with the FISH probes at 1:500 dilution (final concentration 25 nM) in hybridization buffer (10% w/v dextran sulfate, 15% formamide, 2x SSC) overnight. The following day, animals washed 3x in 10% formamide in 4x SSCT for a total of 1.5 hours at 30 °C, with multiple 4x SSCT washes before and after formamide incubation. Animals were then incubated with DAPI (5 ng/mL in PBS). Following two last 4x SSCT washes, animals were stored and mounted in Vectashield (Vector Labs). FISH imaging was performed on an upright Zeiss LSM880 microscope (Carl Zeiss Inc.) equipped with a 594 nm laser using a Zeiss 63x oil objective. Image quantification was performed using FIJI.

Calcium imaging

To image dauers, we adapted an existing microfluidic chip design (90) by incorporating a thinner opening for the worm to accommodate dauers. 1 mM Levamisole was used to semi-immobilize the worms. Each stimulus was delivered to the worm for 15 seconds followed by 30 seconds of H2O. Stimuli were delivered in a random order to account for the effects of memory and adaptation. Fluorescence was recorded with a spinning disc confocal microscope (Dragonfly 200, Andor) and a sCMOS camera (Photometrics Kinetix) that captured fluorescence from GCaMP6.0s (33) in the ASJ neurons of KP9672 (see Table S1) at 10 ms/.5 μm z-slice, 25 z-slices/volume, and 4 volumes/second. To extract calcium traces, we located the center of each neuronal nucleus and took the average pixel intensities of a 5 μm (X) x 5 μm (Y) x 2.5 μm (Z) (rectangular box around those centers. The neuron-independent background signal was removed and $\Delta F/F_0$ calculated for each stimulus-

response, where F_0 was the average fluorescence value during the 2.5 seconds before delivery of the stimulus.

Perturbation assays

For optogenetic assays using the red-shifted channelrhodopsin Chrimson (37, 91), we added all-trans-retinal (Sigma-Aldrich) to a final concentration of 500 µM to 35 mm diameter Petri dishes containing 2 mL of NGM agar (without peptone) supplemented with a high concentration (0.15% w/v) of crude pheromone extract to prevent dauer exit. Dauers were transferred onto these plates and placed in the Wormlab Tracking system (MBF Biosciences) where we then turned on a red LED light. The LED stimulus regime was 100 ms on, 1000 ms off at 100% intensity for two hours. Similarly, for chemogenetic assays using TRPV1 (92), we added capsaicin (Sigma-Aldrich) to a final concentration of 100 µM. For cGMP assays, we added pCPT-cGMP (Sigma-Aldrich) to a final concentration of 1 mM.

Statistical Analysis, Plotting, and Figure Design

Plots were designed and statistical tests were performed using Prism 10.0 (GraphPad). Illustrated figures were designed and drawn using Affinity Designer (Serif).

Acknowledgments

The TRPV1 plasmid was a kind gift from the Bargmann lab (The Rockefeller University). The pQZ::ins-6 plasmid was a kind gift from the Alcedo Lab (Wayne State University). The strain JSR70 was a kind gift from the Srinivasan lab. Some strains (see Table S1) were provided by the National BioResource Project (NBRP) (93), particularly from the lab of Shohei Mitani (Tokyo Women's Medical University Institute for Integrated Medical Sciences), as well as the CGC, which is funded by NIH Office of Research Infrastructure Programs (P40 OD010440). The strain KP9672 nuIs556[ptrx-1::GCaMP6.0s] was a kind gift from the Kaplan lab. Technical support was provided by members of the Sternberg lab including Barbara Perry, Stephanie Nava, and Wilber Palma. Microscopy assistance was provided by the Beckman Institute Biological Imaging Facility at Caltech. Critical

feedback for the manuscript was provided by Sternberg lab members, particularly Hillel Schwartz and Nicholas Markarian.

Competing interests

No competing interests declared.

Author Contributions

M.G.Z. and P.W.S. conceived of the study. M.G.Z., performed experiments and analyzed data with help from S.H. and N.F.. M.S. and V.V. designed and performed calcium imaging experiments. H.P. created CRISPR mutants. F.S. provided synthetic ascarosides. M.G.Z. wrote the manuscript with editorial assistance from P.W.S.

Funding

M.G.Z. was supported by a National Institutes of Health Grant F31 NS120501-01. P.W.S. was supported by a Bren Professorship and by a National Institutes of Health Grant R24-OD023041.

2.6 References

1. A. S. Paintal, Participation by pressure—pain receptors of mammalian muscles in the flexion reflex. J. Physiol. 156, 498–514 (1961).

2. A. C. Hart, “Behavior” in WormBook: The Online Review of C. Elegans Biology [Internet], (WormBook, 2006).

3. X. J. Gao, Drosophila chemotaxis. Fly (Austin) 8, 3–6 (2014).

4. J. Vriens, B. Nilius, T. Voets, Peripheral thermosensation in mammals. Nat. Rev. Neurosci. 15, 573–589 (2014).

5. L. E. Browne et al., Time-resolved fast mammalian behavior reveals the complexity of protective pain responses. Cell Rep. 20, 89–98 (2017).

6. R. Komal, A. Dwivedi, V. Vaish, S. Rani, Conquering the night: understanding nocturnal migration in birds. Biol. Rhythm Res. 48, 747–755 (2017).

7. M. S. Ogonowski, C. J. Conway, Migratory decisions in birds: extent of genetic versus environmental control. Oecologia 161, 199–207 (2009).

8. A. L. Evans et al., Drivers of hibernation in the brown bear. Front. Zool. 13, 7 (2016).

9. S. M. Mohr, S. N. Bagriantsev, E. O. Gracheva, Cellular, molecular, and physiological adaptations of hibernation: the solution to environmental challenges. Annu. Rev. Cell Dev. Biol. 36, 315–338 (2020).

10. D. L. Denlinger, G. D. Yocum, J. P. Rinehart, "Hormonal control of diapause" in Insect Endocrinology, (Elsevier, 2012), pp. 430–463.

11. S. C. Hand, D. L. Denlinger, J. E. Podrabsky, R. Roy, Mechanisms of animal diapause: recent developments from nematodes, crustaceans, insects, and fish. Am. J. Physiol.-Regul. Integr. Comp. Physiol. 310, R1193–R1211 (2016).

12. J. E. Podrabsky, S. C. Hand, Physiological strategies during animal diapause: lessons from brine shrimp and annual killifish. J. Exp. Biol. 218, 1897–1906 (2015).

13. J. W. Golden, D. L. Riddle, The Caenorhabditis elegans dauer larva: Developmental effects of pheromone, food, and temperature. Dev. Biol. 102, 368–378 (1984).

14. J. W. Golden, D. L. Riddle, A pheromone influences larval development in the nematode Caenorhabditis elegans. Science 218, 578–580 (1982).

15. R. C. Cassada, R. L. Russell, The dauerlarva, a post-embryonic developmental variant of the nematode Caenorhabditis elegans. Dev. Biol. 46, 326–342 (1975).

16. A. H. Ludewig, F. C. Schroeder, "Ascaroside signaling in C. elegans" in WormBook: The Online Review of C. Elegans Biology [Internet], (WormBook, 2018).

17. P. T. McGrath, I. Ruvinsky, A primer on pheromone signaling in Caenorhabditis elegans for systems biologists. Curr. Opin. Syst. Biol. 13, 23–30 (2019).

18. R. J. Androwski, K. M. Flatt, N. E. Schroeder, Phenotypic plasticity and remodeling in the stress-induced Caenorhabditis elegans dauer. Wiley Interdiscip. Rev. Dev. Biol. 6, e278 (2017).

19. N. Fielenbach, A. Antebi, C. elegans dauer formation and the molecular basis of plasticity. Genes Dev. 22, 2149–2165 (2008).

20. P. J. Hu, Dauer. WormBook (2007). https://doi.org/10.1895/wormbook.1.144.1.

21. A. Cornils, M. Gloeck, Z. Chen, Y. Zhang, J. Alcedo, Specific insulin-like peptides encode sensory information to regulate distinct developmental processes. Development 138, 1183–1193 (2011).

22. D. A. Fernandes de Abreu et al., An insulin-to-insulin regulatory network orchestrates phenotypic specificity in development and physiology. PLoS Genet. 10, e1004225 (2014).

23. C. I. Bargmann, H. R. Horvitz, Control of larval development by chemosensory neurons in Caenorhabditis elegans. Science 251, 1243–1246 (1991).

24. S. H. Chung, A. Schmalz, R. C. H. Ruiz, C. V. Gabel, E. Mazur, Femtosecond laser ablation reveals antagonistic sensory and neuroendocrine signaling that underlie C. elegans behavior and development. Cell Rep. 4, 316–326 (2013).

25. J. S. Lee et al., FMRFamide-like peptides expand the behavioral repertoire of a densely connected nervous system. Proc. Natl. Acad. Sci. 114, E10726–E10735 (2017).

26. Y. Hao, Z. Hu, D. Sieburth, J. M. Kaplan, RIC-7 promotes neuropeptide secretion. PLOS Genet. 8, e1002464 (2012).

27. S. R. Taylor et al., Molecular topography of an entire nervous system. Cell (2021). https://doi.org/10.1016/j.cell.2021.06.023.

28. X. Li et al., Generation of destabilized green fluorescent protein as a rranscription reporter. J. Biol. Chem. 273, 34970–34975 (1998).

29. S. Speese et al., UNC-31 (CAPS) Is required for dense-core vesicle but not synaptic vesicle exocytosis in Caenorhabditis elegans. J. Neurosci. 27, 6150–6162 (2007).

30. W. Li, S. G. Kennedy, G. Ruvkun, daf-28 encodes a C. elegans insulin superfamily member that is regulated by environmental cues and acts in the DAF-2 signaling pathway. Genes Dev. 17, 844–858 (2003).

31. M. G. Zhang, P. W. Sternberg, Both entry to and exit from diapause arrest in Caenorhabditis elegans are regulated by a steroid hormone pathway. Development 149, dev200173 (2022).

32. P. Ren et al., Control of C. elegans larval development by neuronal expression of a TGF-β homolog. Science 274, 1389–1391 (1996).

33. T.-W. Chen et al., Ultrasensitive fluorescent proteins for imaging neuronal activity. Nature 499, 295–300 (2013).

34. Y. Hao et al., Thioredoxin shapes the C. elegans sensory response to Pseudomonas produced nitric oxide. eLife 7, e36833 (2018).

35. D. Sieburth, J. M. Madison, J. M. Kaplan, PKC-1 regulates secretion of neuropeptides. Nat. Neurosci. 10, 49–57 (2007).

36. N. Pokala, Q. Liu, A. Gordus, C. I. Bargmann, Inducible and titratable silencing of Caenorhabditis elegans neurons in vivo with histamine-gated chloride channels. Proc. Natl. Acad. Sci. 111, 2770–2775 (2014).

37. L. C. Schild, D. A. Glauser, Dual color neural activation and behavior control with Chrimson and CoChR in Caenorhabditis elegans. Genetics 200, 1029–1034 (2015).

38. M. Guo et al., Reciprocal inhibition between sensory ASH and ASI neurons modulates nociception and avoidance in Caenorhabditis elegans. Nat. Commun. 6, 5655 (2015).

39. D. A. Birnby et al., A transmembrane guanylyl cyclase (DAF-11) and Hsp90 (DAF-21) regulate a common set of chemosensory behaviors in Caenorhabditis elegans. Genetics 155, 85–104 (2000).

40. W. Wang et al., cGMP signaling mediates water sensation (hydrosensation) and hydrotaxis in Caenorhabditis elegans. Sci. Rep. 6, 19779 (2016).

41. A. Ward, J. Liu, Z. Feng, X. Z. S. Xu, Light-sensitive neurons and channels mediate phototaxis in C. elegans. Nat. Neurosci. 11, 916–922 (2008).

42. J. Liu et al., C. elegans phototransduction requires a G protein–dependent cGMP pathway and a taste receptor homolog. Nat. Neurosci. 13, 715–722 (2010).

43. J. Park, J. D. Meisel, D. H. Kim, Immediate activation of chemosensory neuron gene expression by bacterial metabolites is selectively induced by distinct cyclic GMP-dependent pathways in Caenorhabditis elegans. PLOS Genet. 16, e1008505 (2020).

44. C. M. Coburn, C. I. Bargmann, A putative cyclic nucleotide–gated channel is required for sensory development and function in C. elegans. Neuron 17, 695–706 (1996).

45. C. M. Coburn, I. Mori, Y. Ohshima, C. I. Bargmann, A cyclic nucleotide-gated channel inhibits sensory axon outgrowth in larval and adult Caenorhabditis elegans: a distinct pathway for maintenance of sensory axon structure. Development 125, 249–258 (1998).

46. N. D. L'Etoile et al., The cyclic GMP-dependent protein kinase EGL-4 regulates olfactory adaptation in C. elegans. Neuron 36, 1079–1089 (2002).

47. J. Stansberry et al., A cGMP-dependent protein kinase is implicated in wild-type motility in C. elegans. J. Neurochem. 76, 1177–1187 (2001).

48. K. Eto et al., Ca2+/Calmodulin-dependent protein kinase cascade in Caenorhabditis elegans: implications in transcriptional activation. J. Biol. Chem. 274, 22556–22562 (1999).

49. Y. Kimura et al., A CaMK cascade activates CRE-mediated transcription in neurons of Caenorhabditis elegans. EMBO Rep. 3, 962–966 (2002).

50. J. Park et al., CREB mediates the C. elegans dauer polyphenism through direct and cell-autonomous regulation of TGF-β expression. PLoS Genet. 17, e1009678 (2021).

51. T. Rojo Romanos, J. G. Petersen, R. Pocock, Control of neuropeptide expression by parallel activity-dependent pathways in Caenorhabditis elegans. Sci. Rep. 7, 38734 (2017).

52. R. A. Butcher, J. R. Ragains, E. Kim, J. Clardy, A potent dauer pheromone component in Caenorhabditis elegans that acts synergistically with other components. Proc. Natl. Acad. Sci. 105, 14288–14292 (2008).

53. R. A. Butcher, M. Fujita, F. C. Schroeder, J. Clardy, Small-molecule pheromones that control dauer development in Caenorhabditis elegans. Nat. Chem. Biol. 3, 420–422 (2007).

54. C. Pungaliya et al., A shortcut to identifying small molecule signals that regulate behavior and development in Caenorhabditis elegans. Proc. Natl. Acad. Sci. 106, 7708–7713 (2009).

55. D. K. Reilly et al., Transcriptomic profiling of sex-specific olfactory neurons reveals subset-specific receptor expression in Caenorhabditis elegans. Genetics 223, iyad026 (2023).

56. Q. Hua et al., A divergent INS protein in Caenorhabditis elegans structurally resembles human insulin and activates the human insulin receptor. Genes Dev. 17, 826–831 (2003).

57. C. T. Murphy, P. J. Hu, “Insulin/insulin-like growth factor signaling in C. elegans” in WormBook: The Online Review of C. Elegans Biology [Internet], (WormBook, 2018).

58. R. Chandra, L. Li, Z. Husain, S. Mishra, J. Alcedo, Axonal transport of an insulin-like peptide mRNA promotes stress recovery in C. elegans. BioRxiv. (2019).

59. M. Ludwig, G. Leng, Dendritic peptide release and peptide-dependent behaviours. Nat. Rev. Neurosci. 7, 126–136 (2006).

60. U. Becherer, J. Rettig, Vesicle pools, docking, priming, and release. Cell Tissue Res. 326, 393–407 (2006).

61. S. O. Rizzoli, W. J. Betz, Synaptic vesicle pools. Nat. Rev. Neurosci. 6, 57–69 (2005).

62. M. Ludwig et al., Intracellular calcium stores regulate activity-dependent neuropeptide release from dendrites. Nature 418, 85–89 (2002).

63. D. Tsuchiya, Y. Yang, S. Lacefield, Positive feedback of NDT80 expression ensures irreversible meiotic commitment in budding yeast. PLOS Genet. 10, e1004398 (2014).

64. W. Xiong, J. E. Ferrell, A positive-feedback-based bistable 'memory module' that governs a cell fate decision. Nature 426, 460–465 (2003).

65. C. Yin, R. Xi, A phyllopod-mediated feedback loop promotes intestinal stem cell enteroendocrine commitment in Drosophila. Stem Cell Rep. 10, 43–57 (2018).

66. O. N. Schaedel, B. Gerisch, A. Antebi, P. W. Sternberg, Hormonal signal amplification mediates environmental conditions during development and controls an irreversible commitment to adulthood. PLOS Biol. 10, e1001306 (2012).

67. F. Kaplan et al., Ascaroside expression in Caenorhabditis elegans is strongly dependent on diet and developmental stage. PLoS ONE 6, e17804 (2011).

68. C. V. Gabel et al., Neural circuits mediate electrosensory behavior in Caenorhabditis elegans. J. Neurosci. 27, 7586–7596 (2007).

69. A. Zaslaver et al., Hierarchical sparse coding in the sensory system of Caenorhabditis elegans. Proc. Natl. Acad. Sci. 112, 1185–1189 (2015).

70. E. R. Troemel, J. H. Chou, N. D. Dwyer, H. A. Colbert, C. I. Bargmann, Divergent seven transmembrane receptors are candidate chemosensory receptors in C. elegans. Cell 83, 207–218 (1995).

71. C. I. Bargmann, "Chemosensation in C. elegans" in WormBook: The Online Review of C. Elegans Biology [Internet], (WormBook, 2006).

72. D. M. Ferkey, P. Sengupta, N. D. L'Etoile, Chemosensory signal transduction in Caenorhabditis elegans. Genetics 217, iyab004 (2021).

73. D. Biron, S. Wasserman, J. H. Thomas, A. D. T. Samuel, P. Sengupta, An olfactory neuron responds stochastically to temperature and modulates Caenorhabditis elegans thermotactic behavior. Proc. Natl. Acad. Sci. 105, 11002–11007 (2008).

74. A. Kuhara et al., Temperature sensing by an olfactory neuron in a circuit controlling behavior of C. elegans. Science 320, 803–807 (2008).

75. E. C. Emery et al., In vivo characterization of distinct modality-specific subsets of somatosensory neurons using GCaMP. Sci. Adv. 2, e1600990 (2016).

76. E. C. Emery, J. N. Wood, Somatosensation a la mode: plasticity and polymodality in sensory neurons. Curr. Opin. Physiol. 11, 29–34 (2019).

77. J.-C. Boivin, J. Zhu, T. Ohyama, Nociception in fruit fly larvae. Front. Pain Res. 4, 1076017 (2023).

78. Y. V. Yu, W. Xue, Y. Chen, Multisensory integration in Caenorhabditis elegans in comparison to mammals. Brain Sci. 12, 1368 (2022).

79. D. D. Ghosh, M. N. Nitabach, Y. Zhang, G. Harris, Multisensory integration in C. elegans. Curr. Opin. Neurobiol. 43, 110–118 (2017).

80. D. Task et al., Chemoreceptor co-expression in Drosophila melanogaster olfactory neurons. eLife 11, e72599 (2022).

81. S. Serizawa, K. Miyamichi, H. Sakano, One neuron–one receptor rule in the mouse olfactory system. Trends Genet. 20, 648–653 (2004).

82. N. E. Schroeder, K. M. Flatt, In vivo imaging of dauer-specific neuronal remodeling in C. elegans. JoVE J. Vis. Exp. e51834 (2014). https://doi.org/10.3791/51834.

83. K. Shen, C. I. Bargmann, The immunoglobulin superfamily protein SYG-1 determines the location of specific synapses in C. elegans. Cell 112, 619–630 (2003).

84. M. Rieckher, N. Tavernarakis, Generation of Caenorhabditis elegans transgenic animals by DNA microinjection. Bio-Protoc. 7 (2017).

85. C. C. Mello, J. M. Kramer, D. Stinchcomb, V. Ambros, Efficient gene transfer in C.elegans: extrachromosomal maintenance and integration of transforming sequences. EMBO J. 10, 3959–3970 (1991).

86. J. F. Etchberger, O. Hobert, Vector-free DNA constructs improve transgene expression in C. elegans. Nat. Methods 5, 3–3 (2008).

87. T. Evans, Transformation and microinjection. WormBook (2006). https://doi.org/10.1895/wormbook.1.108.1.

88. H. Wang, H. Park, J. Liu, P. W. Sternberg, An efficient genome editing strategy to generate putative null mutants in caenorhabditis elegans using CRISPR/Cas9. G3 Genes Genomes Genet. 8, 3607–3616 (2018).

89. J. Schindelin, et al., Fiji: an open-source platform for biological-image analysis. Nat. Methods 9, 676–682 (2012).

90. J. A. Schiffer et al., Modulation of sensory perception by hydrogen peroxide enables Caenorhabditis elegans to find a niche that provides both food and protection from hydrogen peroxide. PLOS Pathog. 17, e1010112 (2021).

91. N. C. Klapoetke et al., Independent optical excitation of distinct neural populations. Nat. Methods 11, 338–346 (2014).

92. D. M. Tobin et al., Combinatorial expression of TRPV channel proteins defines their sensory functions and subcellular localization in C. elegans neurons. Neuron 35, 307–318 (2002).

93. Y. Yamazaki et al., NBRP databases: databases of biological resources in Japan. Nucleic Acids Res. 38, D26–D32 (2010).

94. S. Brenner, The genetics of Caenorhabditis elegans. Genetics 77, 71–94 (1974).

95. The C. elegans Deletion Mutant Consortium, Large-scale screening for targeted knockouts in the Caenorhabditis elegans genome. G3 GenesGenomesGenetics 2, 1415–1425 (2012).

96. J. Kass, T. C. Jacob, P. Kim, J. M. Kaplan, The EGL-3 proprotein convertase regulates mechanosensory responses of Caenorhabditis elegans. J. Neurosci. 21, 9265–9272 (2001).

97. L. X. Liu et al., High-throughput isolation of Caenorhabditis elegans deletion mutants. Genome Res. 9, 859–867 (1999).

98. T. C. Jacob, J. M. . Kaplan, The EGL-21 carboxypeptidase E facilitates acetylcholine release at Caenorhabditis elegans neuromuscular junctions. J. Neurosci. 23, 2122–2130 (2003).

2.7 Figures

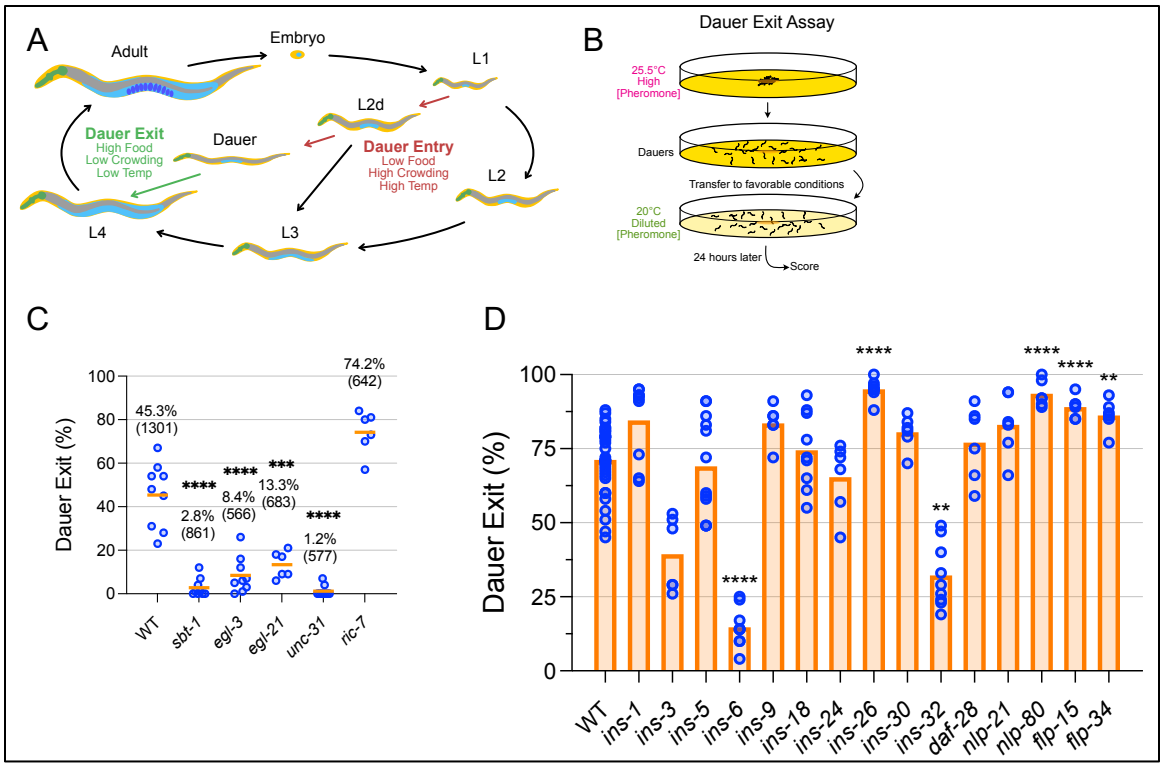

Figure 2.1. Neuropeptides, especially the insulin-like peptide ins-6, are critical for dauer exit.

(A) During development, C. elegans makes multiple developmental decisions including whether to enter and when to exit the developmentally arrested state called dauer. This decision depends mainly on food availability, crowding, and temperature. (B) Overview of the dauer exit assay. Animals were induced to become dauer via growth on conditions of high pheromone concentration and high temperature. Non-dauers were removed using SDS and surviving dauers were transferred to conditions of intermediate pheromone concentrations and lower temperature to stimulate between 40-80% of dauers to exit after 24 hours. (C) Dauer exit rates of mutants defective for neuropeptide processing (sbt-1, egl-3, egl-21) or signaling (unc-31, ric-7) compared to that of wild type (WT). Means are written and shown by the orange line, and total number of animals scored is indicated in parentheses. (D) Dauer exit rates of mutants defective for single neuropeptide genes. Data

compiled from multiple independent experiments, and statistical analyses were only performed between mutant and wild-type samples measured in the same experiment. Bars indicate means. See Figure S1 for analysis of individual mutants. For (C) and (D), each dot is the dauer exit % from an assay plate containing 50-100 animals each. ****, $p<0.0001$, ***, $p<0.001$, **, $p<0.01$, compared to "WT" by Welch ANOVA with Dunnett's T3 multiple comparison correction. Comparisons to "WT" were not statistically significant unless indicated otherwise.

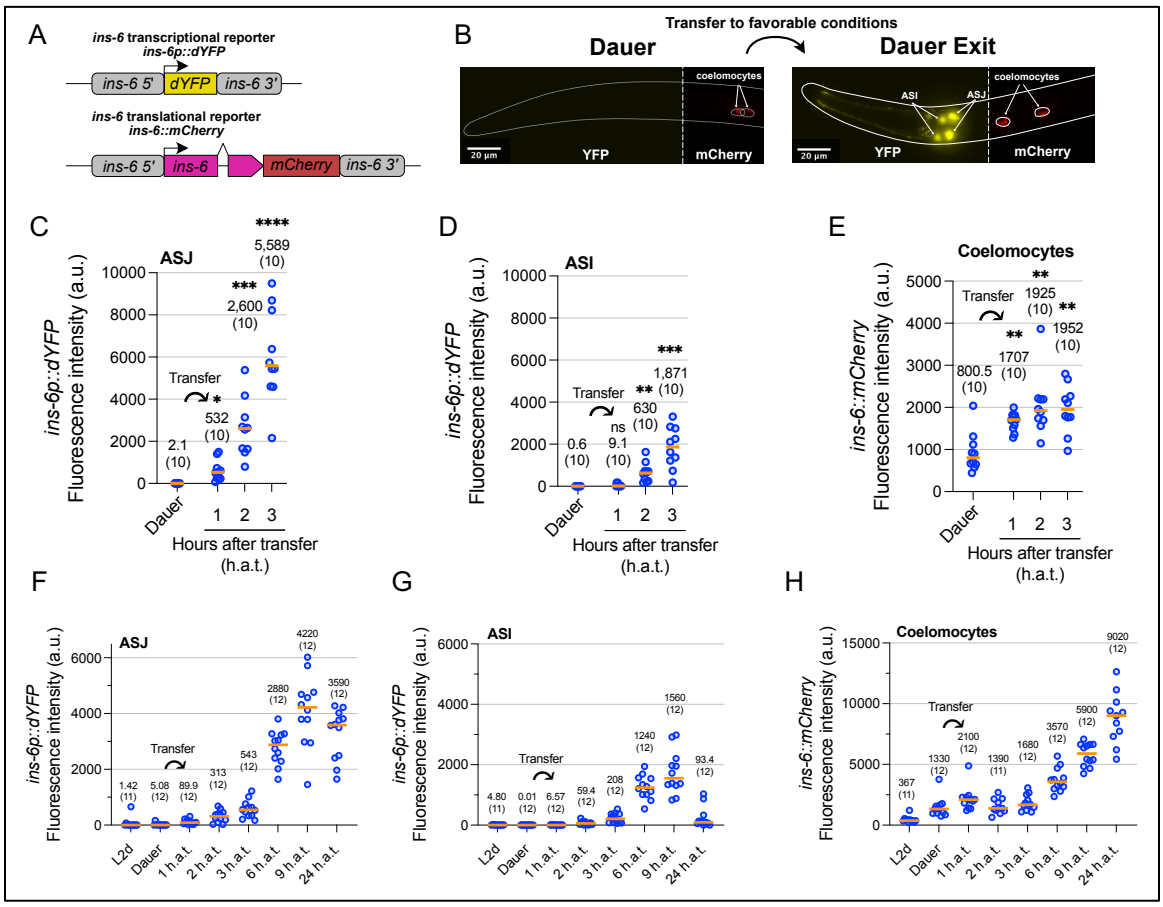

Figure 2.2. ins-6 transcription and INS-6 secretion increase quickly during dauer exit. (A) Design of ins-6 transcriptional and translational reporters. (B) Sample images of merged dYFP and mCherry channels. Left, dauer prior to transfer. Right, dauer six hours after transfer. Anterior is left, ventral is facing the viewer. (C-E) Quantification of ins-6p::dYFP transcriptional reporter activity measured in arbitrary units (a.u.) in ASJ (C) or ASI (D) and mCherry signal in the coelomocytes (E) in dauers and following transfer of dauers to favorable conditions (indicated by curved arrow). Plots are from the same set of animals. ns, not significant. *, $p<0.05$, **, $p<0.01$, ***, $p<0.001$, ****, $p<0.0001$ by Welch ANOVA with Dunnett's T3 multiple comparison correction when compared to "Dauer." (F-H) Additional ins-6 reporter activity experiment performed similarly to (C-E), except

with additional time points, and for dYFP measurements, LED power and exposure time were lowered relative to experiments from (C-E) to prevent pixel saturation. h.a.t., hours after transfer to favorable conditions. In all plots, individual dots represent one animal. Medians are depicted by the orange bar. Medians and sample sizes are written.

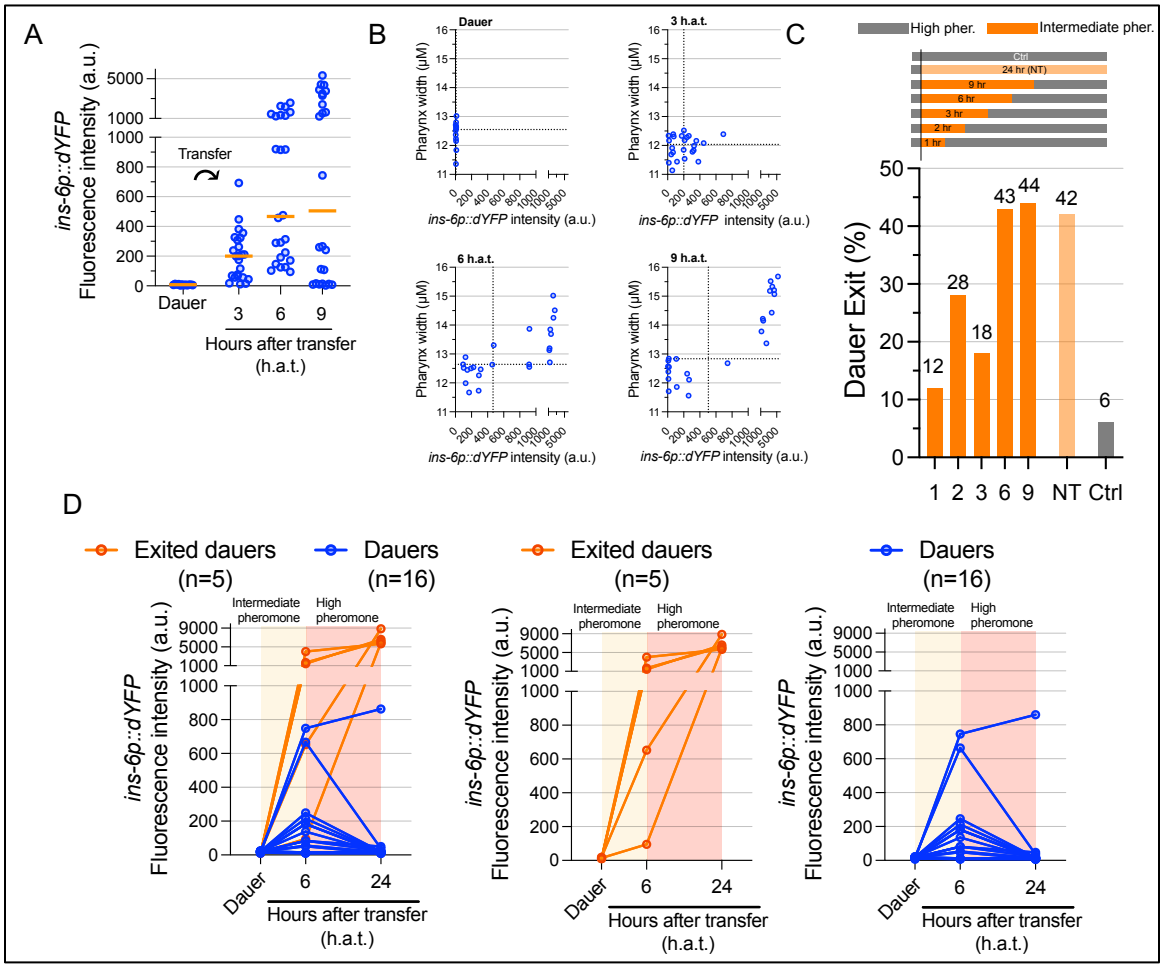

Figure 2.3. ins-6 expression correlates with commitment to exit dauer.

(A) ins-6p::dYFP transcriptional reporter activity in dauers before and after transfer (indicated by curved arrow) onto intermediate-pheromone conditions which stimulate half of dauers to exit. (B) Animals from (A) simultaneously had their pharynx widths measured. Increased pharyngeal width is a key characteristic of ongoing dauer exit. Shown are correlation plots between ins-6p::dYFP signal and pharynx width. Dotted lines are drawn at the median for each measurement. (C) Dauers were induced under high-pheromone growth conditions and transferred to intermediate-pheromone conditions for the indicated duration before being transferred back onto high-pheromone conditions to prevent dauer exit in noncommitted animals. Animals were scored for dauer exit after 24 hours. Included are the following controls: a no-transfer control (NT, light orange) in which dauers were

not transferred but instead remained on intermediate-pheromone conditions and a control in which dauers remained entirely on high-pheromone conditions (Ctrl, grey). Bars and numbers indicate dauer exit rates for >100 animals per sample. (D) ins-6p::dYFP transcriptional reporter activity was measured in the same individuals dauers at the following time points: at the dauer stage, six hours after transfer to intermediate pheromone conditions (shaded yellow), and eighteen hours after transfer to high pheromone conditions (shaded red). Each line indicates the same animal (n=21 total). Animals that exited dauer and remained dauers are indicated in orange and blue, respectively.

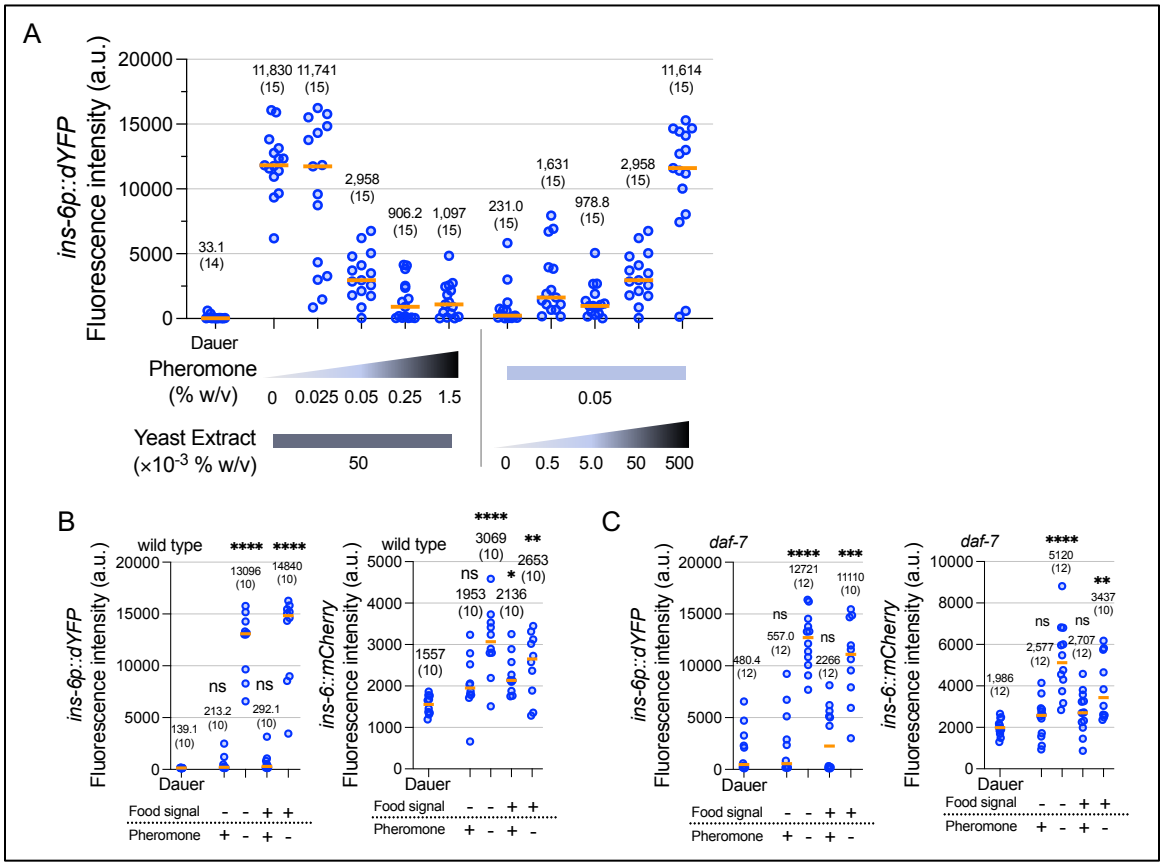

Figure 2.4. ins-6 expression reflects food and pheromone integration.

(A) ins-6p::dYFP transcriptional reporter activity in the ASJ neurons of dauers before transfer ("Dauer") and three hours after transfer to varying concentrations of food signal (yeast extract) and pheromone. Note that the 0.05% w/v pheromone + 0.05% w/v yeast extract sample is shared between the left and right halves of the graph. (B-C) ins-6p::dYFP transcriptional reporter activity in the ASJs (left) and ins-6::mCherry translational reporter activity from coelomocytes (right) were measured in wild-type dauers (B) or daf-7 loss-of-function dauers (which do not exit dauer when kept at high temperatures) (C) before ("Dauer") and three hours after being transferred to plates with different amounts of food and pheromone ("+", 0.5% yeast extract or 0.5% pheromone; "-", 0% yeast extract or 0% pheromone). ns, not significant, *, $p<0.05$, **, $p<0.01$, ***, $p<0.001$, ****, $p<0.0001$ by Kruskal Wallis Test with Dunn's multiple comparison correction when compared to

"Dauer." For all graphs: Each dot represents one animal. Medians are depicted by the orange bar. Medians and sample sizes are written.

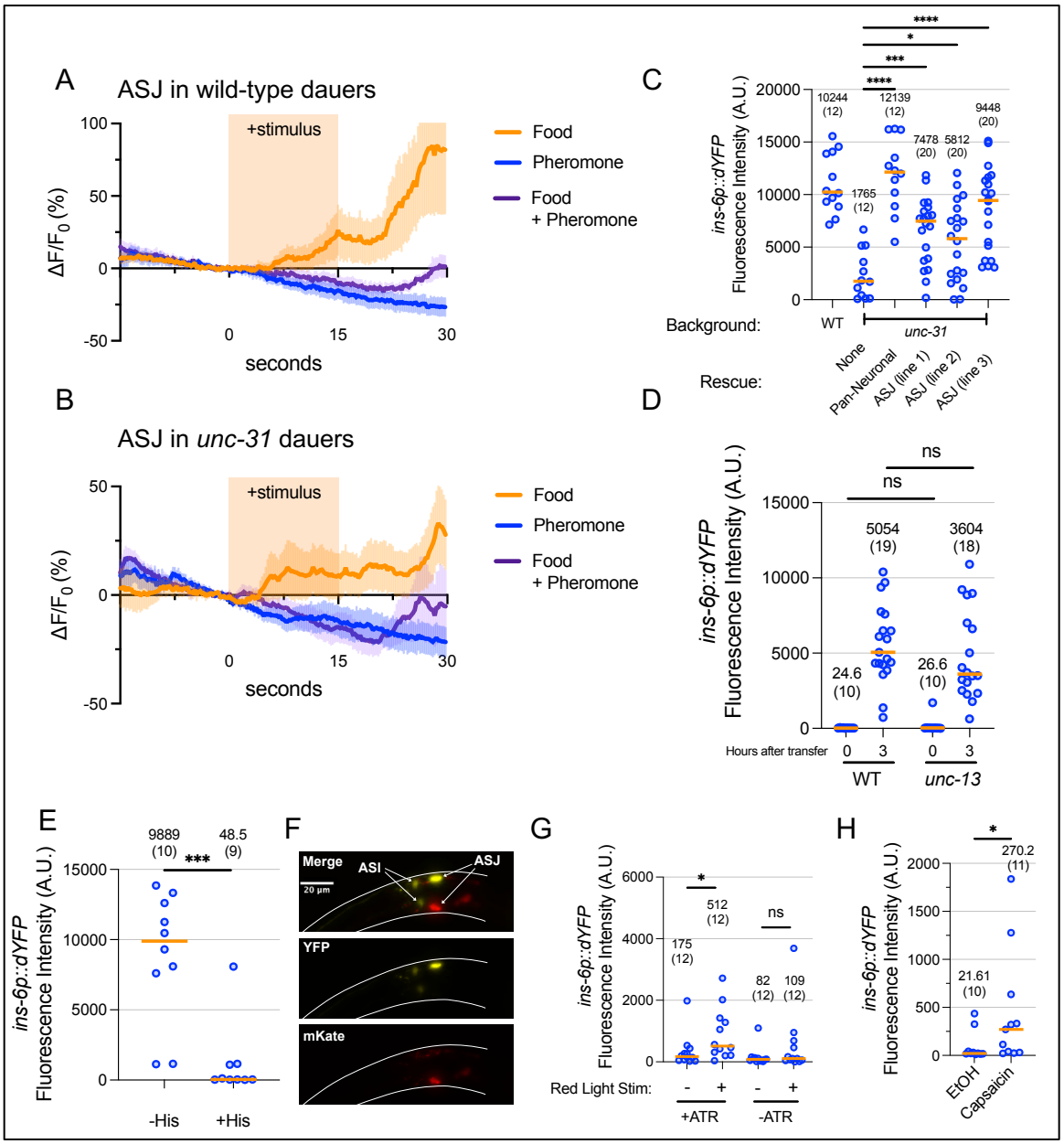

Figure 2.5. ASJ neuronal activity shows sensory integration and is necessary for ins-6 upregulation.

(A,B) Calcium traces of ASJ in wild-type (A) or unc-31 loss-of-function mutant (B) dauers in response to pheromone, food (bacterial supernatant), or a mixture of both. Shown are the mean ± SEM from 10-12 ASJ neurons from six animals. Individual traces can be found in Figure S5. (C) ins-6p::dYFP transcriptional reporter activity in ASJ was measured in wild-type or unc-31 loss-of-function mutant dauers (with or without various rescue

constructs that express unc-31 cDNA pan-neuronally or specifically in ASJ) three hours after transfer to favorable conditions. ns, not significant, **, $p<0.01$, ****, $p<0.0001$ by one-way ANOVA with Dunnett's multiple comparisons correction compared to "WT." (D) ins-6p::dYFP transcriptional reporter activity was measured in the ASJs of wild-type or unc-13 loss-of-function mutant dauers before and three hours after transfer to favorable conditions. ns, not significant, by unpaired t-test. (E) Dauers expressing the histamine-gated chloride channel in the ASJ neurons (trx-1p::HisCl-T2A-mKate2) were transferred to favorable plates with or without histamine and imaged three hours later for ins-6p::dYFP transcriptional reporter activity in the ASJ neurons. ***, $p<0.001$ by Mann Whitney U-Test. (F) Image of a mosaic animal in which the trx-1p::HisCl-T2A-mKate2 extrachromosomal array only expressed in one of the two ASJ nerons. (G, H) Dauers expressing the red-shifted rhodopsin Chrimson (G) or the capsaicin-activated cation channel TRPVI (G) in the ASJs were subjected to the stimulation conditions shown while on high-pheromone conditions and imaged two (F) or three (G) hours later for ins-6p::dYFP transcriptional reporter activity in the ASJs. ns, not significant. *, $p<0.05$ by Mann Whitney U-Test. In all graphs: Each dot represents one animal. Medians are depicted by the orange bar. Medians and sample sizes are written.

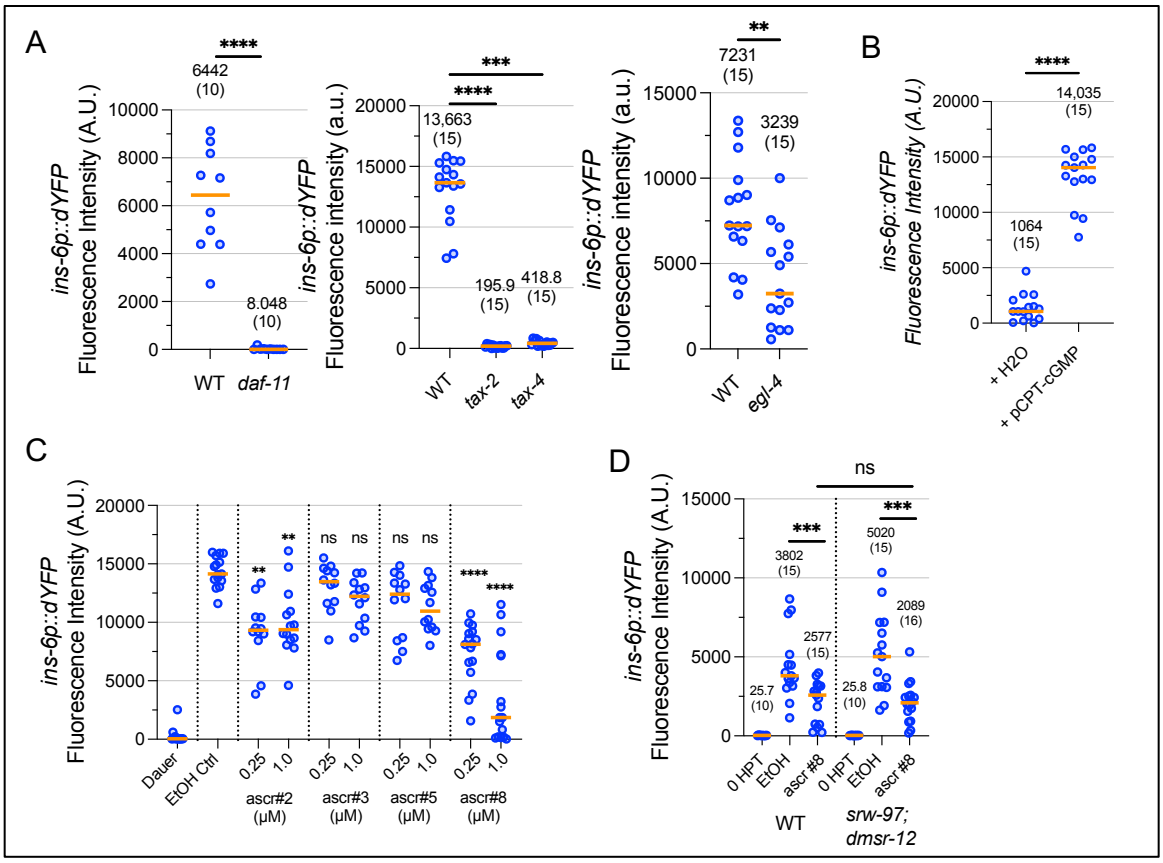

Figure 2.6. ins-6 upregulation is regulated by cGMP signaling and ascr#8.

(A) daf-11, tax-2, tax-4, and egl-4 loss-of-function mutant dauers were transferred to favorable conditions and measured for ins-6p::dYFP transcriptional reporter activity in the ASJ neurons three hours later. ****, p<0.0001 by Mann Whitney U-Test for daf-11. ***, p<0.001, ****, p<0.0001 by Kruskal Wallis Test with Dunn's multiple comparison correction for tax-2 and tax-4 compared to "WT." **, p<0.01 by Mann Whitney U-Test for egl-4. (B) Dauers were transferred to high pheromone plates containing 1 mM pCPT-cGMP or H2O control and measured for ins-6p::dYFP transcriptional reporter activity in the ASJ neurons three hours later. ****, p<0.0001 by Mann Whitney U-Test (C) Dauers were transferred to plates containing ascarosides at 250 nM or 1 μM and measured for ins-6p::dYFP transcriptional reporter activity in the ASJ neurons three hours later. ns, not significant, **, p<0.01, ****, p<0.0001 by Kruskal Wallis Test with Dunn's multiple comparison correction compared to "EtOH Ctrl." (C) srw-97; dmsr-12 loss-of-function

mutants were transferred to ascr#8 (1 μM) or EtOH control plates and measured for ins-6p::dYFP transcriptional reporter activity in the ASJ neurons three hours later. ns, not significant, ***, $p<0.001$ by Mann Whitney U-Test. For all graphs: Each dot represents one animal. Medians are depicted by the orange bar. For (A), (B), and (D), medians and sample sizes are written.

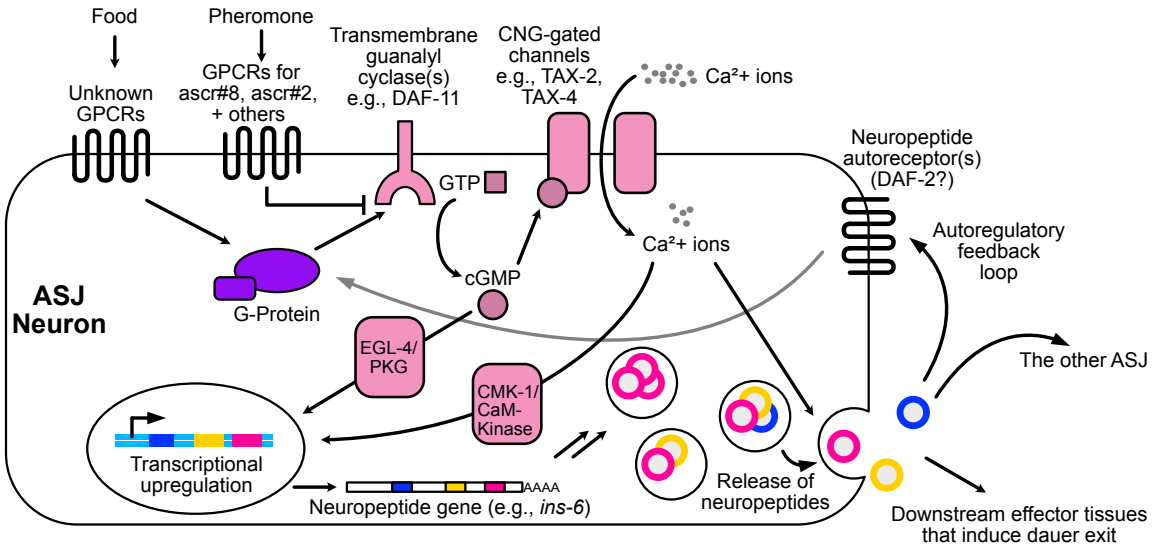

Figure 2.7. Model for ins-6 upregulation during dauer exit.

In each ASJ neuron, GPCRs specific to food signals trigger a G-protein signaling pathway that activates the transmembrane guanylyl cyclase DAF-11 to increase cGMP production. GPCRs specific to pheromone (including the ascarosides ascr#8 and ascr#2) inhibit this activation. cGMP activates cGMP-dependent transcription pathways such as through the cGMP-dependent kinase EGL-4/PKG while also increasing calcium influx through CNG-gated channels such as TAX-2/TAX-4. The resulting calcium increase can both activate calcium-dependent transcription (such as through CMK-1/CaM-Kinase) and promote secretion of neuropeptides, which may include INS-6, in a process dependent on UNC-31/CAPS. Once secreted, these neuropeptides bind to receptors on the same ASJ and/or the other ASJ neuron and, upon reaching a certain threshold, triggers an autoregulatory positive feedback loop that further increases production and secretion of INS-6 from the ASJs. This positive feedback promotes commitment to exit the dauer state by causing an irreversible buildup of INS-6 production and secretion. INS-6 then signals to downstream tissues that execute the relevant dauer exit gene programs.

2.8 Supplementary figures and tables

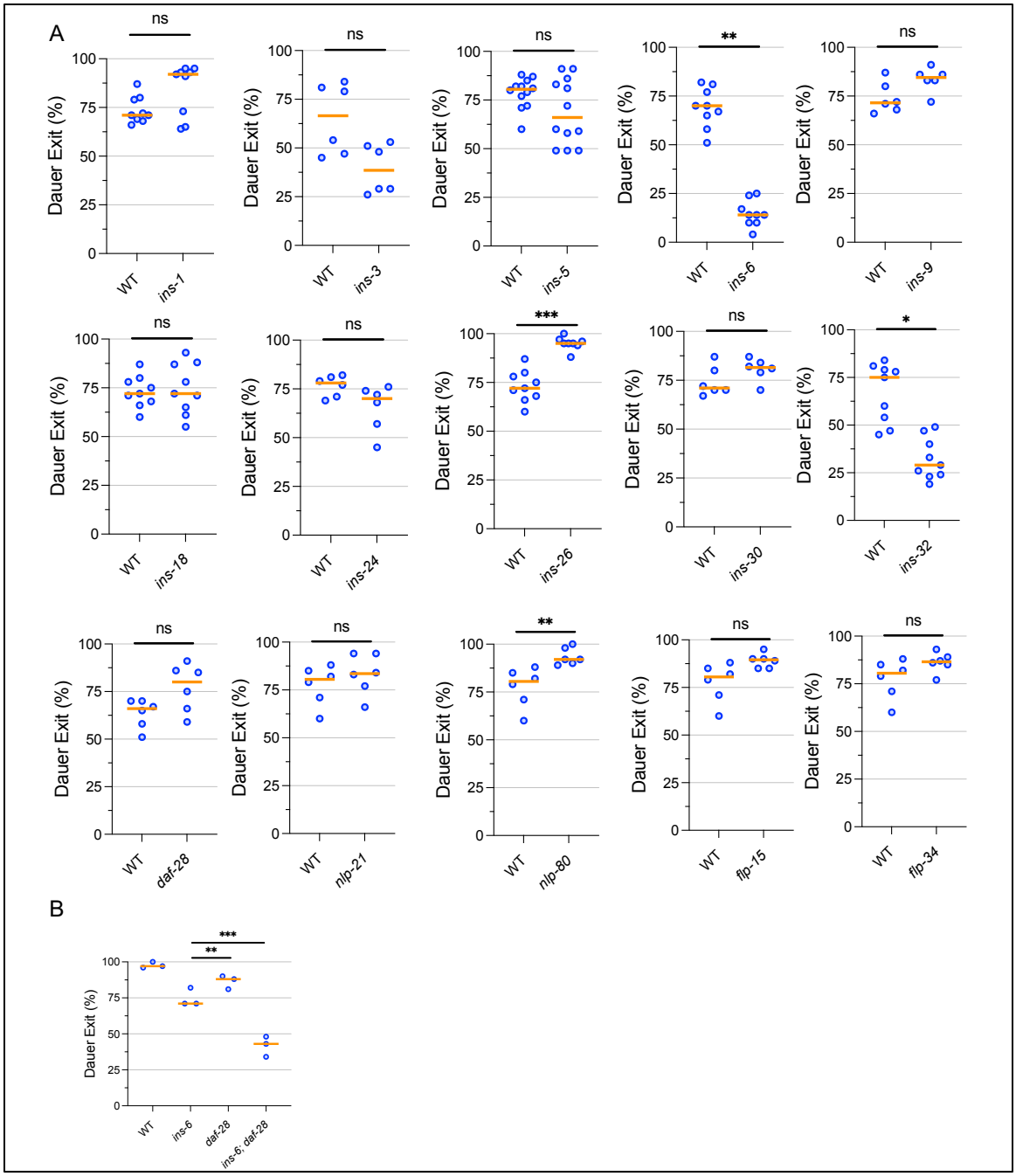

Figure S2.1. Supplementary figure to Figure 2.1

(A) Dauer exit rates of mutants defective for single neuropeptide genes. Refer to Table S1 for list of strains. Bars indicate medians. Each dot is the dauer exit % from an assay plate containing 50-100 animals each. ns, not significant, ***, p<0.001, **, p<0.01, compared

to “WT” by Welch ANOVA with Dunnett’s T3 multiple comparison correction. (B) Dauer exit rates of the double mutant ins-6; daf-28 compared to single mutants defective for each neuropeptide gene alone. Compared to experiments performed for Fig. 2.1D, this assay was performed using a lower pheromone concentration that induces more wild-type dauers to exit. Bars indicate medians. Each dot is the dauer exit % from an assay plate containing 50-100 animals each.

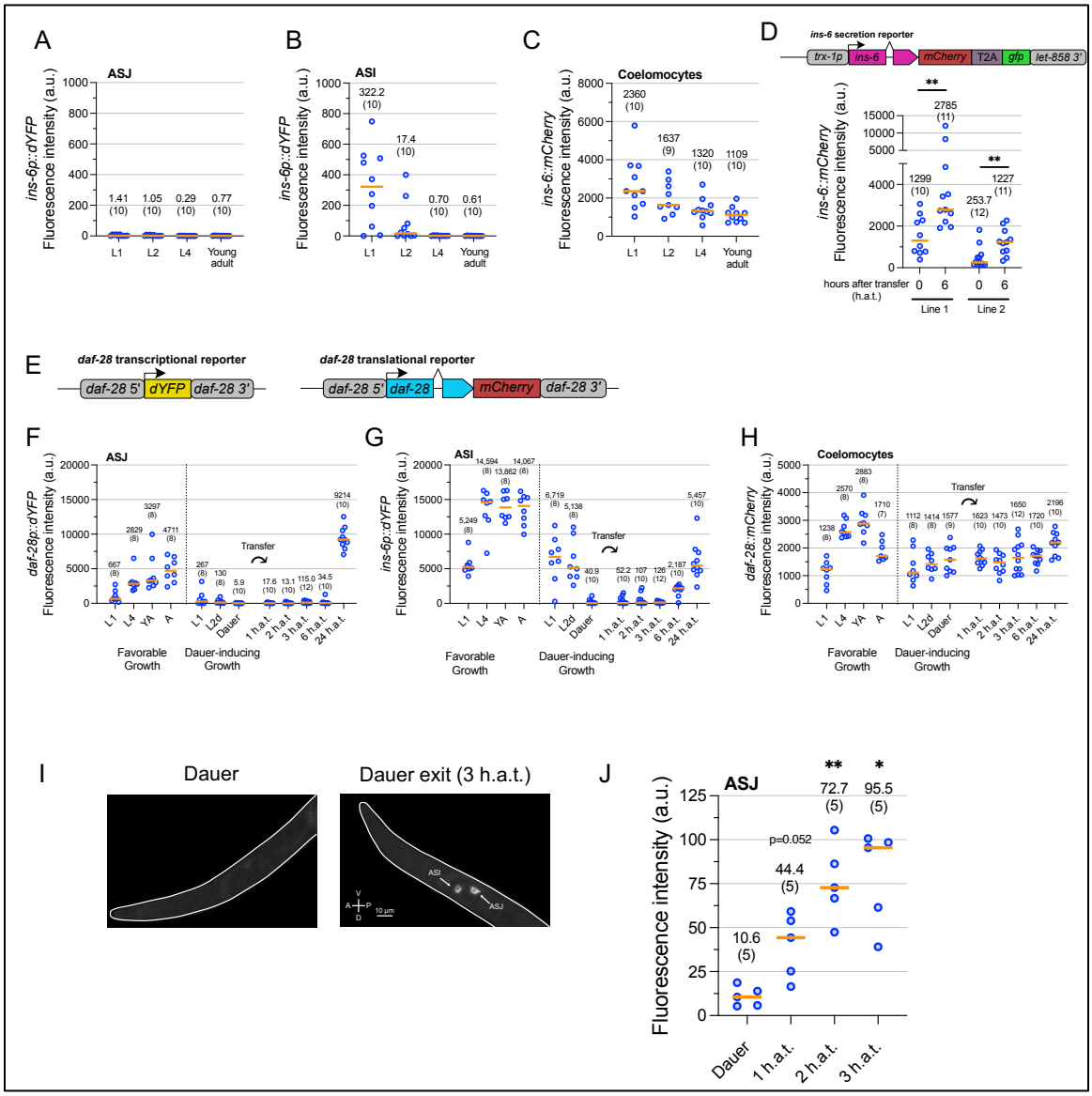

Figure S2.2. Supplementary figure to Figure 2.2

(A-C) Quantification of ins-6p::dYFP transcriptional reporter signal (measured in arbitrary units (a.u.)) in ASJ (A) or ASI (B) and ins-6::mCherry translational reporter signal in the coelomocytes (C) during reproductive growth. (D) An ins-6 secretion reporter was built by driving ins-6::mCherry expression using the ASJ-specific promoter trx-1p and the broadly expressing let-858 3' untranslated region (UTR). Shown are the mCherry fluorescence intensities measured in the coelomocytes for two independent extrachromosomal array lines bearing the ins-6 secretion reporter in dauers before transfer to favorable conditions

(0 h.a.t.) and six hours after transfer to favorable conditions (6 h.a.t.). While the T2A signal was included to simultaneously measure transcriptional activity driven the trx-1p promoter, we did not observe any noticeable GFP signal. (E) Design of daf-28 transcriptional and translational reporters, which were constructed similarly to those for ins-6. (F-H) Quantification of daf-28p::dYFP transcriptional reporter signal (measured in arbitrary units (a.u.)) in ASJ (F) or ASI (G) and daf-28::mCherry translational reporter signal in the coelomocytes (H) during favorable growth (non-dauer-inducing) or dauer-inducing growth, as well as dauers after transfer to favorable conditions (indicated by curved arrow) for the indicated lengths of time. YA, young adult. A, adult. h.a.t., hours after transfer to favorable conditions. See Materials and Methods for precise time points taken during animal development. Dotted lines indicate different populations of animals from which individual animals were sampled for imaging experiments. (I) Representative image of mRNA FISH analysis for ins-6 mRNA in a dauer (left) and an exiting dauer 3 hours after transfer to favorable conditions). (J) mRNA FISH signal quantification in the ASJ neurons measured in arbitrary units (a.u.). **, $p<0.01$, *, $p<0.05$ by Welch ANOVA with Dunnett's T3 multiple comparison correction when compared to "Dauer." For all quantification graphs, individual dots represent one animal. Medians are depicted by the orange bar. Medians and sample sizes are written.

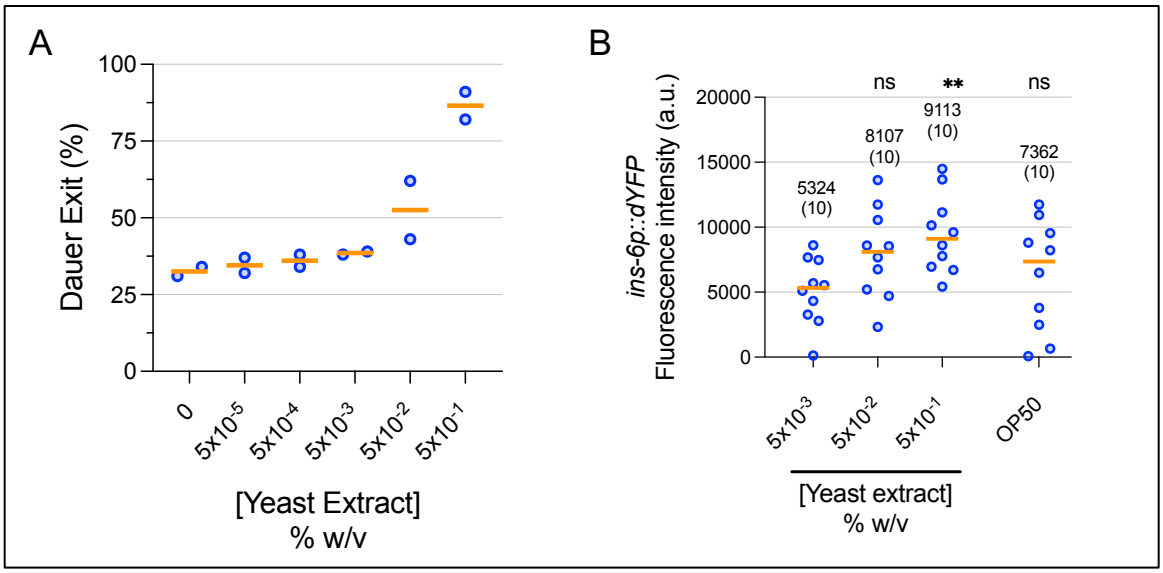

Figure S2.3. Supplementary figure to Figure 2.4

(A) Dauers were transferred onto plates containing an intermediate-pheromone concentration (0.05% w/v) with varying amounts of yeast extract and scored for exit 24 hours later. Bars indicate medians. Each dot is the dauer exit % from an assay plate containing 50-100 animals each. (B) ins-6p::dYFP transcriptional reporter activity was measured in the ASJs of dauers three hours after transfer to plates with an intermediate-pheromone concentration along with various concentrations of yeast extract or a small volume of S-Basal washed live OP50 spotted onto the plate. ns, not significant, **, $p<0.01$ by Welch ANOVA with Dunnett's T3 multiple comparisons correction when compared to "$5x10^{-3}$% w/v yeast extract." Each dot represents one animal. Medians are depicted by the orange bar. Medians and sample sizes are written.

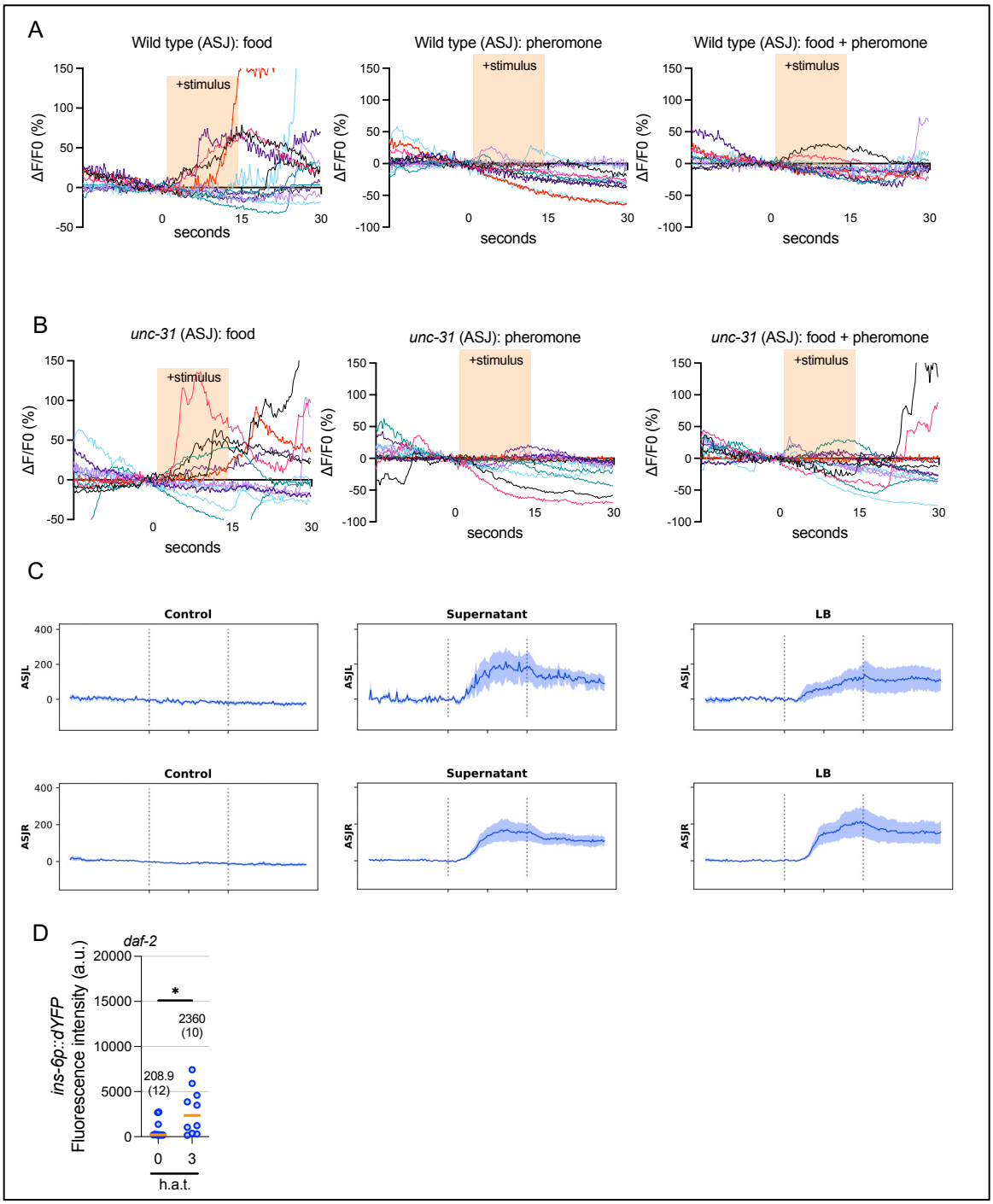

Figure S2.5. Supplementary figure to Figure 2.5

(A,B) Individual calcium traces from 10-12 ASJ neurons across six individual animals in wild-type (A) or unc-31 loss-of-function (B) dauers in response to pheromone, food

(bacterial supernatant), or a mixture of both. Aggregate traces are shown in Figure 5A, B. (C) Calcium traces of ASJ neurons (L and R) in wild-type L4 larvae in response to control (buffer), supernatant, and LB. Shown are mean +/- SEM from 7 animals. Each plot includes 15 seconds before stimulus delivery, 15 s of stimulus delivery, and 15 s period after the delivery; the dotted vertical lines indicate the start and end of the stimulus delivery. F0 was defined as average density of the 5 s period before the stimulus delivery. (C) ins-6p::dYFP transcriptional reporter activity in the ASJ neurons was measured in daf-2(e1370) loss-of-function mutant dauers that were transferred to no-pheromone conditions. Note how the magnitude of ins-6 transcriptional reporter activity is smaller compared to those of comparable experiments such as in Fig. 2.2C and 4B. *, $p<0.05$ by Mann Whitney U-Test. Each dot represents one animal. Medians are depicted by the orange bar. Medians and sample sizes are written.

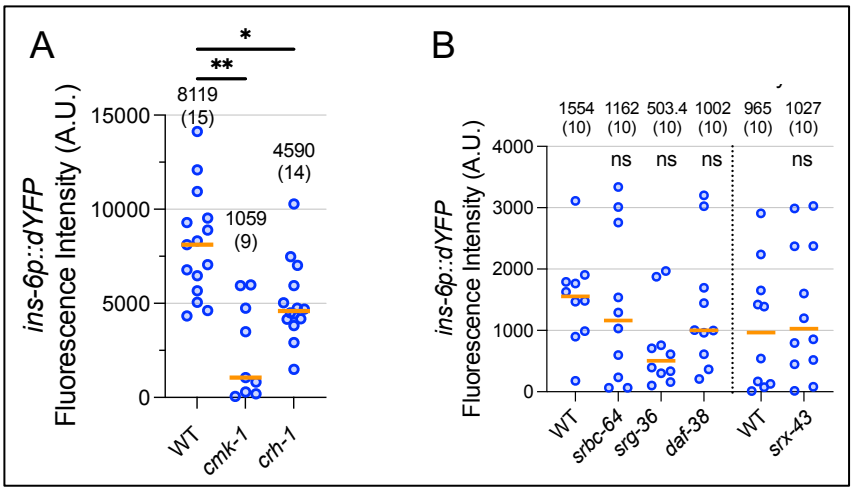

Figure S2.6. Supplementary figure to Figure 2.6

(A) cmk-1 and crh-1 loss-of-function mutant dauers were transferred to favorable conditions and measured for ins-6p::dYFP transcriptional reporter activity in the ASJ neurons three hours later. *, $p<0.05$, **, $p<0.01$ by Kruskal Wallis Test with Dunn's multiple comparison correction when compared to "WT." (B) Left of dotted line: srbc-64, srg-36, and daf-38 loss-of-function mutant dauers were transferred to threshold pheromone conditions and measured for ins-6p::dYFP transcriptional reporter activity in the ASJ neurons three hours later. Right of dotted line: srx-43(sy1959) dauers bearing an extrachromosomal array with the ins-6p::dYFP reporter transgene were transferred to favorable conditions and measured for YFP signal in the ASJ neurons three hours later. ns, not significant, by Kruskal Wallis Test with Dunn's multiple comparison correction compared to "WT." For all graphs: Each dot represents one animal. Medians are depicted by the orange bar. Medians and sample sizes are written.

Table S2.1: List of strains used in this study

Figure	Strain	Genotype	Origin	Notes
1C	N2		(94)	
1C	PS7112	sbt-1(ok901)	(95)	Constructed by outcrossing RB987 to our lab's N2 3x
1C	PS6895	egl-3(nr2090)	(96, 97)	Outcrossed to our lab's N2 4x
1C	KP2018	egl-21(n476)	(98)	
1C	CB169	unc-31(e169)	(94)	
1C	KP2048	ric-7(nu447)	(26)	
1D	FX01888	ins-1(tm1888)	NBRP (93)	
1D	VC1841	ins-3(ok2478)	CGC (95)	
1D	RB2544	ins-4(ok3534)	(95)	
1D	FX2560	ins-5(tm2560)	NBRP (93)	
1D	PS9510	ins-6(tm2416)	NBRP (93)	Constructed by outcrossing FX2416 to our lab's N2 3x
1D	FX3618	ins-9 (tm3618)	NBRP (93)	
1D	VC1218	ins-18(ok1672)	(95)	
1D	PS9417	ins-24(sy1761)	This study	Generated using a CRISPR Stop-In cassette (88)
1D	FX1983	ins-26(tm1983)	NBRP (93)	
1D	RB1809	ins-30(ok2343)	(95)	
1D	PS9712	ins-32(sy1905)	This study	Generated using a CRISPR Stop-In cassette
1D	PS9480	daf-28(tm2308)	NBRP (93)	Outcrossed ZM7963 to N2 4x and isolated the daf-28(tm2308) mutation.
1D	PS9520	nlp-21(sy1807)	This study (88)	Generated using a CRISPR Stop-In cassette

1D	PS8307	nlp-80(sy1264)	This study	Generated using a CRISPR Stop-In cassette
1D	VC2504	flp-15(gk1186)	(95)	
1D	PS7220	flp-34 (sy810)	(25)	
S1B	N2		(94)	
S1B	PS9510	ins-6(tm2416)	NBRP (93)	Already described above
S1B	PS9480	daf-28(tm2308)	NBRP (93)	Outcrossed ZM7963 to N2 4x and isolated the daf-28(tm2308) mutation.
S1B	PS9518	ins-6(tm2416); daf-28(tm2308)	This study	Cross between PS9480 and FX2416
2C-H, S2A-C	PS9750	syIs875	This study	syIs875 [ins-6p::destabilized-YFP; ins-6p::ins-6::mCherry] V constructed via X-Ray mediated integration of syEx1937[pQZ::ins-6p::dYFP::ins-6UTR (100 ng/uL), pQZ::ins-6::mCherry (25 ng/uL), unc-122p(coel)::gfp (40 ng/uL), 1 kb DNA ladder (35 ng/uL)]. Line 1 of 2

S2D	PS10304	syEx1958	This study	syEx1958[trx-1p::ins-6::mCherry-T2A-gfp::let-858UTR (100 ng/uL), unc-122p(coel)::gfp (40 ng/uL), NEB 1 kb ladder (60 ng/uL). Line 1 of 2.
S2D	PS10305	syEx1959	This study	syEx1959[trx-1p::ins-6::mCherry-T2A-gfp::let-858UTR (100 ng/uL), unc-122p(coel)::gfp (40 ng/uL), NEB 1 kb ladder (60 ng/uL). Line 2 of 2.
S2E-H	PS9789	syIs876	This study	Integrated line (via X-Ray irradiation) of PS9725 syEx1941[daf-28p::dYFP (100 ng/uL), daf-28::mCherry (25 ng/uL), unc-122p(coel)::gfp (40 ng/uL), NEB 1 kb ladder (35 ng/uL)]
S2I, J	N2		(94)	
3A, B	PS9750	syIs875	This study	Already described above
4A, B	PS9750	syIs875	This study	Already described above
4C	PS9760	daf-7(e1372); syIs875	This study	

S4A-B	PS9750	syIs875	This study	Already described above
5A	KP9672	nuIs556[ptrx-1::GCaMP6.0s]	(34)	nuIs556[ptrx-1::GcaMP6.0s]
5B	PS10295	unc-31(e169); nuIs556	This study	Cross between CB169 and KP9672 nuIs556[ptrx-1::GcaMP6.0s]
5C	PS9903	unc-31(e169); syIs875	This study	Cross between CB169 and PS9750 syIs875[ins-6p::destabilized-YFP; ins-6p::ins-6::mCherry]
5C	PS10316	unc-31(e169); syIs875; syEx1960	This study	syEx1960[KG#121 rab-3p::unc-31(cDNA) 100 ng/uL, unc-122p(coel)::rfp 40 ng/uL, NEB 1 kb ladder 10 ng/uL]
5C	PS10289	unc-31(e169); syIs875; syEx1956	This study	syEx1956[trx-1p::unc-31(cDNA)::T2A-mKate2-let858UTR 100 ng/uL, unc-122p(coel)::rfp 40 ng/uL, NEB 1 kb ladder 10 ng/uL] Line 1 of 3
5C	PS10290	unc-31(e169); syIs875; syEx1957	This study	syEx1956[trx-1p::unc-31(cDNA)::T2A-mKate2-let858UTR 100 ng/uL, unc-122p(coel)::rfp 40 ng/uL, NEB 1 kb ladder 10 ng/uL] Line 2 of 3

5C	N/A	unc-31(e169); syIs875; mzEx116C2	This study	mzEx116C2[trx-1p::unc-31(cDNA)::T2A-mKate2-let858UTR 100 ng/uL, unc-122p(coel)::rfp 40 ng/uL, NEB 1 kb ladder 10 ng/uL] Line 3 of 3
5D	PS9749	syIs874	This study	syIs874 [ins-6p::destabilized-YFP; ins-6p::ins-6::mCherry] V constructed via X-Ray mediated integration of syEx1937[pQZ::ins-6p::dYFP::ins-6UTR (100 ng/uL), pQZ::ins-6::mCherry (25 ng/uL), unc-122p(coel)::gfp (40 ng/uL), 1 kb DNA ladder (35 ng/uL)]. Line 2 of 2
5D	PS9851	unc-13(e51); syIs874	This study	Cross between MT7929 unc-13(e51) and PS9749 syIs874 [ins-6p::dYFP; ins-6p::ins-6::mCherry]
5E, F	PS10284	pha-1(e2123ts); syIs875; syEx1954	This study	syIs875[ins-6p::destabilized-YFP; ins-6p::ins-6::mCherry] V syEx1954[trx-1p::HisCl-T2A-mKate2 75 ng/µL, pBX pha-1(+) cDNA 75 ng/µL 50 ng/µL, 1 kb ladder (NEB) 25 ng/µL]

5G	PS10282	pha-1(e2123ts); syIs875; syEx1952	This study	syIs875[ins-6p::destabilized-YFP; ins-6p::ins-6::mCherry] V syEx1952[trx-1p::Chrimson-T2A-mKate2 75 ng/µL, pBX pha-1(+) cDNA 75 ng/µL 50 ng/µL, 1 kb ladder (NEB) 25 ng/µL]
5H	PS10330	pha-1(e2123ts); syIs875; syEx1964	This study	syIs875[ins-6p::destabilized-YFP; ins-6p::ins-6::mCherry] V syEx1964[trx-1p::TRPV1-T2A-mKate2 75 ng/µL, pBX pha-1(+) cDNA 60 ng/µL 50 ng/µL, 1 kb ladder (NEB) 40 ng/µL]
S5A	KP9672	nuIs556[ptrx-1::GCaMP6.0s]	(34)	nuIs556[ptrx-1::GcaMP6.0s]
S5B	PS10295	unc-31(e169); nuIs556	This study	Cross between CB169 and KP9672 nuIs556[ptrx-1::GcaMP6.0s]
S5D	PS9759	daf-2(e1370); syIs875	This study	
6A	PS9749	syIs874	This study	Already described above
6A	PS9850	syIs874; daf-11(m47)	This study	Cross between PS9749 syIs874[ins-6p::destabilized-YFP; ins-6p::ins-

				6::mCherry] IV and PS2782 daf-11(m47) V
6A	PS9750	syIs875	This study	Already described above
6A	PS10389	tax-2(p671); syIs875	This study	Cross between PS9750 syIs875 [ins-6p::dYFP; ins-6p::ins-6::mCherry] V and PR671 tax-2(p671) I
6A	PS10390	tax-4(p678); syIs875	This study	Cross between PS9750 syIs875 [ins-6p::dYFP; ins-6p::ins-6::mCherry] V and PR678 tax-4(p678)
6A	PS10411	egl-4(n479); syIs875	This study	Cross between PS9750 syIs875 [ins-6p::dYFP; ins-6p::ins-6::mCherry] and MT1074 egl-4(n479)
6B, C	PS9750	syIs875	This study	Already described above
6D	PS9749	syIs874	This study	Already described above
6D	PS10370	srw-97(knu456); syIs874; dmsr-12(sy1559)	This study	Cross between PS8890 dmsr-12(sy1959) (88), JSR70 (55), and PS9749. ins-6 reporter in a srw-97; dmsr-12 double mutant background. Note that the original dmsr-12 mutation from

				JSR70 was exchanged for the new sy1959 allele created via CRISPR STOP-IN, and the him-5 mutation was crossed out.
S6A	PS9750	syIs875	This study	Already described above
S6A	PS10391	cmk-1(oy21); syIs875	This study	Cross between PS9750 syIs875 [ins-6p::dYFP; ins-6p::ins-6::mCherry] and PY1589 cmk-1(oy21)
S6A	PS10396	crh-1(tz2); syIs875	This study	Cross between PS9750 syIs875 [ins-6p::destabilized-YFP; ins-6p::ins-6::mCherry] V and YT17 crh-1(tz2)
S6B	PS9941	srbc-64(tm1946); syIs875	This study	Cross between PS9750: syIs875[ins-6p::dYFP; ins-6::mCherry] and PY6560 srbc-64(tm1946)
S6B	PS9942	syIs875; srg-36(sy1961)	This study	Cross between PS9750: syIs875[ins-6p::dYFP; ins-6::mCherry] and PS9886 srg-36(sy1961), which was generated using a CRISPR Stop-In cassette (88)
S6B	PS9944	daf-38(ok2765); syIs875	This study	Cross between PS9750 syIs875[ins-

				6p::dYFP; ins-6::mCherry] and PS9943 daf-38(ok2765), AKA RB2090 (outcrossed to our lab's N2 3x)
S6B	PS9704	syEx1937	This study	syEx1937[ins-6p::dYFP::ins-6UTR (100 ng/uL), ins-6::mCherry (25 ng/uL), unc-122p(coel)::gfp (40 ng/uL), 1 kb DNA ladder (35 ng/uL)]
S6B	PS10138	srx-43(sy1959); syEx1937	This study	Cross between PS9704 syEx1937 and PS9884 srx-43(sy1959) , which was generated using a CRISPR Stop-In cassette (88)

Table S2.2: List of probes used in ins-6 mRNA FISH

Probe #	Sequence
1	gttgctagatactcgtcaaa
2	aacggaaaatgagtacgggg
3	ttggagtgcgcacaaaacga
4	ttgacggaaacttgcagcga
5	ttcagacattgaaggaccga
6	aagttgcatgcttgctgatt
7	gttgtgttgaagttcacgga
8	attggtcggtgagctgattc
9	tggaacacgtcttgctcgtg
10	agatgagttttcttccgcag
11	ccacagacagccatgactaa
12	cttcttgtgggttgcaaaga
13	attcagtcgcaatgtccttt

14	cagaacactgatttccgcag
15	catggacaacaagcagatct
16	actgatatcggagtaaaggt
17	acgagattgtatggtacaga
18	cacgggtgaaacgagattca
19	gggatgacagatttgatgag
20	aggtttattgtacaagccac

Chapter 3

Both entry to and exit from diapause arrest in Caenorhabditis elegans are regulated by a steroid hormone pathway

M.G. Zhang, P.W. Sternberg, Both entry to and exit from diapause arrest in Caenorhabditis elegans are regulated by a steroid hormone pathway. Development 149, dev200173 (2022). https://doi.org/10.1242/dev.200173

3.1 Abstract

Diapause arrest in animals such as Caenorhabditis elegans is tightly regulated so that animals make appropriate developmental decisions amidst environmental challenges. Fully understanding diapause requires mechanistic insight of both entry and exit from the arrested state. While a steroid hormone pathway regulates the entry decision into Caenorhabditis elegans dauer diapause, its role in the exit decision is less clear. A complication to understanding steroid hormonal regulation of dauer has been the peculiar fact that steroid hormone mutants such as daf-9 form partial dauers under normal growth conditions. Here, we corroborate previous findings that daf-9 mutants remain capable of forming full dauers under unfavorable growth conditions and establish that the daf-9 partial dauer state is likely a partially exited dauer that has initiated but cannot complete the dauer exit decision. We show that the steroid hormone pathway is both necessary for and promotes complete dauer exit, and that the spatiotemporal dynamics of steroid hormone regulation during dauer exit resembles that of dauer entry. Overall, dauer entry and dauer exit are distinct developmental decisions that are both controlled by steroid hormone signaling.

3.2 Introduction

Animals must be able to adapt to changing environments to survive against uncertain and stress-inducing circumstances. One such adaptive mechanism is diapause, a state of developmental arrest typically characterized by metabolic depression and stress resistance (1). Diapause is a dynamic process that involves successive developmental decisions dictating entry, maintenance, and exit from the dormant state (2, 3). Diapause is well conserved across the animal kingdom including nematodes, insects, crustaceans, fish, and mammals (1, 3–5).

Upon encountering adverse conditions during larval growth, Caenorhabditis elegans exit the cycle of reproductive development and instead enter the alternative, diapause state, termed dauer, which grants them increased durability and longevity to protect against environmental insults and allows them to disperse in search of a more favorable

environment (4, 6). The dauer entry decision-making process comprises two distinct subdecisions. First-stage (L1) larvae decide between developing into L2 or pre-dauer L2d larvae, depending on whether conditions are favorable or unfavorable, respectively (the "L1 to L2/L2d subdecision"). If conditions sufficiently improve, then L2d larvae choose reproductive development by becoming L3 larvae, but if not they become dauer larvae (the "L2d to L3/Dauer subdecision"; Golden and Riddle, 1984). While in the dauer state, animals continuously assess their environment and, when conditions improve by way of an increased food to pheromone ratio, exit the dauer state to return to the reproductive cycle as L4 larvae (8). A complete understanding of this developmental decision-making process requires a synthesis of information involving both the dauer entry subdecisions and the dauer exit decision. The majority of dauer studies in C. elegans have focused on dauer entry (4, 9, 10), leaving much to be explored for dauer exit.

Previous studies have found multiple pathways that govern the dauer entry decision, including cGMP signaling, insulin growth factor signaling, TGF-β signaling, and steroid hormone signaling (4, 10). The steroid hormone pathway has been placed genetically downstream in the dauer entry process and is thought to serve as a convergence point for both the insulin and the TGF-β signaling (10) in controlling dauer development. The steroid hormone pathway centers on DAF-12, a nuclear hormone receptor with homology to the vertebrate farnesoid-X receptor (FXR; Antebi, 2015; Antebi et al., 1998). The major endogenous ligands for DAF-12/FXR are steroid hormones collectively referred to as dafachronic acids (DA), which include Δ7-DA (dafa#2) and Δ4-DA (dafa#4) among others (13–15). DAF-12/FXR regulation of its transcriptional targets depends on environmental growth conditions, which in turn dictate the presence of DAF-12/FXR ligands. Under favorable conditions, DAF-9 catalyzes the formation of DAs such as Δ-7 DA that bind to DAF-12/FXR and specify reproductive adulthood. Under unfavorable conditions, unliganded DAF-12/FXR interacts with the corepressor DIN-1/CoR to specify dauer entry (10).

Biosynthesis of all known DAs require the cytochrome P450 enzyme DAF-9, and therefore daf-9 null mutants are completely dauer formation constitutive (Daf-c) (13, 16, 17). daf-9 is constitutively expressed in a pair of neuroendocrine cells termed the XXX cells but shows variable upregulation in the hypodermis depending on environmental conditions and developmental state (16, 18). When larvae choose the reproductive pathway during either of the two dauer entry subdecisions, daf-9 is upregulated throughout the hypodermis and amplifies steroid hormone production to instigate reproductive development (16, 18). While the role of the steroid hormone pathway in regulating dauer entry is well-characterized, how the same steroid hormone pathway governs the dauer exit decision remains substantially less clear.

A complete analysis concerning how steroid hormone signaling regulates dauer arrest must also account for the well-documented observation that Daf-c mutants impaired for steroid hormone biosynthesis and/or signaling such as daf-9, daf-36 (encoding a Rieske-like oxygenase that catalyzes the first step of steroid hormone biosynthesis), ncr-1 and ncr-2 (encoding two putative cholesterol transporters), and Daf-c alleles of daf-12 do not form full dauers under favorable growth conditions as do other Daf-c strains such as daf-2(e1370) or daf-7(e1372) (12, 16, 19, 20). Full dauers are characterized by radial and pharyngeal constriction, immobility, pumping quiescence, and a darkened intestine owing to increased fat storage (6, 21). Steroid hormone mutants such as daf-9 instead form “partial” or “dauer-like” larvae that resemble dauers but exhibit non-dauer traits such as sporadic pumping, increased mobility, a slightly enlarged pharynx, and a lighter body (16, 22). Partial dauers are not exclusive to steroid hormone mutants, as they are also observed in double mutants involving daf-16 (23, 24), which encodes a homolog of the forkhead transcription factor FOXO and is the major downstream target of the insulin pathway (25).

Whether steroid hormone mutants form partial or full dauers appear to depend on growth conditions since daf-9(dh6) and daf-12(rh273) become full dauers under unfavorable growth conditions (12, 16). Why this distinction occurs remains unclear, but it has been speculated that the partial dauer may have first been a full dauer that attempted dauer exit

(owing to favorable growth conditions) but could not complete it (12). A comprehensive model of how steroid hormones govern dauer entry and exit should be able to explain why steroid hormone mutants form partial dauers under favorable growth conditions unlike other Daf-c strains (Fig. 3.1).

Here we provide evidence that daf-9 partial dauers are likely animals in a state of incomplete dauer exit rather than a state of incomplete dauer formation. Furthermore, we show that the daf-9 partial dauer state requires insulin and TGF-β signaling, and that activation of these pathways is sufficient to induce a partial dauer state. We characterize the regulatory role of steroid hormones in dauer exit, demonstrating that the steroid hormone biosynthesis pathway is both necessary for and sufficient to induce dauer exit. We also show that the spatiotemporal regulation of daf-9 during dauer exit closely mirrors that of the L1 to L2 vs. L2d dauer entry subdecision, which means that C. elegans use steroid hormone signaling in similar ways to regulate both the dauer entry and exit developmental decisions.

3.3 Results

daf-9 mutants form full dauers under unfavorable growth conditions

To assess the role of steroid hormones in the C. elegans dauer exit developmental decision (Fig. 3.1), we chose to focus on daf-9 since it is the only gene acting in a steroid hormone pathway for which null mutants such as daf-9(dh6) and daf-9(e1406) show completely penetrant Daf-c phenotypes, suggesting that its loss severely abrogates steroid hormone signaling (11, 16, 20, 26). We first confirmed that daf-9 null mutants could form full dauers that would be suitable for subsequent dauer exit analysis. Previous reports indicate that the Daf-c steroid hormone mutants daf-9(dh6) and daf-12(rh273) form full dauers under unfavorable growth conditions (12, 16). To confirm these findings, we grew daf-9(dh6) animals under unfavorable conditions, which involves high temperature (25.5°C) and the presence of dauer-inducing pheromone extract (see Materials and Methods). These unfavorable growth conditions yielded daf-9(dh6) dauer larvae that matched the characteristics of full dauers formed by wild-type animals. Namely, both daf-9(dh6) and

daf-9(e1406) dauers showed no pumping, low motility, and a darkened, radially constricted body (Fig. 3.2 and Video 3.1 for daf-9(dh6), Fig. 3.3E-F for daf-9(e1406)). daf-9(dh6) full dauers are also completely SDS resistant, which is a hallmark of the dauer state (Fig. S3.1A). In contrast, when daf-9(dh6) mutants were grown under favorable conditions, we observed partial dauers that pumped more frequently, moved faster, and showed enlarged pharynxes compared to full dauers (Fig. 3.2). Comparisons to L3 larvae show that these partial dauers have pharynx sizes and pharyngeal pumping rates between those of full dauers and L3 larvae, but their movement speeds are comparable to or faster than that of L3 larvae (Fig. 3.2).

Evaluating the daf-9 partial dauer state

Having confirmed that daf-9 mutants form partial or full dauers depending on the environmental conditions, we further probed the robust daf-9 partial dauer phenotype, reasoning that it would provide insights into understanding how steroid hormones regulate the dauer process. We reasoned two likely possibilities for how daf-9 partial dauers fit into the developmental pathway: (1) Partial dauers are en route to becoming full dauers but require unfavorable environmental stimuli to complete the dauer entry process; (2) partial dauers are partially exited dauers that have gone through a full dauer state and then initiate, but cannot complete, dauer exit (Fig. 3.1A).

To test possibility (1), in which daf-9 partial dauers require unfavorable conditions to become full dauers, we grew daf-9(dh6) mutants under favorable conditions to first form partial dauers and then transferred them to unfavorable conditions to determine if they could form WT-dauers (Fig. 3.3A-C). We found that, despite a 24-hour incubation under unfavorable conditions, daf-9(dh6) partial dauers did not transition towards a full dauer state. These daf-9(dh6) animals continued to move and pump at high rates in comparison to daf-9(dh6) full dauers. Thus, we find it unlikely that the partial dauer state obtained under favorable growth conditions represents a transition state that is en route to becoming full dauer.

daf-9 partial dauers are likely partially exited dauers

To assess possibility (2), in which daf-9 partial dauers are first full dauers that then partially exit dauer, we grew daf-9(dh6) mutants under unfavorable conditions to first form full dauers, and then we transferred them to favorable conditions to examine if they became partial dauers. We found that 24 hours post-transfer, daf-9(dh6) larvae actively pumped, moved significantly more, and had wider pharynxes compared to before the transfer (Fig. 3.3D-G, and Video 3.2), thereby recapitulating the daf-9 partial dauer state. These partially exited dauers slowly continued to grow radially and develop a larger pharynx even past the 24-hour mark, although they never develop into healthy reproductive adults (16). We obtained similar results using daf-9 alleles e1406 (another putative null mutation) and m540 (a weaker loss-of-function allele) (Fig. 3.3E, F). Together, these findings suggest that transfer to favorable conditions causes full daf-9 dauers to initiate dauer exit and engage in concomitant behavioral and morphological changes such as increased pumping, motility, and pharyngeal expansion.

We also examined whether this partial dauer exit phenotype could be recapitulated at the level of the nuclear hormone receptor DAF-12/FXR. Daf-c alleles of daf-12 that bear mutations altering DAF-12's putative ligand binding domain form partial dauers with low penetrance under favorable growth conditions. (12, 27). We analyzed a Daf-c mutant, daf-12(rh273), and found that we were able to induce full dauers under unfavorable growth conditions that could become partial dauers upon transfer to favorable conditions (Fig. S3.1B, C). Therefore, daf-12(rh273) mutants can phenocopy the partial dauer exit phenotype of daf-9 putative null mutants, consistent with DAF-12/FXR mediating this phenotype.

A feature of dauer exit is its irreversibility: wild-type dauers that have been shifted to favorable conditions commit to dauer exit within an hour since shifting them back onto unfavorable conditions afterwards cannot maintain or restore the dauer state (7). We asked whether daf-9(dh6) partial dauers were in an irreversible state of partial dauer exit, or if a return to unfavorable conditions could cause the animal to become a full dauer again. We grew daf-9(dh6) mutants under unfavorable conditions to induce full dauers, transferred the resulting dauers to favorable conditions to stimulate partial dauer formation, and then transferred them back onto unfavorable conditions to see if they could become full dauers

again (Fig. S3.1D-F). Transfer into unfavorable conditions neither dramatically altered pumping rate nor movement speed compared to the mock transfer control, nor did it produce larvae that were similar to full dauers, even 24 hours after a return to unfavorable conditions. This observation suggests that partial dauers may be animals that have committed to, but can only partially complete, dauer exit.

Having concluded that daf-9(dh6) partial dauers resemble partially exited dauers, we compared the temporal progression of dauer exit in wild-type versus daf-9(dh6) animals (Fig. S3.2). When wild-type and daf-9(dh6) dauers are transferred to favorable conditions, they both gradually develop dauer exit behaviors and morphologies such as increased pumping, movement speed, and pharyngeal expansion. daf-9(dh6) dauers develop these exit characteristics more slowly than wild-type dauers do. With the exception of movement speed, daf-9(dh6) partial dauers at 24 hours post-transfer resembles wild-type partially exited dauers at over 8 hours post-transfer (Fig. S3.2). This delay suggests that daf-9 may be involved in the pace with which these exit characteristics manifest. As for movement speed, daf-9(dh6) partially exited dauers move at higher speeds than wild-type dauers do after four hours following transfer to favorable conditions. These data highlight the similarities between daf-9(dh6) partial dauers and wild-type animals during the early stages of dauer exit.

Assessing if daf-9 partial dauers pass through a transient state of full dauer

Under the hypothesis that daf-9 partial dauers were once full dauers that then partially exited, it should be possible to observe daf-9 mutants pass through a period of being full dauers before they become partial dauers even under favorable conditions. We grew daf-9(dh6) mutants under favorable conditions and scored animals every two hours as being late L2d, full dauer, or partial dauer based on metrics such as pharyngeal pumping, locomotion, and morphology (Fig. 3.4A, B, and see Materials and Methods). As controls, we also grew daf-9(dh6) and wild-type animals under unfavorable conditions in parallel. To maintain synchrony across the different growth conditions, we grew all animals at a high temperature of 25.5°C but withheld pheromone from the daf-9(dh6) mutants grown under favorable conditions. Although growth at 25.5°C favors dauer formation, it alone

cannot induce dauer formation in wild-type animals (23). At 44 hours post egg-lay, the vast majority of animals were late L2d (Fig. 3.4A). By 49 hours, around 25% of daf-9(dh6) mutants grown in the absence of pheromone could be scored as full dauers, while by 52 hours, 75% of animals were found to be full dauers. By 69 hours, the majority of animals were partial dauers. In contrast, both the wild-type and daf-9(dh6) animals grown under high pheromone conditions showed a steady increase in the proportion of dauers over time, and few if any partial dauers could be found at any time point (Fig. 3.4A). These results show that a proportion of daf-9(dh6) mutants grown in the absence of pheromone become full dauers for some period of time.

To determine what fraction of daf-9(dh6) mutants pass through a transient dauer state, we repeated the above experiment but with single animals. We grew daf-9(dh6) mutants without pheromone at 25.5°C and, after 43 hours post egg-lay, we transferred the resulting late L2ds onto new plates without pheromone (one per plate), and we scored individual animals over time (Fig. 3.4C). In concordance with our bulk tracking assay, we observed full dauers between 45 and 50 hours that later became partial dauers. Of 12 tracked animals, we observed seven that went through a period of being full dauers. For these animals, we observed an L2d molt in which the animal detached from and sometimes rolled inside its cuticle (28). Afterwards, the animal would cease both movement and pharyngeal pumping before completing radial constriction to become a full dauer. Within a few hours, these dauers slowly began pumping and moving more (a sign of partial dauer exit), but radial expansion did not occur until many hours later. Some animals were never observed as having formed full dauers (Fig. 3.4C), which may be because their transition through full dauers occurred in between time points or because they skipped the full dauer state.

We also performed the above single animal observation experiments under more favorable conditions by lowering the temperature to 20°C. However, under these conditions, we were unable to find any daf-9(dh6) larvae that went through a full dauer state, despite making observations every hour (Fig. S3.3). daf-9(dh6) grown under these conditions passed through an L2d stage and L2d molt indistinguishable from that of wild-type L2d larvae and L2d larvae formed by daf-9(dh6) mutants grown under unfavorable

conditions. Following the L2d molt, these daf-9(dh6) mutants instead passed through an intermediate state that involved both elements of being a dauer (a darkened body) as well as a partial dauer (pumping, motility), before becoming well-recognizable partial dauers usually within one hour. These observations suggest that high temperatures facilitate formation of full dauers in daf-9(dh6) mutant animals in the absence of exogenously added pheromone.

Genetic and physiological factors that could affect partial dauer formation

We sought to characterize the genetic and physiological underpinnings of the daf-9 partial dauer exit state. We asked whether the daf-9(dh6) partial dauer exit phenotype was dependent on other genes in the dauer pathway by performing double mutant analysis of daf-9(dh6) with strong loss-of-function mutations in the insulin pathway gene daf-2(e1370) (encoding a homolog of the insulin growth factor receptor) and the TGF-β pathway gene daf-7(e1372) (encoding an ortholog of human GDF11). Mutants in daf-2 and daf-7 possess strong Daf-c phenotypes and form full dauers in the absence of exogenous pheromone at high temperatures. We grew daf-2(e1370); daf-9(dh6) and daf-7(e1372); daf-9(dh6) double mutants under favorable conditions alongside daf-9(dh6), daf-2(e1370), and daf-7(e1372) single mutants to see which would form partial dauers (Fig. 3.5A, B). We found that only daf-9(dh6) formed partial dauers under these conditions, while the daf-2(e1370); daf-9(dh6) and daf-7(e1372); daf-9(dh6) double mutants were phenotypically identical to the daf-2(e1370) and daf-7(e1372) single mutants in that they formed full dauers. These results indicate that the daf-9(dh6) partial dauer phenotype is dependent on the insulin pathway as well as the TGF-β pathway.

We also evaluated whether stimulation of the insulin and TGF-β pathways was sufficient to induce partial dauer phenotypes. To do so, we overexpressed ins-6 and daf-7 pan-neuronally in a daf-9(dh6) background. ins-6 encodes an insulin-like peptide shown to activate the insulin pathway and promote dauer exit (29, 30). We grew these transgenic animals under unfavorable conditions to induce full dauer development, and we found that animals overexpressing daf-7 or ins-6 exhibited partial dauer phenotypes (Fig. 3.5C-F). Overexpression of daf-7 weakly increased locomotion speed, pumping frequency, and

pharyngeal expansion, while overexpression of ins-6 strongly bolstered these traits. These phenotypes were not due to abnormal growth or dauer development defects since these transgenic animals underwent a wild-type L2d molting process before becoming partial dauers. Taken together, these data suggest that the insulin and TGF-β pathways are necessary and sufficient for partial dauer formation in a daf-9(dh6) background.

We speculated that a potential reason for the partial dauer exit phenotype could be that a small amount of reproduction-promoting steroid hormones continues to be produced even in daf-9 putative null mutants, and that these steroid hormones might trigger partial dauer exit. We reasoned that withholding cholesterol, a precursor for the vast majority of DAF-12 steroid hormone ligands (13), could hinder partial dauer exit. We found that withholding cholesterol from the NGM media did not hinder the formation of partial dauers (Fig. S4), suggesting that the partial dauer state is not a result of residual steroid hormone production. We cannot rule out the possibility that there was sufficient cholesterol or sterol derivatives contained in the medium and/or passed on by previous generations to induce a partial dauer exit state.

daf-9 dependent steroid hormone biosynthesis is necessary for and promotes dauer exit

Having confirmed that steroid hormone mutants retain the ability to form full dauers, we proceeded to assess the role of the steroid hormone biosynthesis pathway in dauer exit using daf-9(dh6) full dauers. daf-9 encodes a cytochrome P450 enzyme that catalyzes the formation of all known steroid hormones (Fig. 3.6A) (15). Among the dafachronic acids, Δ7-DA has been shown to rescue the Daf-c phenotype of daf-9(dh6) mutants by allowing them to bypass dauer entry to become healthy adults (14, 15). We determined whether Δ7-DA could also rescue the partial dauer exit phenotype of daf-9(dh6) mutants (Fig. 3.6B). We let daf-9(dh6) full dauers form under unfavorable growth conditions and then transferred them to favorable conditions with varying concentrations of Δ7-DA and scored for complete dauer exit the next day. At low Δ7-DA concentrations, animals become partial dauers, while at 100 nM Δ7-DA nearly all daf-9(dh6) mutants fully exit the dauer state and resume reproductive development. Nonlinear regression analysis of the dose response curve reveals an EC_{50} of 7.56 nM. We also determined whether Δ7-

DA could induce dauer exit of daf-9(dh6) mutants in the presence of pheromone. Even at 100 nM Δ7-DA, almost all animals remained full dauers (89.4%, n=284). This could be because Δ7-DA is insufficient to induce dauer exit without the dauer first being exposed to favorable conditions that activate insulin and TGF-β pathways. Another possibility could be that their lack of feeding and/or their thickened cuticle (6) preclude access to Δ7-DA.

We examined whether overexpression of daf-9 was sufficient to induce dauer exit in a wild-type background. Since constitutive and ubiquitous overexpression of daf-9 would likely preclude dauer formation, we drove expression of daf-9 cDNA from the col-183 promoter (31). col-183 shows maximal expression during dauer and within the hypodermis, a tissue that exhibits high daf-9 expression levels during reproductive development (16, 18). Overexpression of daf-9 from the col-183 promoter significantly increased the fraction of dauers that exited, indicating that hypodermal daf-9 expression during dauer promotes dauer exit (Fig. 3.6C).

Spatiotemporal regulation of daf-9 during dauer exit resembles that of dauer entry

We characterized the spatiotemporal regulation of daf-9 during dauer exit to examine whether it differs from that during dauer entry. Prior to the dauer entry decision, daf-9 is expressed exclusively in the XXX neuroendocrine cells. When animals decide to enter the reproductive life cycle, daf-9 expression increases throughout the hypodermis (16, 18). To test whether this expression pattern holds true during dauer exit, we used the same DAF-9::GFP translational fusion-bearing strain (16) and monitored GFP expression as animals exited dauer (Fig. 3.7A,B). Upon shifting dauer larvae from unfavorable to favorable conditions to induce exit, we observed an increase in the proportion of animals displaying hypodermal GFP expression. The proportion peaked at 18 hours post-shift, which is when larvae have nearly entered L4, at which point nearly 75% of animals showed hypodermal GFP. After 36 hours post-shift, the vast majority of animals (~90%) lost all hypodermal GFP but retained GFP expression in the XXX cells. Thus, the spatiotemporal dynamics of daf-9 expression for the dauer exit decision seem to match those of the dauer entry decision in that there is widespread hypodermal daf-9 expression as the animal chooses the reproductive route during development.

The constitutive expression of daf-9 in the XXX cells throughout dauer led us to ask whether the XXX cells might be important for dauer exit. Published reports indicate if the XXX cells are ablated by a laser microbeam during the L1 stage, only a small fraction of animals become partial dauers even under favorable conditions (16, 32). However, if ablation occurs during the L2d stage after the animals have been reared under unfavorable conditions, then nearly all larvae form dauers even after a shift to favorable conditions (18). To examine whether the XXX cells are dispensable for dauer exit, we bilaterally ablated the XXX cells in dauers using a laser microbeam in dauer animals and transferred the ablated animals to a recovery plate under favorable conditions to induce dauer exit. We found that all XXX-ablated dauer larvae were able to exit dauer, similar to their mock ablated counterparts (Fig. 3.7C). To validate this finding, we also genetically ablated the XXX cells by expressing the human caspase gene ICE from the XXX-specific promoter eak-3p using the cGal bipartite expression system for C. elegans (33). While we observed some artifacts owing to the UAS::ICE transgene, such as formation of SDS-sensitive dauers that exited dauer at rates higher than the cGAL XXX cell-specific driver strain, genetic ablation of the XXX cells did not substantially prevent dauer larvae from exiting more when compared to control animals expressing the UAS::ICE effector transgene without the XXX cell-specific driver (Fig. S3.5). These findings suggest that the XXX cells may not be essential for dauer exit.

3.4 Discussion

Partial dauers formed by steroid hormone mutants are likely partially exited dauers

We evaluated how the steroid hormone pathway regulates both the dauer entry and dauer exit developmental decisions by first addressing why steroid hormone mutants such as daf-9 form partial dauers. Our evidence favors the hypothesis that these partial dauers are dauers that have commenced but cannot complete dauer exit. We find that forming daf-9 full dauers under unfavorable conditions followed by transfer to favorable conditions to induce dauer exit produces animals that resemble the partial dauers that are formed when daf-9 mutants are grown constantly under favorable conditions (Fig. 3.2, 3.3E-G). We also show that even when pheromone is omitted from the growth medium, some daf-9(dh6)

animals pass through a state of full dauer before initiating dauer exit owing to the favorable environment (Fig. 3.4). But given the lack of reproduction-promoting steroid hormones such as Δ7-DA, these larvae can only partially exit from dauer, resulting in a partial dauer state that slowly grows to unhealthy and sterile adulthood.

Under completely favorable conditions (i.e., no pheromone and low temperature), daf-9(dh6) larvae could not be found in a full dauer state (Fig. S3.3). Following the L2d molt, we were only able to find daf-9(dh6) mutants in a transient, intermediate state that looked like a hybrid between an L2d and a partial dauer in terms of morphology and behavior. Within an hour, these animals then quickly went on to become familiar partial dauers. We could not observe a similar intermediate state in wild-type animals, which we attempted to do by transferring wild-type L2d larvae that had committed to becoming dauers from unfavorable to favorable conditions (18). Instead, these animals passed through a full dauer state These observations suggest that daf-9(dh6) mutants skip or fail to enter the full dauer state under favorable conditions. One possibility for this observation is that constant growth under favorable conditions activates insulin and TGF-β pathways in daf-9(dh6) mutants and prevents full dauer formation. Alternatively, daf-9 may be required for full dauer formation under favorable conditions but not unfavorable conditions. Untangling these possibilities requires a better understanding of the molecular effectors downstream of the insulin, TGF-β, and steroid hormone pathways that are directly responsible for the behavioral and morphological changes associated with full dauer formation.

The daf-9 partial dauer state provides new insights into the dauer exit process

Recognizing that the daf-9 partial dauer state may be a partially exited dauer prompts a consideration of what genetic, developmental, and physiological factors may be responsible for partial dauer exit. We considered that residual steroid hormone production, either through non-daf-9-dependent biosynthesis or transgenerational rescue, suffices to trigger partial dauer exit. The former is improbable because there are no characterized biochemical pathways to form DAF-12 ligands that do not involve DAF-9 (13). The latter seems unlikely because growing daf-9(dh6) mutants on media lacking cholesterol does not

suppress partial dauer formation (Fig. S3.4). Moreover, a double mutant defective in both daf-9 and daf-36, which would presumably have lower steroid hormone levels than daf-9 single mutants alone, phenocopies daf-9 to produce partial dauers (20).

The partial dauer exit phenotype can be suppressed by mutations in important components of the insulin or TGF-β pathways, and a partial dauer state be induced by activation of either of these two pathways (Fig. 3.5). This is consistent with a model in which steroid hormone mutants form partial dauers because insulin and TGF-β pathways are activated in response to the animal sensing favorable conditions, subsequently triggering initial dauer exit behaviors and morphologies. This model is further supported by the fact that the transcriptional outputs of the insulin pathway, mediated by DAF-16/FOXO, are distinct from those of DAF-12/FXR, although the two pathways have significant crosstalk (34). While DAF-16/FOXO directly regulates the transcription of genes related to metabolism, stress resistance, and longevity, DAF-12/FXR is known to transcriptionally regulate heterochronic gene pathways that govern developmental timing (35, 36). Given these different transcriptional networks, one hypothesis is that favorable conditions activate insulin and TGF-β pathways that transcriptionally upregulate target genes to initiate dauer exit. However, without liganded DAF-12/FXR activity to stimulate heterochronic gene expression, the larvae cannot proceed to reproductive adulthood and remain as partial dauers. When Δ7-DA is supplemented to these partial dauers, full dauer exit occurs (Figure 6B).

In summary, our results are consistent with a model in which dauer exit comprises two stages. The first stage involves the transition from a full dauer to a partially exited dauer and is not dependent on daf-9 but is instead mediated by insulin and TGF-β signaling (Fig. 3.5), Since insulin and TGF-β pathway ligand-encoding genes are regulated in response to dauer-specific cues such as pheromone and food levels (37, 38), this first stage could be considered a “sensory integration” step in the dauer exit decision. The second stage in this dauer exit model describes the transition from a partially exited dauer to a reproductive L4 larvae and is mediated by the steroid hormone pathway (Fig. 3.6). Because this stage encompasses the important developmental steps that entail escape from diapause into reproduction, it could be considered the “execution” step in the dauer exit decision.

Further experiments that manipulate insulin, TGF-β, and steroid hormone pathway activity in full and partial dauers with temporal precision will help evaluate such a model.

It remains an open question as to whether other described partial dauers, such as those produced by double mutant strains carrying daf-16 (23, 24), are identical to the partial dauers formed by steroid hormone mutants. One distinction is that daf-16 double mutant partial dauers were described to quickly and spontaneously exit to adulthood (24), while daf-9(dh6) partial dauers cannot ever fully exit. We have not rigorously tested those strains using our partial dauer exit analyses.

Steroid hormone biosynthesis governs dauer exit in a manner similar to the L1 to L2 versus L2d dauer entry decision

We evaluated how the C. elegans steroid hormone pathway regulates dauer exit in comparison to dauer entry. We established that steroid hormones are essential for full dauer exit by showing that daf-9(dh6) dauers only partially exit in the absence of Δ7-DA but completely exit when supplemented with Δ7-DA at nanomolar concentrations (Fig. 3.6B). Previous dose response curves showing the relationship between Δ7-DA and the Daf-c dauer entry phenotype of daf-9(dh6) animals show an EC50 of ~5-25 nM, while 100 nM fully rescues the dauer entry phenotype (18). These results suggest that similar concentrations of Δ7-DA mediate both dauer entry and dauer exit in daf-9(dh6) animals. We further show that hypodermal overexpression of daf-9 during dauer promotes dauer exit (Fig. 3.6C), therefore demonstrating a parallel role for daf-9-dependent steroid hormones in regulating both dauer entry and dauer exit.

In comparing how the steroid hormone pathway regulates dauer exit versus dauer entry, our results suggest that the role of the steroid hormone pathway in dauer exit closely mirrors its role in the L1 to L2 vs. L2d dauer entry subdecision (see Fig. 3.1A). First, our daf-9::gfp translational fusion analysis shows that hypodermal upregulation of daf-9::gfp begins around 10-14 hours following transfer of dauers onto favorable conditions (Fig. 3.7A). This delay in hypodermal daf-9::gfp expression nearly matches that of the L1 to L2 vs. L2d decision, in which it was shown that daf-9::gfp expression increased starting at 24 to 27 hours post hatch in animals grown under favorable conditions, while larvae commit

to reproductive adulthood much earlier at around 14 to 16 hours post hatch (18). In stark contrast, during the L2d to dauer versus L3 decision, hypodermal daf-9::gfp expression closely aligned with the time window in which L2d larvae committed to reproductive adulthood (18). Importantly, given that dauer exit commitment occurs within one to two hours following transfer onto favorable conditions (7), the fact that hypodermal DAF-9::GFP fluorescence does not appear until hours later suggests that hypodermal upregulation of daf-9 may be a consequence of, rather than a cause of, the commitment to exit dauer.

Second, our XXX ablation experiments argue against an essential role for the XXX cells in dauer exit, as ablation of XXX cells do not prevent dauers from exiting (Figs. 3.7C and S3.5). Such observations are consistent with the nonessential role of XXX cells in the L1 to L2 versus L2d decision, in which groups have reported that ablation of XXX cells in L1 larvae has only a minor effect on dauer entry (16, 32). In contrast, the XXX cells are required for reproductive adulthood in the L2d to L3 versus dauer subdecision, as ablation of the XXX cells in L2d larvae prevents development into the L3 stage even under favorable conditions (18).

Hormonal regulation of diapause entry and exit in other organisms

The DAF-12 steroid hormone pathway in C. elegans is conserved in other parasitic nematode species, whose infective larvae stage are comparable to C. elegans dauers. Treatment of multiple parasitic species during early larval growth with Δ7-DA prevents entry into the infective stage, while treatment of infective larvae prompts exit from the infective stage (39, 40), mirroring our results using Δ7-DA to induce full dauer exit (Fig. 3.6B). Such conservation suggests that mechanistic knowledge of how steroid hormones control dauer exit in C. elegans could yield potential therapeutic insights to combat other parasitic species.

Diapause is evolutionarily conserved and phylogenetically widespread, and hormonal control of both diapause entry and exit is especially well-studied in insects (41). In Heliothis and Helicoverpa species of moth, diapause entry is likely caused by insufficient levels of diapause hormone (DH) and prothoracicotropic hormone (PTTH) (42).

Administration of DH or DH mimics to diapausing pupae results in diapause termination, indicating that DH is sufficient to cause diapause exit (43). The notion that diapause occurs in the absence of a pro-development hormone(s) and that diapause terminates in its presence may therefore be conserved between nematodes and insects, but in some insect species where diapause is maternally controlled, diapause entry and exit are regulated via different hormonal processes. Studies of embryonic diapause in the silkworm Bombyx mori have demonstrated a central role for DH in triggering, rather than preventing, diapause in developing embryos (44). Diapause termination, on the other hand, does not appear to depend on the absence of DH but instead on the presence of pro-development ecdysteroids such as 20-hydroxyecdysone (45, 46). In C. elegans and other animal species, co-opting the same hormonal signaling process for preventing diapause entry and inducing diapause exit could be an adaptive strategy that efficiently uses pre-existing molecular pathways for multiple purposes.

3.5 Materials and Methods

C. elegans Strains and Maintenance

C. elegans strains were derived from the wild-type strain N2 (Bristol) and were cultured according to standard laboratory conditions on Nematode Growth Medium (NGM) agar seeded with E. coli OP50 as the food source. A list of strains used in this study, including their genotypes and origins, can be found in Table S1. Maintenance and propagation of C. elegans, with the exception of daf-9 loss-of-function mutants, were performed under typical growth conditions with Nematode Growth Medium (NGM) agar seeded with OP50 E. coli cultures as described previously (47). The daf-9(dh6), daf-9(e1406), and daf-9(m540) mutants were propagated in the presence of 100 nM Δ7-Dafachronic Acid (Δ7-DA) to promote reproductive development. The daf-9(dh6) strain was obtained by propagating non-array carrying animals from PS5511 (daf-9(dh6); dhEx24[T13C5, pTG96(+)]) on Δ7-DA.

Dauer Entry Induction

To induce full dauers in wild-type and daf-9 mutants, 10-20 young adults were placed on 35 mm diameter Petri dishes containing 2 mL of NGM agar (without peptone) supplemented with a quantity of crude pheromone extract (48) that normally induce 95-100% of dauers in wild-type animals—typically 10-30 µL per 2 mL of agar. Plates were seeded with 10 µL of 8% w/v E. coli OP50 that was heat-killed at 95°C for 5 minutes. Adults were picked onto the plate and allowed to lay eggs at room temperature (RT; 22-23°C) for 5-9 hours before being removed, during which time they typically laid 200-300 eggs. The plates were then further seeded with an additional 20 µL of heat-killed OP50. Afterwards, the plates were wrapped with parafilm and incubated at 25.5°C for 60-72 hours.

Dauer Exit Assay

Dauers were formed according to Dauer Entry Induction, above. In most cases, dauers were selected for by an SDS wash (2%, 30 minutes, 25°C) to kill non-dauers before being washed 3x in M9 solution (1 minute, room temperature, 1000 x g). Surviving dauers were then plated onto dauer exit plates, which were identical to dauer entry plates but contained a lower concentration of crude pheromone extract (typically 0.5-2 µL per 2 mL of agar) that had been determined to induce ~40-60% of wild-type dauers to exit within 24 hours. In the case of the genetic ablation assay using the UAS::ICE construct, the SDS wash step was omitted since dauers bearing the UAS::ICE construct were SDS sensitive. Dauers were instead washed directly onto the dauer exit plate. Following 24 hours after dauers were transferred onto dauer exit plates, dauer exit was scored using the following criteria. Larvae were scored as having exited dauer if they showed any pharyngeal pumping or if their body had thickened and lightened considerably. Additional factors that favored scoring an animal as having exited dauer included whether the larva showed foraging behavior (such as increased head turns) or increased and consistent locomotory behavior, both of which are absent from dauers.

Microscopy and Image Analysis

Worms were immobilized on a 4-10% agarose pad (10% for dauer imaging, 4% for others) in 1-2 µL of 10 mg/mL levamisole, 50 mM sodium azide, or 0.1 µm polystyrene beads

(Polysciences, Warrington, PA) for dauer imaging. Imaging was performed on a Zeiss AxioImager2 equipped with a Colibri 7 for LED fluorescence illumination and an Axiocam 506 Mono camera (Carl Zeiss Inc., White Plains, NY). Pharyngeal bulb width measurements were performed using Zen Blue 2.3 (Zeiss) software by using the length tool to measure the widest section of the posterior pharyngeal bulb. Images were processed using FIJI (ImageJ). Pharyngeal outlines were drawn using Affinity Designer (Serif, Nottingham, UK). DIC images without the pharyngeal outlines can be found in Fig. S3.6.

Laser Ablation in Dauers

PS8568 animals expressing gfp in the XXX cells were induced to form dauers and then immobilized on a 4% agarose pad with 10 mg/mL levamisole. Laser ablation was performed on a Zeiss Axioskop (Carl Zeiss Inc.) equipped with an Andor MicroPoint nitrogen-pulsed laser microbeam (Oxford Instruments, Abingdon, UK). XXX cells were visualized under fluorescence, and the laser was fired at ~5 Hz for a total 20-30 pulses, or until all discernable fluorescence was gone. Cellular damage could often be visualized under DIC. Following surgery, animals were recovered onto a 35 mm NGM plate seeded with OP50 washed in S Basal and scored for dauer exit 24 hours later. GFP was no longer discernable under stereomicroscopy in successfully ablated animals. Mock ablated animals were prepared and rescued identically to ablated animals but without receiving laser treatment.

Partial Dauer Induction

Partial dauers of daf-9 mutants were successfully obtained using two methods. The first method (favorable growth) is as follows. 10-20 young adults were placed on 35 mm Petri dishes containing 2 mL of NGM agar (without peptone) seeded with 10 µL of 8% w/v OP50 washed twice in S Basal and including 50 µg/mL streptomycin to limit bacterial growth (7). Adults were allowed to lay eggs at RT before being removed, after which an additional 20 µL of 8% S Basal-washed OP50 was added. Plates were wrapped in parafilm and grown at 20°C for 60-72 hours to yield partial dauers. The second method (unfavorable growth followed by transfer to favorable conditions) involved forming dauers according to

Dauer Entry Induction. Dauers were then washed in 2% SDS (30 minutes, 25°C) before being washed 3x in M9, collected by centrifugation (1 minute, room temperature, 1000 x g), and then plated onto 35 mm NGM Petri plates lacking pheromone. Partial dauers could be found 24 hours later.

Behavioral Scoring

For all behavioral scoring events, animals were first allowed to acclimate to room temperature for thirty minutes prior to scoring. For pumping frequency scoring, animals were manually scored under a stereomicroscope at 100x magnification over a twenty second period. A pumping event was scored as a contraction of the pharyngeal grinder. For locomotion analysis, one-minute videos were recorded and analyzed using the WormLab Imaging System and software (MBF Bioscience, Willston, VT). Videos contained on average 8-12 animals per recording event, and multiple videos were pooled together for each experiment. Recordings were performed in areas of the plate that were away from food to maximize contrast, since recordings performed on food prevented accurate tracking of Animals. In all cases, the Peristaltic Speed (Absolute) output, measured in μm/second, was reported for these experiments. We note that the non-zero absolute speed output of many plotted dauers (i.e., Figure 3) were a result of noise owing to unstable camera movements. These dauers were often perfectly still when viewed by eye (see Video 1).

Time Course Tracking of Dauer Status in daf-9(dh6) Mutants

Wild-type and daf-9(dh6) full dauer controls were grown according to Dauer Entry Induction. Simultaneously, daf-9(dh6) mutants were grown in the absence of exogenous pheromone. All strains were grown at 25.5°C in order to maximize developmental synchrony across the different conditions. For single animal tracking of daf-9(dh6) partial dauers, individual L2ds grown under the conditions described above were picked onto new non-pheromone-containing plates starting at 43 hours post egg-lay and scored every two hours. An animal was scored as being a partial dauer if any pumping was observed and/or the body thickened and lightened compared to a normal dauer.

Cholesterol Deprivation

Cholesterol deprived plates were made similarly to normal dauer plates (i.e., in 35 mm petri dishes with 2 mL NGM agar without peptone) except that ethanol solvent was added in place of cholesterol. This method was sufficient to enhance the Daf-c phenotype of daf-9(m540) mutants, as previously described (34). More severe methods of cholesterol starvation, such as using agarose in place of agar and passaging the animals over two generations in the absence of cholesterol (16), yielded unhealthy larvae that could not grow to become dauers.

Double Mutant Analysis between daf-9(dh6) and daf-2(e1370) or daf-7(e1372)

Double mutants were constructed as follows. Wild-type males were mated to the balancer strain sC1(s2023) [dpy-1(s2170) umnIs21], which are marked by a recessive Dumpy (Dpy) phenotype and a dominant pharyngeal GFP phenotype. The resulting male sC1heterozygotes were mated to daf-9(dh6); dhEx24 hermaphrodites. dhEx24 is an extrachromosomal array containing the cosmid T13C5, containing a rescuing wild-type copy of the daf-9 locus and a sur-5p::gfp marker expressing GFP throughout the body. Hemizygous daf-9(dh6)/0 male progeny with both whole-body GFP+ (from dhEx24) and pharyngeal GFP+ (from sC1) were mated again to daf-9(dh6) dhEx24 hermaphrodites, and the Dpy F_2 double GFP+ progeny were obtained to yield sC1(s2023) [dpy-1(s2170) umnIs21]; daf-9(dh6); dhEx24. This strain was then crossed into a daf-2(e1370) or daf-7(e1372) background to yield daf-2(e1370)/sC1(s2023) [dpy-1(s2170) umnIs21]; daf-9(dh6); dhEx24 or daf-7(e1372)/sC1(s2023) [dpy-1(s2170) umnIs21]; daf-9(dh6); dhEx24, respectively. The sC1 balancer could then be used to follow daf-2(e1370) and daf-7(e1372) in trans to facilitate the construction of double mutants between these mutations and daf-9(dh6). For pharyngeal pumping and locomotion assays, the balanced double mutants were grown from eggs at 25.5° without pheromone for three days, and daf-2(e1370); daf-9(dh6) or daf-7(e1372); daf-9(dh6) dauer larvae were identified by looking for non-GFP dauers and picked onto new plates. These dauers were allowed to acclimate on the new plates for at least thirty minutes prior to scoring.

Statistical Analysis and Plotting

Plots were designed using Prism 9.0 (GraphPad, San Diego, CA). All plots are representative of at least 2 independent experiments. Dose response curves for steroid hormones were calculated using Prism's nonlinear regression tool ([Agonist] vs response) with four parameters and the EC50 parameter constrained to be greater than zero. Mann-Whitney tests were performed in Prism. Permutation tests for dauer exit proportion between two samples were performed by first binarizing dauer exit data, pooling the two samples together, and simulating experiments by drawing two samples out of the pooled binarized data. The p value was calculated by comparing the number of simulated experiments, out of 10^4, in which the difference between the simulated proportions was greater than the observed difference between the actual proportions.

Acknowledgements

Δ7-DA was a gift from the lab of Frank Schroeder (Cornell University). We thank Mengyi Cao and Stephanie Nava for the XXX cGAL driver. Some strains were provided by the CGC, which is funded by NIH Office of Research Infrastructure Programs (P40 OD010440). We are grateful to members of the Sternberg lab for their feedback on the manuscript, particularly Hillel Schwartz.

Competing interests

No competing interests declared.

Author Contributions

M.G.Z. and P.W.S. conceived of the study. M.G.Z. performed the experiments and analyzed the data. M.G.Z. wrote the manuscript with editorial assistance from P.W.S.

Funding

M.G.Z. was funded by National Institutes of Health Grant F31 NS120501-01. A National Institutes of Health Grant UF1-NS111697 (P.W.S) supported the research material and research assistance.

3.6 References

1. S. C. Hand, D. L. Denlinger, J. E. Podrabsky, R. Roy, Mechanisms of animal diapause: recent developments from nematodes, crustaceans, insects, and fish. Am. J. Physiol.-Regul. Integr. Comp. Physiol. 310, R1193–R1211 (2016).

2. V. Koštál, Eco-physiological phases of insect diapause. J. Insect Physiol. 52, 113–127 (2006).

3. G. J. Ragland, D. L. Denlinger, D. A. Hahn, Mechanisms of suspended animation are revealed by transcript profiling of diapause in the flesh fly. Proc. Natl. Acad. Sci. 107, 14909–14914 (2010).

4. P. J. Hu, Dauer. WormBook (2007). https://doi.org/10.1895/wormbook.1.144.1.

5. J. E. Podrabsky, S. C. Hand, Physiological strategies during animal diapause: lessons from brine shrimp and annual killifish. J. Exp. Biol. 218, 1897–1906 (2015).

6. R. C. Cassada, R. L. Russell, The dauerlarva, a post-embryonic developmental variant of the nematode Caenorhabditis elegans. Dev. Biol. 46, 326–342 (1975).

7. J. W. Golden, D. L. Riddle, The Caenorhabditis elegans dauer larva: Developmental effects of pheromone, food, and temperature. Dev. Biol. 102, 368–378 (1984).

8. J. W. Golden, D. L. Riddle, A pheromone influences larval development in the nematode Caenorhabditis elegans. Science 218, 578–580 (1982).

9. R. J. Androwski, K. M. Flatt, N. E. Schroeder, Phenotypic plasticity and remodeling in the stress-induced Caenorhabditis elegans dauer. Wiley Interdiscip. Rev. Dev. Biol. 6, e278 (2017).

10. N. Fielenbach, A. Antebi, C. elegans dauer formation and the molecular basis of plasticity. Genes Dev. 22, 2149–2165 (2008).

11. A. Antebi, Nuclear receptor signal transduction in C. elegans. WormBook Online Rev. C Elegans Biol. 1–49 (2015). https://doi.org/10.1895/wormbook.1.64.2.

12. A. Antebi, J. G. Culotti, E. M. Hedgecock, daf-12 regulates developmental age and the dauer alternative in Caenorhabditis elegans. Development 125, 1191–1205 (1998).

13. H. Aguilaniu, P. Fabrizio, M. Witting, The role of dafachronic acid signaling in development and longevity in Caenorhabditis elegans: Digging deeper using cutting-edge analytical chemistry. Front. Endocrinol. 7 (2016).

14. P. Mahanti et al., Comparative metabolomics reveals endogenous ligands of DAF-12, a nuclear hormone receptor, regulating C. elegans development and lifespan. Cell Metab. 19, 73–83 (2014).

15. D. L. Motola et al., Identification of ligands for DAF-12 that govern dauer formation and reproduction in C. elegans. Cell 124, 1209–1223 (2006).

16. B. Gerisch, C. Weitzel, C. Kober-Eisermann, V. Rottiers, A. Antebi, A hormonal signaling pathway influencing C. elegans metabolism, reproductive development, and life span. Dev. Cell 1, 841–851 (2001).

17. K. Jia, P. S. Albert, D. L. Riddle, DAF-9, a cytochrome P450 regulating C. elegans larval development and adult longevity. Development 129, 221–231 (2002).

18. O. N. Schaedel, B. Gerisch, A. Antebi, P. W. Sternberg, Hormonal signal amplification mediates environmental conditions during development and controls an irreversible commitment to adulthood. PLOS Biol. 10, e1001306 (2012).

19. J. Li, G. Brown, M. Ailion, S. Lee, J. H. Thomas, NCR-1 and NCR-2, the C. elegans homologs of the human Niemann-Pick type C1 disease protein, function upstream of DAF-9 in the dauer formation pathways. Development 131, 5741–5752 (2004).

20. V. Rottiers, et al., Hormonal control of C. elegans dauer formation and life span by a Rieske-like oxygenase. Dev. Cell 10, 473–482 (2006).

21. D. L. Riddle, P. S. Albert, “Genetic and environmental regulation of dauer larva development” in C. Elegans II, 2nd Ed., D. L. Riddle, T. Blumenthal, B. J. Meyer, J. R. Priess, Eds. (Cold Spring Harbor Laboratory Press, 1997).

22. P. S. Albert, D. L. Riddle, Mutants of Caenorhabditis elegans that form dauer-like larvae. Dev. Biol. 126, 270–293 (1988).

23. M. Ailion, J. H. Thomas, Dauer formation induced by high temperatures in Caenorhabditis elegans. Genetics 156, 1047–1067 (2000).

24. J. J. Vowels, J. H. Thomas, Genetic analysis of chemosensory control of dauer formation in Caenorhabditis elegans. Genetics 130, 105–123 (1992).

25. S. Ogg et al., The Forkhead transcription factor DAF-16 transduces insulin-like metabolic and longevity signals in C. elegans. Nature 389, 994–999 (1997).

26. B. Gerisch, A. Antebi, Hormonal signals produced by DAF-9/cytochrome P450 regulate C. elegans dauer diapause in response to environmental cues. Development 131, 1765–1776 (2004).

27. A. Antebi, W.-H. Yeh, D. Tait, E. M. Hedgecock, D. L. Riddle, daf-12 encodes a nuclear receptor that regulates the dauer diapause and developmental age in C. elegans. Genes Dev. 14, 1512–1527 (2000).

28. R. N. Singh, J. E. Sulston, Some observations on moulting in Caenorhabditis elegans. Nematologica 24, 63–71 (1978).

29. A. Cornils, M. Gloeck, Z. Chen, Y. Zhang, J. Alcedo, Specific insulin-like peptides encode sensory information to regulate distinct developmental processes. Development 138, 1183–1193 (2011).

30. Q. Hua et al., A divergent INS protein in Caenorhabditis elegans structurally resembles human insulin and activates the human insulin receptor. Genes Dev. 17, 826–831 (2003).

31. P.-Y. Shih, J. S. Lee, P. W. Sternberg, Genetic markers enable the verification and manipulation of the dauer entry decision. Dev. Biol. (2019). https://doi.org/10.1016/j.ydbio.2019.06.009.

32. K. Ohkura, N. Suzuki, T. Ishihara, I. Katsura, SDF-9, a protein tyrosine phosphatase-like molecule, regulates the L3/dauer developmental decision through hormonal signaling in C. elegans. Development 130, 3237–3248 (2003).

33. H. Wang et al., cGAL, a temperature-robust GAL4–UAS system for Caenorhabditis elegans. Nat. Methods 14, 145–148 (2017).

34. M.-H. Jeong, I. Kawasaki, Y.-H. Shim, A circulatory transcriptional regulation among daf-9, daf-12, and daf-16 mediates larval development upon cholesterol starvation in Caenorhabditis elegans†. Dev. Dyn. 239, 1931–1940 (2010).

35. D. Hochbaum et al., DAF-12 regulates a connected network of genes to ensure robust developmental decisions. PLOS Genet. 7, e1002179 (2011).

36. S. Kumar, K. P. Smith, J. L. Floyd, M. F. Varela, Cloning and molecular analysis of a mannitol operon of phosphoenolpyruvate-dependent phosphotransferase (PTS) type from Vibrio cholerae O395. Arch. Microbiol. 193, 201–208 (2011).

37. W. Li, S. G. Kennedy, G. Ruvkun, daf-28 encodes a C. elegans insulin superfamily member that is regulated by environmental cues and acts in the DAF-2 signaling pathway. Genes Dev. 17, 844–858 (2003).

38. P. Ren et al., Control of C. elegans larval development by neuronal expression of a TGF-β homolog. Science (1996). https://doi.org/10.1126/science.274.5291.1389.

39. A. Ogawa, A. Streit, A. Antebi, R. J. Sommer, A conserved endocrine mechanism controls the formation of dauer and infective larvae in nematodes. Curr. Biol. 19, 67–71 (2009).

40. Z. Wang et al., Identification of the nuclear receptor DAF-12 as a therapeutic target in parasitic nematodes. Proc. Natl. Acad. Sci. 106, 9138–9143 (2009).

41. D. L. Denlinger, G. D. Yocum, J. P. Rinehart, "Hormonal control of diapause" in Insect Endocrinology, (Elsevier, 2012), pp. 430–463.

42. W.-H. Xu, D. L. Denlinger, Molecular characterization of prothoracicotropic hormone and diapause hormone in Heliothis virescens during diapause, and a new role for diapause hormone. Insect Mol. Biol. 12, 509–516 (2003).

43. Q. Zhang, R. J. Nachman, K. Kaczmarek, J. Zabrocki, D. L. Denlinger, Disruption of insect diapause using agonists and an antagonist of diapause hormone. Proc. Natl. Acad. Sci. 108, 16922–16926 (2011).

44. Y. Sato et al., A New Diapause Hormone Molecule of the Silkworm, Bombyx mori. Proc. Jpn. Acad. Ser. B 68, 75–79 (1992).

45. K. Iwata et al., Temperature-dependent activation of ERK/MAPK in yolk cells and its role in embryonic diapause termination in the silkworm Bombyx mori. J. Insect Physiol. 51, 1306–1312 (2005).

46. H. Sonobe, R. Yamada, Ecdysteroids during early embryonic development in silkworm Bombyx mori: Metabolism and Functions. Zoolog. Sci. 21, 503–516 (2004).

47. S. Brenner, The genetics of Caenorhabditis elegans. Genetics 77, 71–94 (1974).

48. N. E. Schroeder, K. M. Flatt, In vivo imaging of dauer-specific neuronal remodeling in C. elegans. JoVE J. Vis. Exp. e51834 (2014). https://doi.org/10.3791/51834.

3.7 Figures

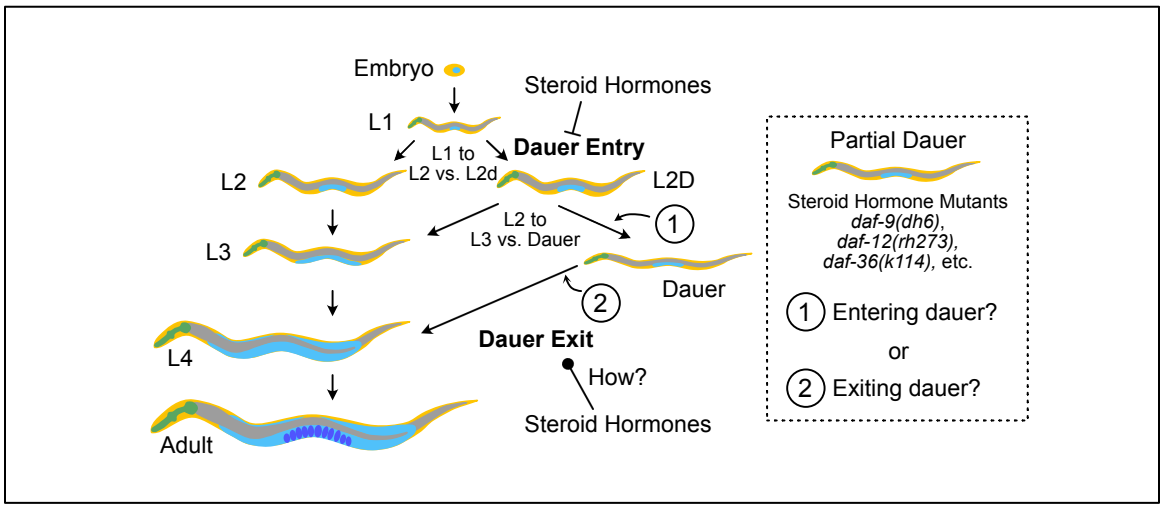

Figure 3.1. Regulation of Caenorhabditis elegans dauer development by steroid hormones.

The C. elegans dauer pathway includes multiple developmental decisions. The dauer entry decision comprises two subdecisions made at L1 and then L2d, whereas dauer exit is a singular, continuous decision. Leftward or rightward arrows indicate the decision that is made under favorable or unfavorable conditions, respectively. Steroid hormones inhibit dauer entry and promote reproductive development. How steroid hormones regulate dauer exit is less understood. A model of how steroid hormones regulate the dauer pathway requires understanding why steroid hormone mutants such as daf-9(dh6), daf-12(rh273), daf-36(k114), etc., form partial dauers rather than full dauers like other Daf-c mutants. Partial dauers could be (1) animals that have yet to enter a full dauer state or (2) partially exited dauers.

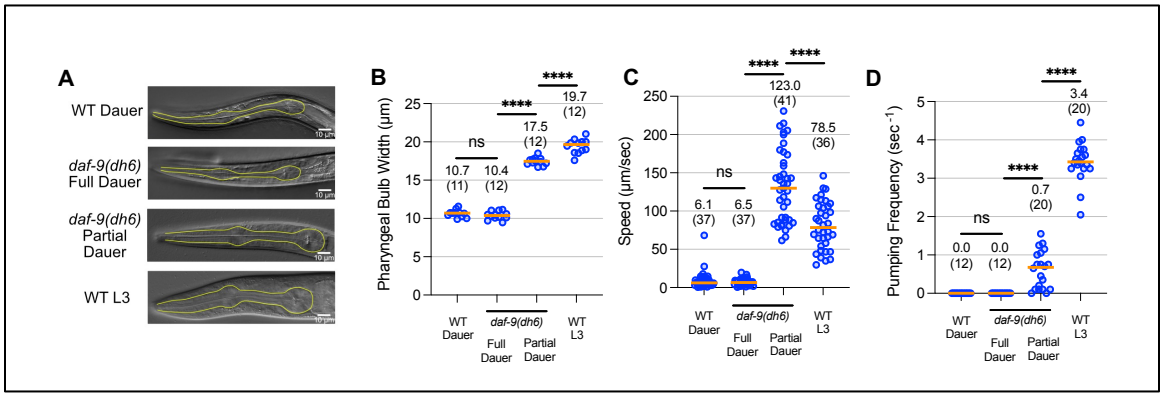

Figure 3.2. Characterization of full versus partial dauers formed by daf-9 null mutants. daf-9(dh6) full dauers formed under unfavorable growth conditions phenocopy wild-type dauers and are distinct from daf-9(dh6) partial dauers formed under favorable growth conditions. Phenotypes measured include (A, B) terminal pharyngeal bulb width, (C) speed, and (D) pumping frequency. Wild-type L3 animals are shown for comparison. The pumping frequencies for WT and daf-9(dh6) full dauers in (B) are from the same experiment shown in Figure 3F. ns, not significant. ****, $p<0.0001$ by Mann Whitney Test. Horizontal bars and in-graph numbers show median values. Numbers in parentheses indicate number of animals. Each dot is one animal.

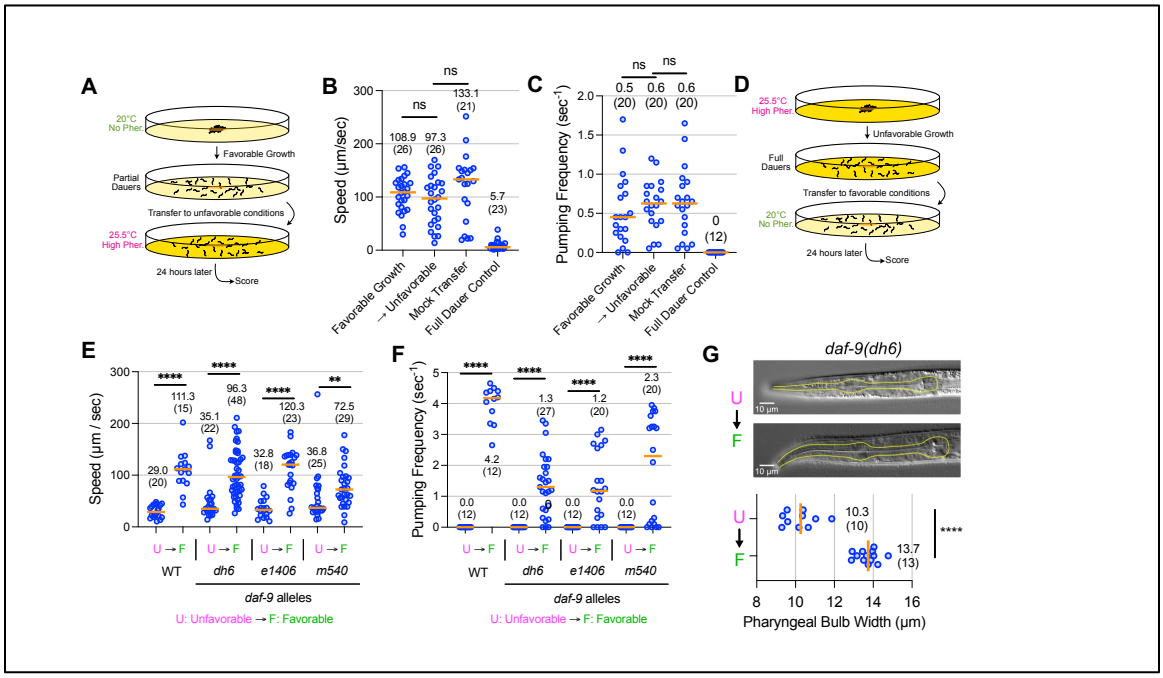

Figure 3.3. daf-9 partial dauers may be partially exited dauers.

(A) Experimental schematic to test whether daf-9(dh6) partial dauers become full dauers upon transfer to unfavorable conditions. daf-9(dh6) partial dauers obtained under favorable growth conditions were transferred to unfavorable conditions or again to favorable conditions (mock transfer) and scored 24 hours later for (B) speed and (C) pumping frequency. Also shown are daf-9(dh6) full dauers grown under unfavorable conditions (Full Dauer Control). (D) Experimental schematic to test whether daf-9(dh6) full dauers become partial dauers upon transfer to favorable growth conditions. daf-9(dh6) full dauers were obtained under unfavorable, dauer-inducing growth conditions, transferred to favorable conditions, and then scored 24 hours later for (E) speed and (F) pumping frequency. daf-9 alleles e1406 (null) and m540 (weak loss-of-function) show similar partial dauer exit phenotypes. (G) daf-9(dh6) partially exited dauers obtained via the method in (D) have wider pharynxes than their full dauer counterparts. ns, not significant. **, $p<0.01$. ****, $p<0.0001$ by Mann Whitney test. Horizontal bars and in-graph numbers show median values. Numbers in parentheses indicate number of animals. Each dot is one animal.

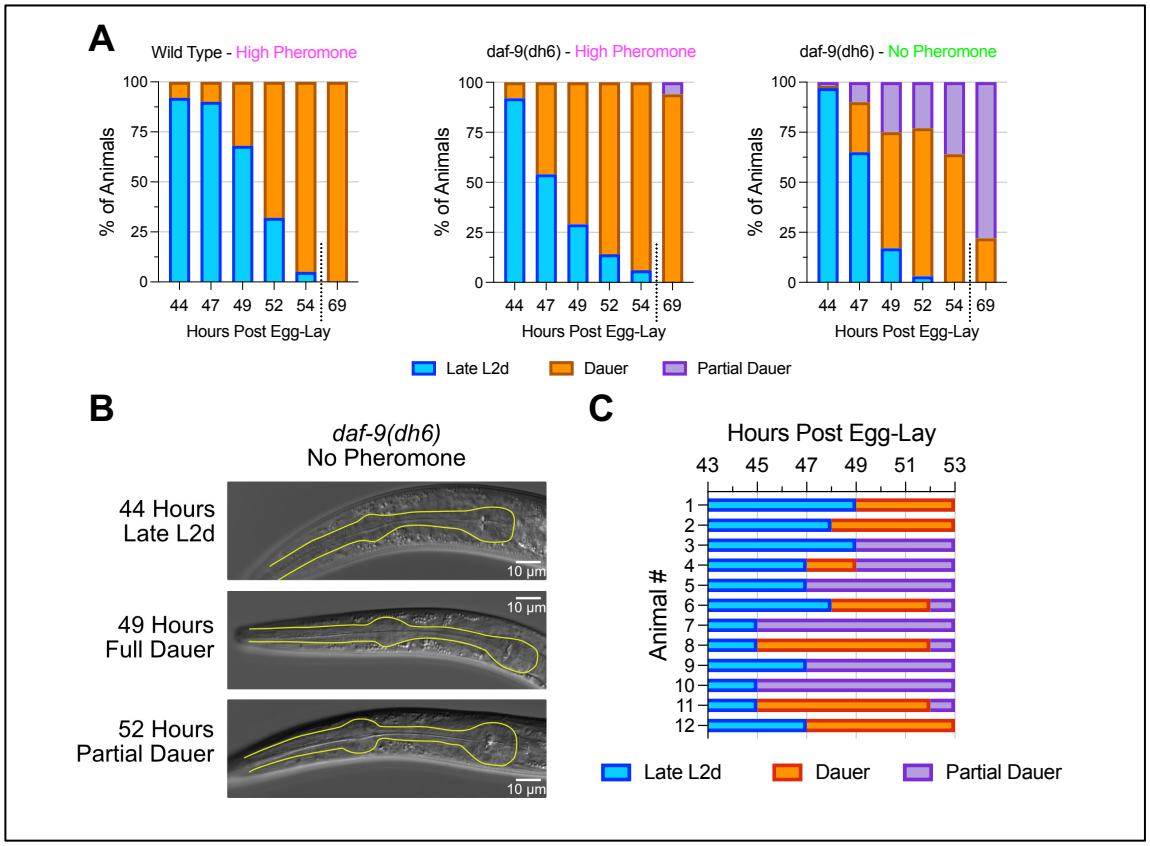

Figure 3.4: daf-9(dh6) larvae transiently become full dauers in the absence of exogenous pheromone.

(A) daf-9(dh6) worms were grown in the presence or absence of exogenously added pheromone and then scored as late L2d, full dauer, or partially exiting dauer animals. n ≥ 53 animals for all observations (B) Representative images of pharynxes from worms grown as in (A). Note the shrinkage of the posterior pharyngeal bulb at 49 hours, indicative of full dauer status, followed by an enlargement of the pharynx at 52 hours, indicative of partial dauer exit. (C) daf-9(dh6) worms grown as in (A), but worms were individually grown and observed every 2 hours starting at 43 hours post egg-lay. 7 out of 12 animals could be observed in a full dauer state.

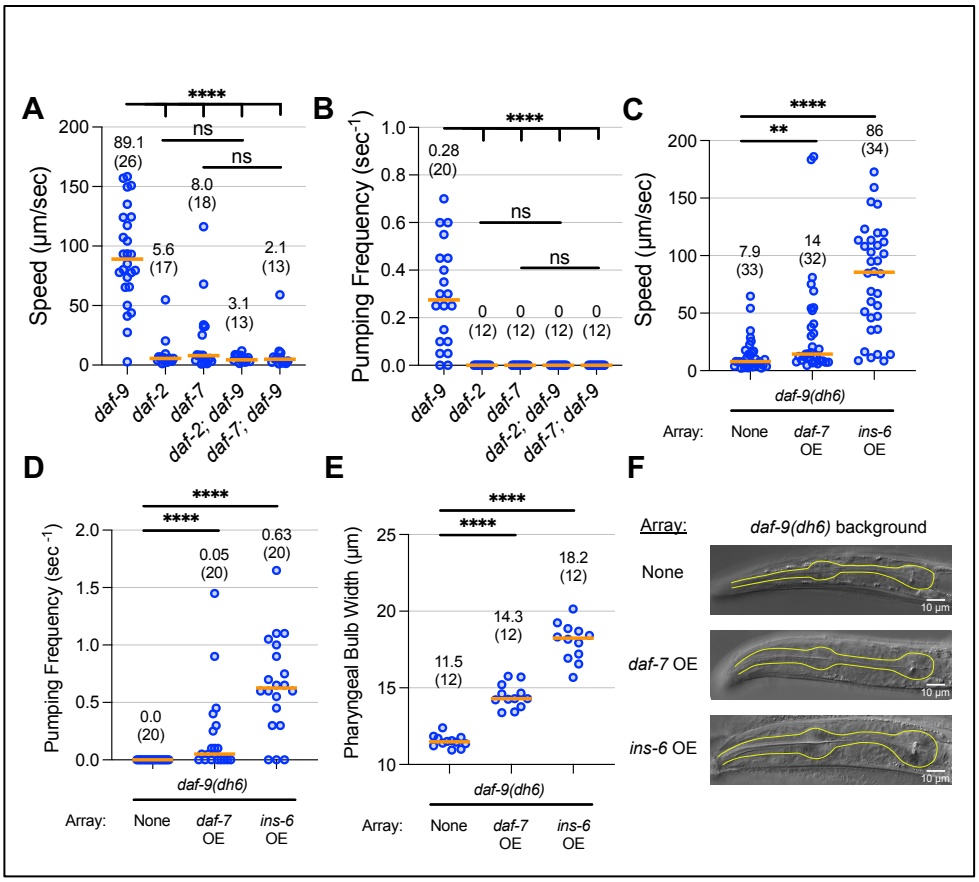

Figure 3.5. Effects of daf-2 and daf-7 on the daf-9 partial dauer phenotype. (A,B) Single and double mutants between daf-9(dh6) and daf-2(e1370) or daf-7(e1372) were grown under favorable conditions. While daf-9(dh6) worms form partial dauers, daf-2(e1370), daf-7(e1372), and their respective daf-9(dh6) double mutants do not form partial dauers. $p<0.0001$ by Mann Whitney test between daf-9 single mutant and all other double mutants. (C-F) Overexpression of daf-7 or ins-6 in a daf-9(dh6) background is sufficient for partial dauer phenotypes. daf-9(dh6) mutants with or without an extrachromosomal array that pan-neuronally overexpresses (OE) daf-7 or ins-6 were grown under unfavorable conditions. While animals without the array form full dauers, animals overexpressing daf-7 or ins-6 exhibit weaker or stronger partial dauer phenotypes, respectively. ns, not significant. **, $p<0.01$. ****, $p<0.0001$ by Mann Whitney test. Horizontal bars and in-graph numbers show median values. Numbers in parentheses indicate number of animals. Each dot is one animal.

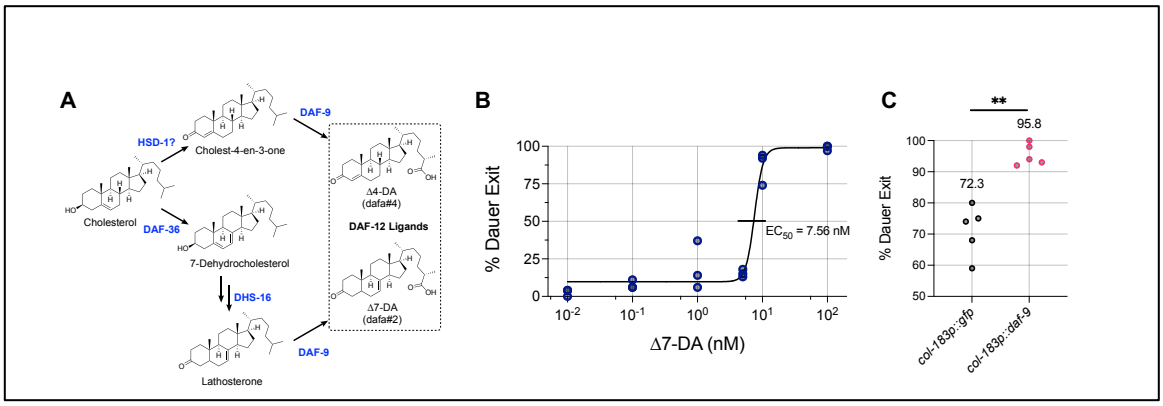

Figure 3.6. The daf-9 steroid hormone pathway is necessary for and promotes dauer exit. (A) Steroid hormone biosynthetic pathway. DAF-9 catalyzes the final oxidation step required to form all known endogenous ligands of DAF-12, which promote reproductive development over dauer. Figure adapted from Mahanti et al., 2014 and Aguilaniu et al., 2016. (B) Dose response curve for the efficacy of Δ7-Dafachronic Acid (Δ7-DA) to rescue the dauer exit defect of daf-9(dh6) mutants. daf-9(dh6) full dauers were transferred to favorable conditions containing various concentrations of Δ7-DA. 24 hours later, animals were scored for complete dauer exit. Lower concentrations yielded partially exited dauers, while 100 nM induced nearly all animals to completely exit dauer. (C) Overexpression of daf-9 from the hypoderm-specific and dauer-specific promoter col-183p in a wild-type background promotes dauer exit. For (B) and (C), each dot is a biological replicate of scored dauer exit plates, with each group having a total n ≥ 100 animals. **, $p<0.01$ by bootstrapped permutation test using 10^4 samples.

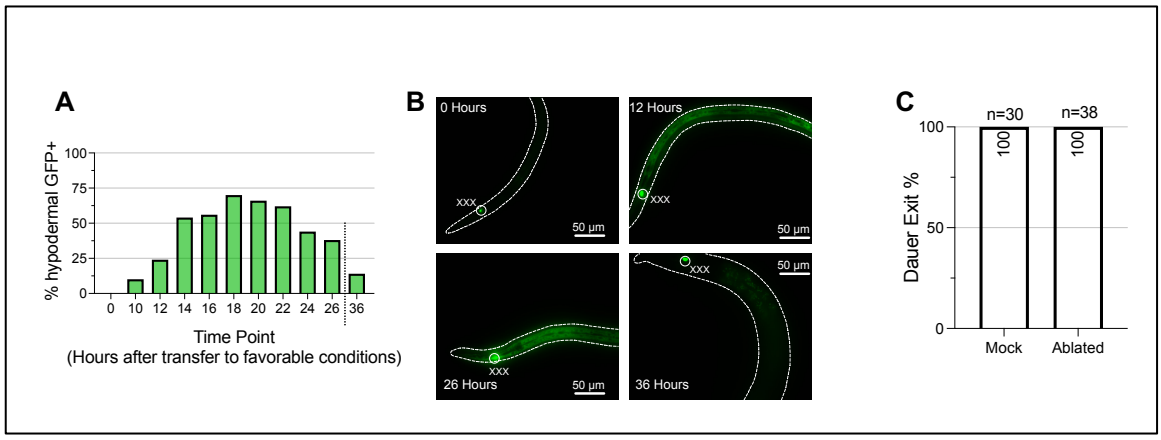

Figure 3.7. Spatiotemporal dynamics of daf-9 expression during dauer exit.

(A) Time course of hypodermal daf-9::gfp expression during dauer exit. Dauers expressing a daf-9::gfp translational fusion were transferred to favorable conditions and imaged for the presence or absence of GFP signal in the hypoderm. daf-9::gfp is expressed in the highest percentage of animals at ~16-20 hours after transfer to favorable conditions. $n \geq 20$ for all time points. (B) Representative images of animals observed in (A), with bodies outlined and the XXX neuroendocrine cells (which constitutively express daf-9::gfp) labeled. Note the increase in DAF-9::GFP in images for 12 and 26 hours. (C) Laser ablation of XXX cells does not prevent dauer exit. Following ablation of the XXX cells using a laser microbeam, dauers and mock-ablated control dauers were transferred to favorable conditions and scored for dauer exit 24 hours later.

3.8 Supplemental figures and tables

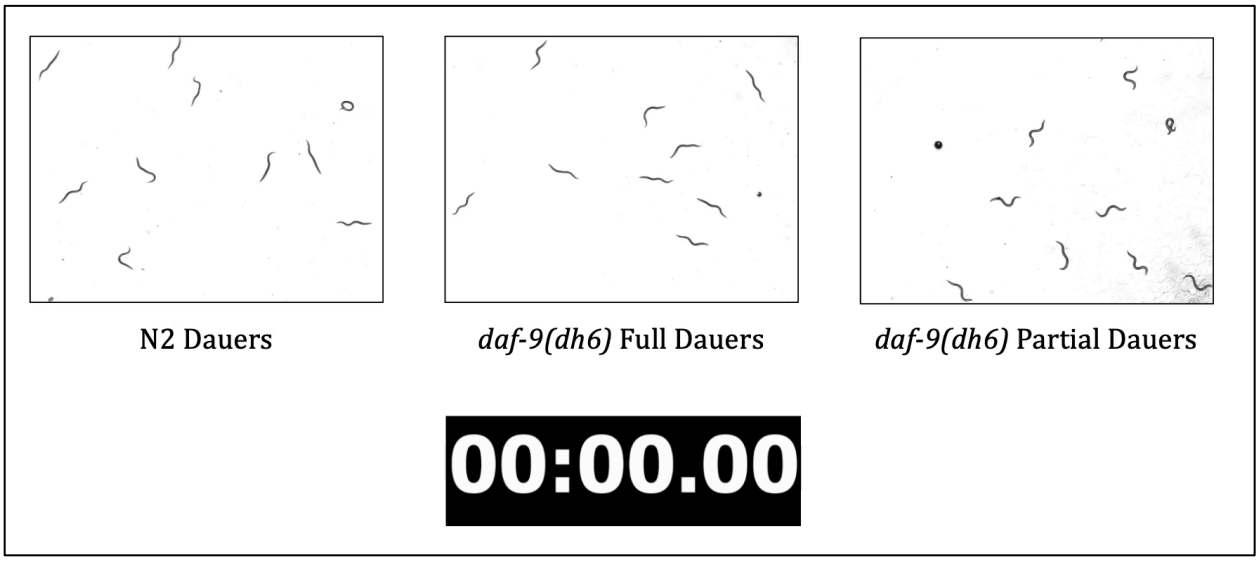

Full video available as a .mov file from the published online article:
https://doi.org/10.1242/dev.200173

Video 1: daf-9(dh6) full dauers resemble wild-type dauers in terms of locomotion. Shown are 1-minute video recordings of N2 (wild-type) and daf-9(dh6) dauers formed under unfavorable growth conditions in comparison to daf-9(dh6) partial dauers formed under favorable growth conditions. N2 (wild-type) and daf-9(dh6) worms move much more slowly, if at all, compared to daf-9(dh6) partial dauers.

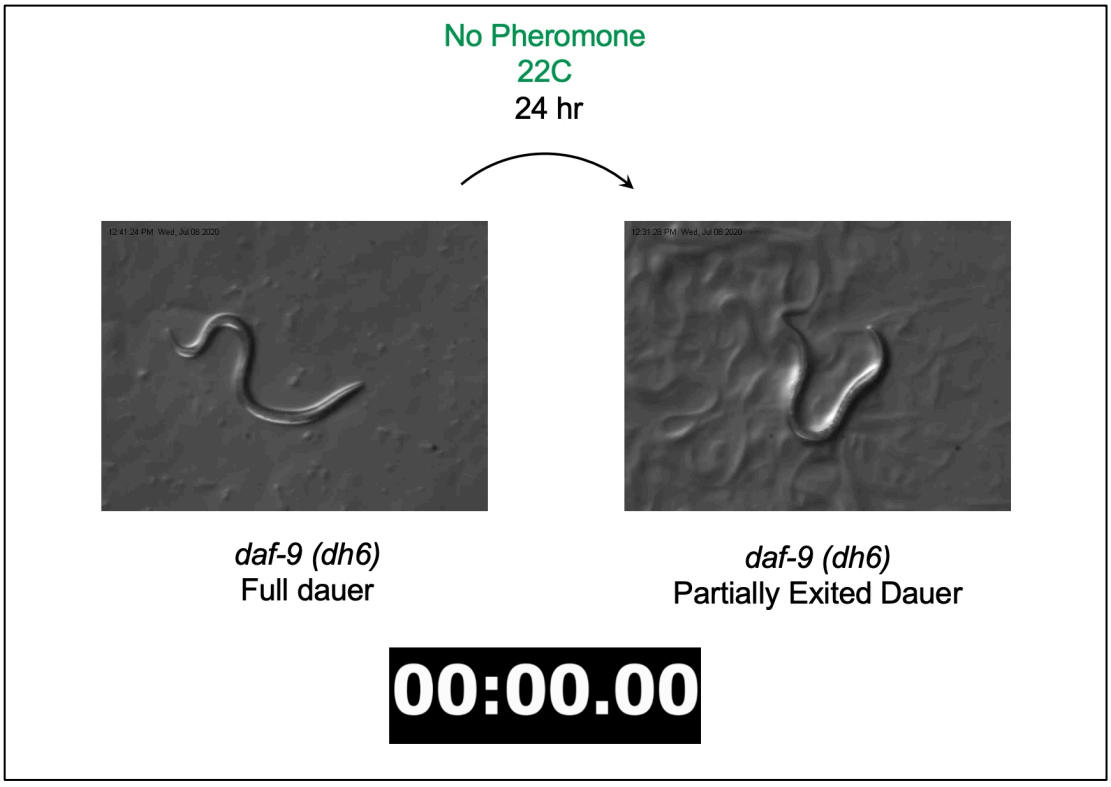

Full video available as a .mov file from the published online article:
https://doi.org/10.1242/dev.200173

Video 2: Locomotion behavior of daf-9(dh6) partially exited dauers.
Shown are ten-second recordings of (left) a daf-9(dh6) full dauer formed under unfavorable growth conditions and (right) a daf-9(dh6) partially exited dauer formed by transferring full daf-9(dh6) dauers from unfavorable to favorable conditions for 24 hours. A second partially exited dauer can be seen crawling at high speed in the background midway through the recording. The daf-9(dh6) partially exited dauer performs many small head movements and frequently reverses, unlike daf-9(dh6) full dauers which remain idle.

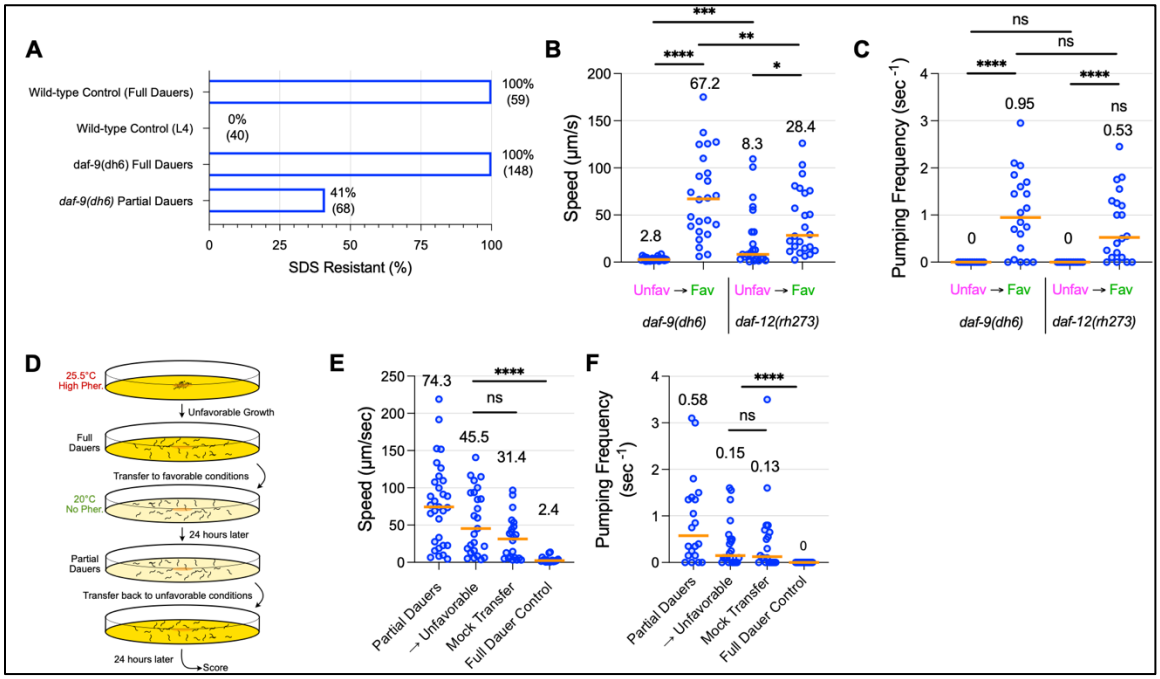

Figure S3.1. daf-9(dh6) full dauer SDS resistance, daf-12(rh273) partial dauer phenotype, and irreversibility of the partial dauer phenotype

(A) daf-9(dh6) full dauers are completely SDS resistant, while daf-9(dh6) partial dauers are SDS sensitive. Also shown are wild-type control animals grown under unfavorable conditions to form full dauers or under favorable conditions to form SDS-sensitive L4 larvae. Displayed are the percentages of animals that survived SDS treatment and the corresponding number of animals treated. (B,C) daf-12(rh273) phenocopies the daf-9(dh6) partial dauer exit phenotype. The Daf-c allele daf-12(rh273) shows a similar partial dauer exit phenotype to daf-9(dh6) as measured by locomotion speed and pumping frequency, as daf-12(rh273) full dauers formed under unfavorable conditions were induced to become partially exited dauers that (B) moved faster and (C) pumped more frequently following transfer to favorable conditions. Note that daf-12(rh273) full dauers tend to be slightly more mobile than N2 or daf-9(dh6) dauers, despite being fully pumping quiescent. (D-F) The partial dauer exit phenotype is not reversible. (D) Experimental schematic for reversibility assay. daf-9(dh6) partial dauers were produced by first inducing full dauers under unfavorable growth conditions followed by transfer to favorable conditions for 24

hours (Partial Dauers). Partially exited dauers were then transferred back to unfavorable conditions for a further 24 hours (→Unfavorable) and assessed for full dauer characteristics, including locomotion and pumping frequency. A 24-hour incubation under unfavorable conditions did not significantly decrease (E) locomotion speed nor (F) pumping quiescence compared to a mock transfer control, in which partially exited dauers were transferred to favorable conditions for 24 hours. ns, not significant. *, $p<0.05$. ***, $p<0.01$. ****, $p<0.001$ by Mann Whitney test. Each dot is one animal. $n \geq 12$ animals for each experimental sample.

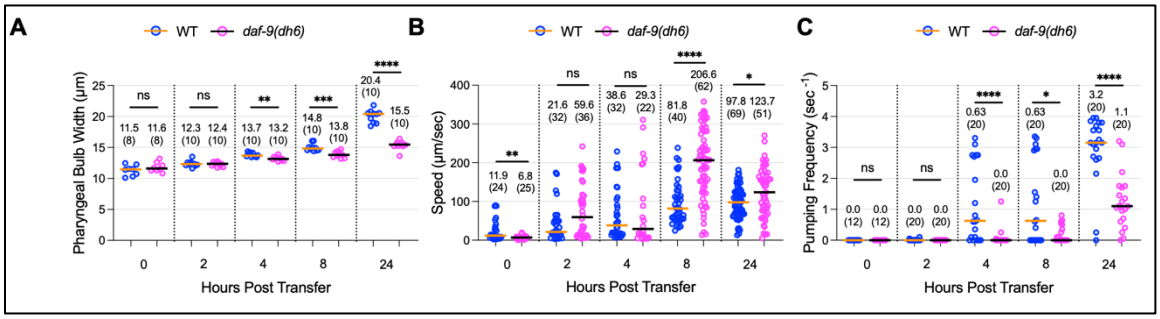

Figure S3.2. Comparison of daf-9(dh6) dauer exit with wild-type dauer exit. Wild-type dauers and daf-9(dh6) full dauers were obtained by growth under unfavorable conditions and then transferred to favorable conditions to induce dauer exit. Animals were scored for (A) speed, (B) pumping frequency, and (C) pharyngeal terminal bulb width before transfer (0 hours post transfer) and at various intervals following transfer. Animals at 0 hours post transfer are identical to "Full Dauers" described elsewhere in the paper, while daf-9(dh6) mutants at 24 hours post transfer are identical to "Partial Dauers" obtained through favorable transfer as described elsewhere in the paper. The statistically significant difference between wild-type and daf-9(dh6) full dauers at 0 hours post transfer was not consistently observed and occur here because wild-type dauers sporadically show bursts of movement. ns, not significant. *, $p<0.05$. **, $p<0.01$. ***, $p<0.001$. ****, $p<0.0001$ by Mann Whitney test. Horizontal bars and in-graph numbers show median values. Numbers in parentheses indicate number of animals. Each dot is one animal.

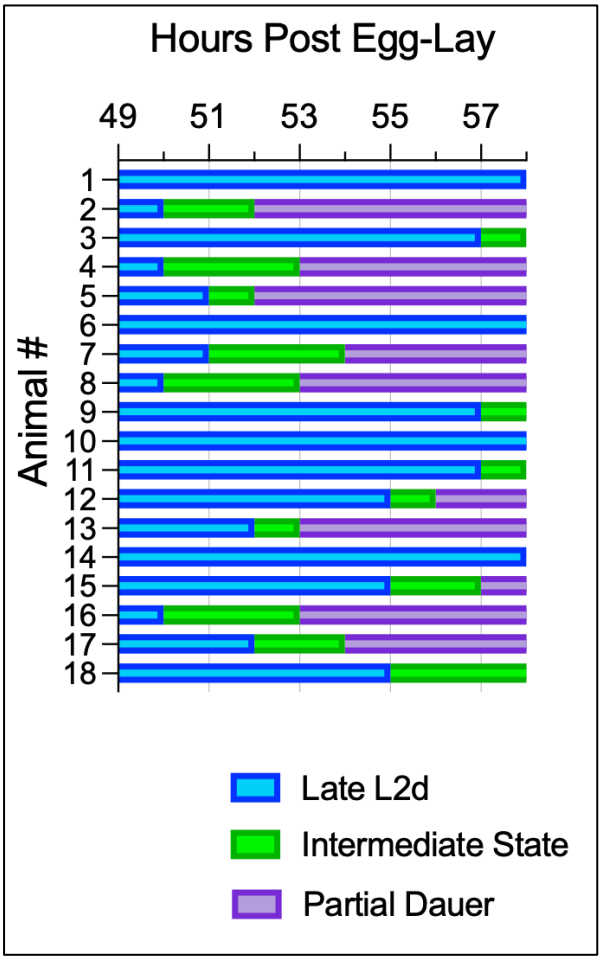

Figure S3.3. daf-9(dh6) mutants do not enter a full dauer state at lower temperatures. daf-9(dh6) worms were grown in absence of exogenously added pheromone at 20.0°C. At 49 hours post egg-lay, animals were individually transferred to new plates and observed every hour. Animals could not be found to pass through a full dauer state as they did at 25.5°C. Instead, following the L2d molt, they passed through an intermediate state that showed characteristics between those of an L2d and a partial dauer larva (see Main Text).

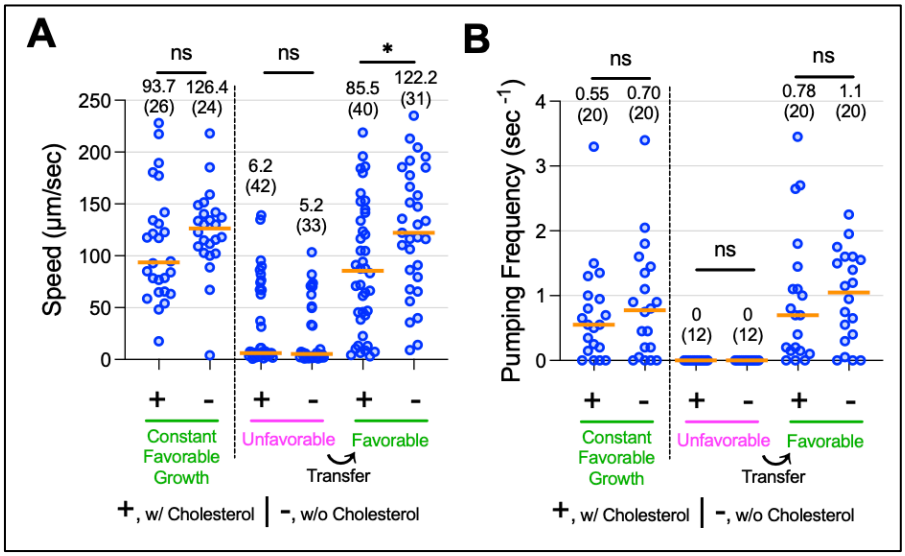

Figure S3.4. Effects of cholesterol on the partial dauer phenotype.

daf-9(dh6) partial dauers were formed by constant growth under favorable conditions, or by first inducing full dauers under unfavorable conditions before transferring to favorable conditions to induce dauer exit. In either case, omission of cholesterol from the growth media does not hinder the formation of partial dauers as measured by (A) speed or (B) pumping frequency. ns, not significant. *, $p<0.05$, ****,$p<0.0001$ by Mann Whitney test. Horizontal bars and in-graph numbers show median values. Numbers in parentheses indicate number of animals. Each dot is one animal.

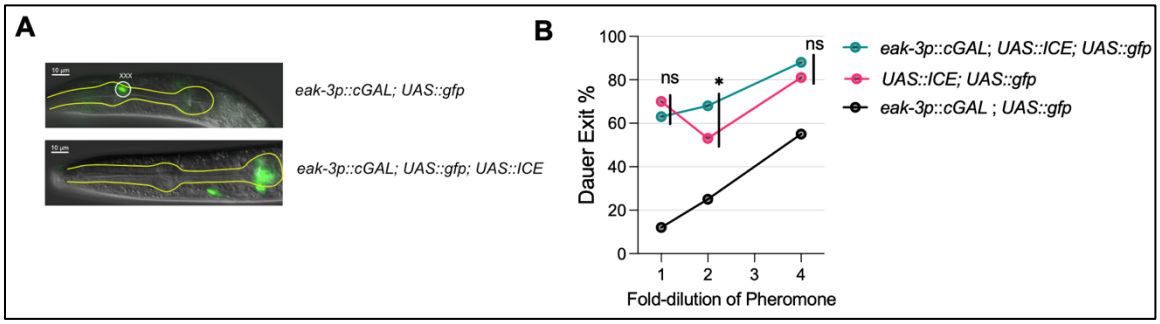

Figure S3.5. Genetic ablation of the XXX neuroendocrine cells using the human caspase ICE gene.

(A) A transgenic strain using the cGAL bipartite gene expression system expresses UAS::gfp using the cell-specific driver eak-3p::cGAL in the XXX neuroendocrine cells. The XXX cells are located near the anterior bulb of the pharynx. Expression of the human caspase gene ICE using the same XXX-specific eak-3 cGAL driver shows a loss of fluorescence in the XXX cells. The labeled neuron in the bottom image comes from RFP bleed-through from a co-injection marker labeling the AIY neuron, and the GFP signal in the posterior pharynx is nonspecific expression inconsistently observed in strains bearing the UAS::gfp transgene. (B) Genetic ablation of the XXX cells does not drastically impact dauer exit. Dauers whose XXX cells were genetically ablated were transferred to plates with decreasing pheromone concentrations and scored for dauer exit 24 hours later. Note that animals bearing the integrated UAS::ICE transgene formed SDS-sensitive dauers that exited at higher rates than the cGAL driver strain (see Materials and Methods). $n \geq 102$ animals for each sample. ns, not significant. *, $p<0.05$ by bootstrapped permutation test for a proportion using 10^4 samples.

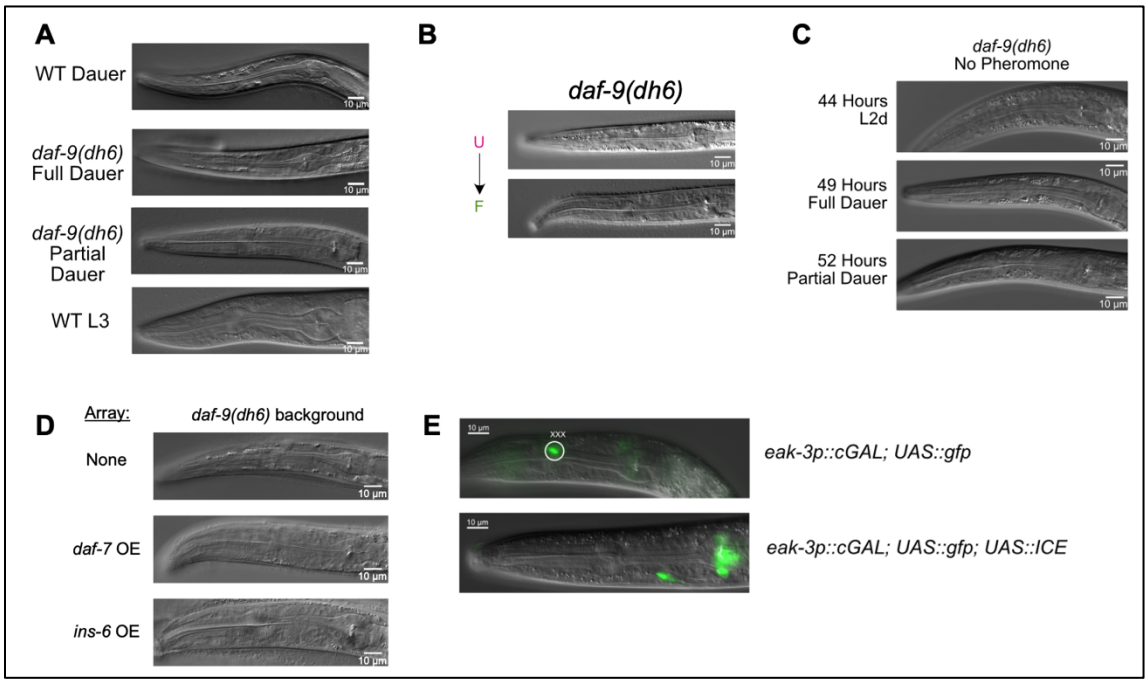

Figure S6. DIC images without pharyngeal outlines.

DIC images of pharynxes shown in (A) Figure 2A, (B) Figure 3G, (C) Figure 4B, (D) Figure 5F, and (E) Figure S5A but with the pharyngeal outlines omitted.

Table S3.1: Strain names, genotypes, and origins

Strain	Genotype	Origin	Notes
N2		Brenner, 1974	Wild-type
CB1370	daf-2(e1370) III	CGC, Riddle et al., 1981	
CB1372	daf-7(e1372) III	CGC, Riddle et al., 1981	
PS5511	daf-9(dh6) X; dhEx24(T13C5, pTG96(+))	Schaedel et al., 2012	
PS5513/AA277	lin-15(n765) X; dhIs64[daf-9::gfp, lin-15(+)]	Gerisch et al., 2001; Schaedel et al., 2012	AA277 was outcrossed 3x to make PS5513
CB2620	daf-9(e1406)/lon-2(e678) X	CGC	
DR2281	daf-9(m540) X	CGC, Jia et al., 2002	
AA87	daf-12(rh273) X	CGC, Antebi et al., 1998	
PS7949	syEx1628[col-183p::gfp; unc-122p::rfp]	Shih et al., 2019	col-183p is a hypoderm and dauer-specific promoter

PS7931	syEx1629[col-183p::daf-9 cDNA; unc-122p::rfp]	Shih et al., 2019	
PS9089	daf-2(e1370)/ sC1(s2023) [dpy-1(s2170) umnIs21] III; daf-9(dh6) X; dhEx24(T13C5, pTG96(+))	This study	
PS9187	daf-7 (e1372) / sC1(s2023) [dpy-1(s2170) umnIs21] III; daf-9(dh6) X; dhEx24(T13C5, pTG96(+))	This study	
PS9574	daf-9(dh6) X; syEx1913[rab-3p::cGal; UAS::ins-6(cDNA)::SL2::gfp; unc-122p::gfp]	Wang et al., 2017, and this study	Propagated on 100 nM Δ7-DA
PS9575	daf-9(dh6) X; syEx1914[rab-3p::cGal; UAS::daf-7(gDNA); unc-122p::gfp]	Wang et al., 2017, and this study	Propagated on 100 nM Δ7-DA
PS9186	syIs416[UAS::ICE; unc-122p::gfp] II; syIs300[UAS::gfp; ttx-3p::rfp] V; syIs669[eak-3p::cGal; unc-122p::rfp]	This study	Cross between PS7195 and PS8568
PS8568	syIs300[UAS::gfp; ttx-3p::rfp] V; syIs669[eak-3p::cGal; unc-122p::rfp]	M. Cao, S. Nava, and P. Sternberg, in prep.	Drives gfp in XXX cells. Used for laser ablation experiment
PS7195	syIs416[UAS::ICE; unc-122p::gfp] II	Wang et al., 2017	

Chapter 4
Conclusion and future directions

This thesis has advanced our previously limited understanding of the dauer exit decision, particularly when it comes to how dauers perform sensory integration (Chapter Two) and how dauers utilize steroid hormone signaling during the exit decision (Chapter Three). In doing so, this thesis has also underscored critical questions that remind us of how far we still are from fully understanding the complexity and nuance of neurogenetic computations performed during the dauer entry and exit decisions. In this concluding chapter, I identify outstanding questions that stem from the findings in Chapters Two and Three, and I provide suggestions for how we might address them in the future.

4.1 How do the TGF-β-like and insulin-like signaling pathways convey different sensory information?

Historically, signal transduction models depict the TGF-β-like and insulin-like/insulin-like growth factor signaling (IIS) pathways as working in parallel that converge onto steroid hormone signaling (see Fig. 1.2) (1–3). Further, these two pathways are thought to provide different streams of information. But what kinds of distinct information do these two pathways communicate?

An easy explanation would have been that each pathway conveys information pertaining to a specific class of sensory input, such as food availability or population density. However, this clearly cannot be the case. I showed in Chapter Two that ins-6 expression integrates both food and pheromone, and work from previous groups demonstrate that daf-7 expression also responds to both food and pheromone (4, 5). Thus, expression of key signal transduction molecules from both pathways are sensitive to both food and pheromone changes.

This leaves at least three remaining possibilities. The first possibility is that these pathways might respond to different individual components that collectively constitute "food signal" or "pheromone." The chemical composition of dauer pheromone is relatively well understood and is known to be composed of ascarosides (6, 7). In Chapter Two, I showed that production of the insulin-like peptide INS-6 is downregulated most strongly by ascr#8, weakly by ascr#2, and less so (if at all) by ascr#3 and ascr#5 when tested at 1 μM (Fig. 2.6). Kim and colleagues showed that production of DAF-7/ TGF-β is downregulated by ascr#1, ascr#3, and ascr#5 in adult animals, although they used concentrations that were 5-50x higher than those used in Fig. 2.6 of this thesis. Therefore, work from this thesis and others suggest that the TGF-β-like and IIS pathways may respond to different ascarosides.

Compared to pheromone, the precise chemical composition of the food signal is considerably less understood. However, recent studies (8–10) have made inroads to show that a multitude of different secreted bacterial metabolites, including polyamines and fatty acids, may constitute an appetitive odor that could contribute to a collective food signal. Food signals also differ for C. elegans from one environment to the next, as different natural habitats comprise different microbial populations (11). Therefore, the TGF-β-like and IIS pathways might respond to different bacterial metabolites as to expand C. elegans' capacity to respond to disparate microbial environments.

The second possibility is that the TGF-β-like and IIS pathways respond to the same environmental stimuli, but these two pathways may be differentially tuned to those stimuli. For instance, a specific bacterial metabolite may trigger activity in the TGF-β-like pathway at lower concentrations than for the IIS pathway, or the TGF-β-like pathway might respond more quickly than the IIS pathway. The third possibility is that the TGF-β-like and IIS pathways respond to the same environmental stimuli with the same tuning, but the site-of-action for these pathways differ. For instance, although the insulin-like growth factor receptor DAF-2/IGFR and the receptors for DAF-7/TGF-β are both expressed broadly, some tissues likely express receptors for one pathway more strongly than for the other.

These three possibilities are not mutually exclusive, and in fact all three may be true to some extent. The TGF-β-like and IIS pathways could show completely disparate responses to some stimuli, nearly identical responses to others, and influence gene expression in different tissues. Later in the next section, I provide suggestions to experimentally delineate how the TGF-β-like and IIS pathways respond to different environmental inputs.

4.2 How does information flow between the dauer-relevant signal transduction pathways?

While the question I raised above deals with how environmental stimuli affect activity within pathways, the dauer field also needs to reckon with the question of how activity varies between pathways. In other words, how does activity in one pathway correlate with or influence activity in another pathway?

Most studies that have examined the genetic pathways underlying the dauer entry and exit decisions have done so largely by measuring gene expression patterns of a limited number of genes in response to different environmental conditions or in the context of different loss- or gain-of-function mutants (4, 5, 12–14). What the dauer field critically needs is an integrative model that explains how information flows through and between the various signal transduction pathways that govern dauer entry and exit, starting from the nervous system at the level of sensory perception of dauer-related cues and ending with the transcriptional outputs that manifest the relevant physiological changes.

To create such an integrative model would require the ability to simultaneously measure neuronal activity as well as gene expression patterns across multiple tissues. Thankfully, these requirements are well within the realm of our current C. elegans experimental toolkit. If we take dauer exit as an example decision, an ideal experimental setup would be one in which we could follow individual dauers in real time as it contemplates the dauer exit decision, either using a microfluidic device or via live imaging in free roaming animals, after exposure to intermediate pheromone conditions. For us to measure specific parameters, these dauers would also express one or multiple of the following genetically encoded reporters:

- calcium indicators in a number of key chemosensory neurons such as the ASJ, ASI, ASG, and ADF neurons (12, 15, 16) to measure calcium dynamics
- cGMP reporters in the same neurons to measure cGMP levels (17)
- fluorescence reporters to measure the production or subcellular localization of key signal transduction components such as INS-6, DAF-28, or DAF-16/FoxO for the IIS pathway, DAF-7/TGF-β and DAF-8/R-SMAD for the TGF-β-like pathway, and DAF-9/CYP450 for the steroid hormone pathway. To avoid signal convolution, these reporters would need to be orthogonal in their spatial profile (i.e., expressed in different tissues) or their spectral profiles (i.e., have orthogonal excitation and emission wavelengths)

While we would be limited in the number of measurements (such as calcium traces and number of gene reporters) we could capture in a single animal, we could image different sets of parameters over the course of multiple animals to construct a more complete model. As an alternative to fluorescence reporters to measure gene expression, we could also utilize mRNA FISH or single-cell RNA sequencing to measure transcripts, but this technique would prevent longitudinal studies of the same individual worms due to the requirement of fixing or lysing the animal as part of sample preparation.

The goal of this experimental paradigm would be to collect measurements along multiple dimensions of biological information and use this vast dataset to gain insight into the decision-making process. Much like how systems neuroscientists construct models using activity across neuronal populations to understand computation within neural circuits, we could similarly construct models that relate neuronal activity to secondary messenger production and gene expression patterns to better understand the holistic computations that C. elegans performs during dauer entry or exit.

4.3 How do dynamical inputs into the dauer entry and exit decisions influence the decision-making process?

In their natural habitats, animals rarely encounter static environmental conditions such as those seen in the controlled lab environment. In Chapters Two and Three, I induced C.

elegans dauers to exit by transferring animals from unfavorable, high-pheromone conditions to favorable conditions without pheromone. But in the wild, C. elegans rarely experience such sudden shifts from one constant concentration to another. Instead, changes in the environment occur sporadically and dynamically. Worms may experience an increasing gradient of pheromone one moment and then a steep concentration decline the next.

This issue also relates to the timescale discrepancy alluded to in Chapter Two: the dauer decisions draw upon sensory inputs that can be measured over shorter timescales on the order of seconds via calcium dynamics, but the decision-making process occurs over a much longer timescale on the order of hours as measured via gene expression and physiological changes. In Chapter Two (Fig. 2.2), I demonstrated that ins-6 transcription increases in as little as one hour following transfer to favorable conditions, meaning that a continuous one-hour exposure to stimuli can induce a measurable change in gene expression. Similarly, our lab has previously shown that a three hour exposure to favorable, no-pheromone conditions is sufficient to commit a pre-dauer L2d worm to non-dauer, reproductive growth (18).

In both cases, an environmental stimulus on the order of hours results in a noticeable physiological response. Does that hours-long exposure need to be continuous, or can it be provided in disconnected pulses or as an increasing concentration gradient (Fig. 4.1)? Would an even higher pheromone concentration shorten the duration of the exposure needed? How are the temporal dynamics of the stimulus encoded by calcium dynamics, secondary messenger levels, and gene expression patterns? Such questions are commonly asked by systems biologists who analyze information flow within gene circuits; we ought to employ a similar strategy while studying the C. elegans dauer decisions. To answer these questions, we could utilize the same experimental setup described above and measure changes in GCaMP and other fluorescence reporters in response to different sensory input paradigms (Fig. 4.1)

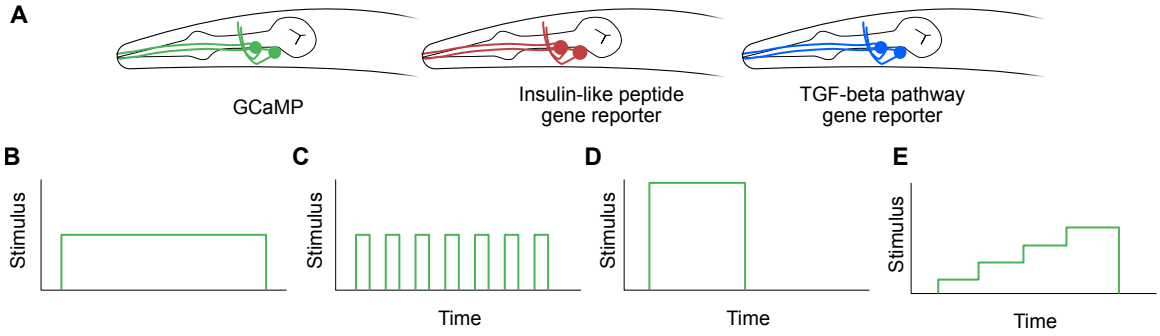

Figure 4.1 Experimental paradigm to measure and model multiple parameters during the dauer decision

Shown is a simplified example of how one might measure multiple biological parameters relevant to the dauer decision-making process in response to dynamical inputs in real time. In this example, suppose we are analyzing the dauer exit decision, although this setup would theoretically work for the dauer entry decision as well. (A) A transgenic dauer should express multiple genetically encoded fluorescence reporters that measure relevant parameters such as calcium activity via GCaMP, gene expression of key signaling pathways, and more. These reporters need to be non-overlapping in terms of their spatial (i.e. expressing in different neurons) or spectral (i.e., different excitation/emission wavelengths) properties. (B-E) Under a microfluidic setup, the exit-promoting stimulus can be provided in different temporal patterns to test how the parameters measured in (A) respond. These patterns include a flat concentration (B), a series of discontinuous pulses (C), an increased concentration for a shorter amount of time (D), or an increasing concentration gradient (E).

4.4 Why do some dauers exit but not others? Where does inter-worm variability arise?

Even within a genotypically identical population there is phenotypic variability or heterogeneity due to the inherent stochasticity of how biological molecules behave (19). The degree of phenotypic variability can be shaped over time by evolution via small

changes in the biophysical parameters that sculpt such variability. In microorganisms such as bacteria and yeast, it has been shown that greater phenotypic variability confers a competitive advantage in unstable, fluctuating environments (19–21). This effect is known as bet hedging, wherein organisms manifest multiple phenotypes in the hopes that at least one of those phenotypes will prove advantageous in the environment that eventually comes to pass. Bet hedging is exemplified by the C. elegans dauer entry and exit decisions (22); under uncertain environmental conditions, a population of C. elegans can commit a fraction of its population to become dauers while leaving others to grow reproductively, therefore diversifying its survival strategy to maximize the chance that at least some progeny survive to reproductive adulthood.

In Chapter Two (Fig. 2.3D), I showed that six hours of exposure to intermediate-pheromone concentrations (which induce approximately 25-75% of dauers to exit) greatly increases ins-6 transcriptional reporter activity in the ASJ neurons of dauers that end up exiting after 24 hours but only slightly increases reporter activity in worms that remain dauers. This begs the question: why do these two populations of dauers respond differently?

The experiment performed in Fig. 2.3D highlights the power of longitudinal studies to examine how individual worms behave over time. The experimental paradigm to study dauer exit described above in Fig. 4.1, in which individual dauers are followed over time in a microfluidic or free roaming setup, could similarly be used to address this question. By comparing the different parameters between dauers that end up remaining dauers or exiting the dauer state, we can determine if an individual worm is biased towards deciding one way or the other based on differences such as calcium activity in response to food signals or ascarosides, production of secondary messengers such as cGMP, gene expression levels of components of the TGF-β-like, insulin-like, or steroid hormone signaling pathways, or degree of subcellular localization of key transcription factors. The decision parameter(s) must be encoded in one of the above steps.

4.5 Concluding remarks

Through this thesis, I hope to have illustrated that while the C. elegans dauer entry and exit decisions are some of the most well-studied biological processes, there remains much that we do not know. As is the case with any scientific endeavors, our efforts to study the dauer decisions are limited by our technical capabilities. Over the past few decades, the dauer decisions have been studied using the classic tools of genetics and molecular biology, including forward mutagenesis screens, epistasis analysis, mutant constructs, transgenic reporters, and more. But now we are in a period in which high throughput, multiplex measurements can be made in real time, such as whole brain imaging (23–25). These techniques are perfectly suited to address the complexities of the dauer entry and exit decisions, which invite analyses of how multiple neurons, tissues, and genes interact to compute and execute a whole-organism decision. I hope that this thesis brings us one step closer to appreciating and understanding how such a simple roundworm, whose nervous system comprises only 302 neurons in the hermaphrodite, can accomplish a rich repertoire of multifaceted behaviors and decisions.

4.6 References

1. R. J. Androwski, K. M. Flatt, N. E. Schroeder, Phenotypic plasticity and remodeling in the stress-induced Caenorhabditis elegans dauer. Wiley Interdiscip. Rev. Dev. Biol. 6, e278 (2017).

2. N. Fielenbach, A. Antebi, C. elegans dauer formation and the molecular basis of plasticity. Genes Dev. 22, 2149–2165 (2008).

3. P. J. Hu, Dauer. WormBook (2007). https://doi.org/10.1895/wormbook.1.144.1.

4. S. J. Neal et al., Feeding state-dependent regulation of developmental plasticity via CaMKI and neuroendocrine signaling. eLife 4, e10110 (2015).

5. P. Ren et al., Control of C. elegans larval development by neuronal expression of a TGF-β Homolog. Science (1996). https://doi.org/10.1126/science.274.5291.1389.

6. A. H. Ludewig, F. C. Schroeder, “Ascaroside signaling in C. elegans” in WormBook: The Online Review of C. Elegans Biology [Internet], (WormBook, 2018).

7. P. T. McGrath, I. Ruvinsky, A primer on pheromone signaling in Caenorhabditis elegans for systems biologists. Curr. Opin. Syst. Biol. 13, 23–30 (2019).

8. B. Brissette et al., Chemosensory detection of polyamine metabolites guides C. elegans to nutritive microbes. Sci. Adv. 10, eadj4387 (2024).

9. T. K. Kaul, P. R. Rodrigues, I. V. Ogungbe, P. Kapahi, M. S. Gill, Bacterial fatty acids enhance recovery from the dauer larva in Caenorhabditis elegans. PLOS ONE 9, e86979 (2014).

10. S. E. Worthy et al., Identification of attractive odorants released by preferred bacterial food found in the natural habitats of C. elegans. PLOS ONE 13, e0201158 (2018).

11. H. Schulenburg, M.-A. Félix, The Natural biotic environment of Caenorhabditis elegans. Genetics 206, 55–86 (2017).

12. A. Cornils, M. Gloeck, Z. Chen, Y. Zhang, J. Alcedo, Specific insulin-like peptides encode sensory information to regulate distinct developmental processes. Development 138, 1183–1193 (2011).

13. J. C. Fierro-González, A. Cornils, J. Alcedo, A. Miranda-Vizuete, P. Swoboda, The thioredoxin TRX-1 modulates the function of the insulin-like neuropeptide DAF-28 during dauer formation in Caenorhabditis elegans. PloS One 6, e16561 (2011).

14. W. L. Hung, Y. Wang, J. Chitturi, M. Zhen, A Caenorhabditis elegans developmental decision requires insulin signaling-mediated neuron-intestine communication. Development 141, 1767–1779 (2014).

15. C. I. Bargmann, H. R. Horvitz, Control of larval development by chemosensory neurons in Caenorhabditis elegans. Science 251, 1243–1246 (1991).

16. D. A. Fernandes de Abreu et al., An insulin-to-insulin regulatory network orchestrates phenotypic specificity in development and physiology. PLoS Genet. 10, e1004225 (2014).

17. S. Woldemariam et al., Using a robust and sensitive GFP-based cGMP sensor for real-time imaging in intact Caenorhabditis elegans. Genetics 213, 59–77 (2019).

18. O. N. Schaedel, B. Gerisch, A. Antebi, P. W. Sternberg, Hormonal signal amplification mediates environmental conditions during development and controls an irreversible commitment to adulthood. PLOS Biol. 10, e1001306 (2012).

19. M. Ackermann, A functional perspective on phenotypic heterogeneity in microorganisms. Nat. Rev. Microbiol. 13, 497–508 (2015).

20. M. Acar, J. T. Mettetal, A. van Oudenaarden, Stochastic switching as a survival strategy in fluctuating environments. Nat. Genet. 40, 471–475 (2008).

21. H. J. E. Beaumont, J. Gallie, C. Kost, G. C. Ferguson, P. B. Rainey, Experimental evolution of bet hedging. Nature 462, 90–93 (2009).

22. L. Avery, A model of the effect of uncertainty on the C elegans L2/L2d decision. PLOS ONE 9, e100580 (2014).

23. E. Yemini et al., NeuroPAL: A Multicolor Atlas for Whole-Brain Neuronal Identification in C. elegans. Cell 184, 272-288.e11 (2021).

24. V. Susoy et al., Natural sensory context drives diverse brain-wide activity during C. elegans mating. Cell 184, 5122-5137.e17 (2021).

25. J. P. Nguyen et al., Whole-brain calcium imaging with cellular resolution in freely behaving Caenorhabditis elegans. Proc. Natl. Acad. Sci. 113, E1074–E1081 (2016).